Chapter 1: Introduction

1.1 Introduction

Wood is used in many structural applications around the world due to its economy, its good strength to weight ratio, and its status as a renewable resource. This widespread use demands a comprehensive understanding of the material properties and the mechanical behaviors of wood and wood connections. Connections, in particular, are vital to the safety and stability of wood structures, as they distribute load between structural members, and provide ductility within the system.

Dowel-type fasteners, such as nails, screws, and bolts are the primary active components in most structural wood connections. Bolts are useful in connections involving large members and substantial loads, and multiple-bolt connections are often encountered in construction. The design of multiple-bolt wood connections is not easy, as connection strength is not simply proportional to the number of bolts present, but is also a function of bolt spacing, among other things. If bolts are spaced too closely, the wood may split prematurely. On the other hand, if bolts are spaced too far apart, strength may be lost in locations where it is most needed.

Currently the National Design Specification for Wood Construction (NDS) recommends a spacing of four times the bolt diameter (4D) between bolts in a row. However, recent experimentation by Anderson (2002) and Billings (2004) suggests that a 4D spacing may lead to premature splitting failures, and Billings, in particular, recommended a 7D spacing in her conclusions. Her results, however, do not apply to connections subject to mode III or mode IV yielding, in which bolts bend prior to wood splitting. Despite efforts to the contrary, she was unable to develop these yield modes due to lower-than-expected wood strength and higher-than-expected bolt bending strength.

The project described in this thesis was designed to develop connections subject to yield modes III and IV, and to use test data to recommend a between-bolt spacing for these

connections. Since an accurate estimate of wood strength and bolt bending strength is vital to predicting yield modes, the design of the wood connections was based on preliminary dowel bearing and bolt bending tests. The measurement of bolt bending strength is particularly difficult, and the details of this issue are also explored in this thesis.

In addition to the issues of bolt bending and between-bolt spacing, this project is part of a growing effort to better understand the effects of reverse-cyclic loading on multiple-bolt, single-shear connections between wood members. While much monotonic experimentation has been devoted to developing design guidelines for wood members and connections under gravity loads, less is known about the effects of dynamic loading situations. Reverse-cyclic loading is a dynamic loading procedure designed to simulate natural hazard loads, like those produced by earthquakes or high winds. This project, like the projects of Heine (2001), Anderson, and Billings before it, employed reverse-cyclic loading in order to further investigate the response of bolted connections to dynamic loads.

1.2 Objectives

Recent experimentation by Heine, Anderson, Billings, and others has contributed to a better understanding of bolted connection behavior under reverse-cyclic loading. However, there are still questions remaining. Billings was unable to consistently develop yield modes III and IV, meaning that her suggested bolt spacing of 7D may not apply to connections subject to true mode III and mode IV behavior. In addition, research has confirmed the important influence of bolt bending yield strength on connection behavior. However, questions remain regarding the proper measurement of bending yield strength and the relationship between the bending yield strength and the tensile yield strength. With these questions in mind, the following objectives for this project were developed:

a) To determine the relationship between the tensile yield strength, three-point bending yield strength, and cantilever bending yield strength of bolts.

b) To quantify the bending yield strengths of 3/8”x6” and 3/8”x8” low-carbon steel bolts.
c) To use these bending yield strengths and the NDS yield limit equations to predict multiple-bolt, single-shear connection configurations that will produce yield modes III and IV, and to validate these predictions with preliminary monotonic and reverse-cyclic testing.
d) To compare a 7D between-bolt spacing to an 8D between-bolt spacing for the mode III and IV configurations under reverse-cyclic loading. Optimization will be based on the seven strength and serviceability parameters employed by Billings (2004). These include maximum load, failure load, E.E.P. yield load, 5% offset load, elastic stiffness, E.E.P. energy, and ductility ratio.

1.3 Significance

The research conducted in one phase of this project pertains to the reliable measurement of bolt bending strength. The results of this experimentation can be used by future researchers to inform their own measurements of bolt bending strength. The research conducted in the other phase of this project pertains to the between-bolt spacing in multiple-bolt, single-shear connections subjected to reverse-cyclic loading. The results of this experimentation, paired with the work of Anderson and Billings, can be used to reevaluate the 4D bolt spacing currently recommended by NDS. In addition, the research presented in this thesis represents further insight into the response of wood connections to dynamic loading, and is thereby valuable for limiting earthquake and high wind damage in wood structures.

1.4 Thesis Overview

Chapter 2 of this document contains a literature review of previous research related to wood connections and bolt properties. Chapter 3 describes the test methods and materials used during the course of experimentation. Chapter 4 contains the presentation and discussion of test results. Chapter 5 contains a summary of important results, conclusions drawn from testing, and suggestions for further research. Appendix A contains

preliminary measurements and yield mode calculations. Appendix B contains all results from the connection testing. Appendix C contains all results from the bolt testing.

Chapter 2: Background

2.1 Introduction

The importance of connections in wood structures cannot be overstated. In addition to their role in transferring static loads between members, connections are especially vital in dynamic loading situations. It has been suggested that up to 90% of a wood structure's dampening capacity comes from its connections (Chui and Smith, 1989)(Yeh, et. al., 1971). The catastrophic annual damages associated with hurricanes and earthquakes serve to affirm the importance of damping and dynamic stability in timber structures. While much experimentation has been devoted to wood connections, more research is necessary to quantify their response to dynamic loading situations.

2.2 Dowel-Type Wood Connections

2.2.1 Single-Fastener Connections

Single fastener, dowel-type connections under lateral load were the subject of early tests by Trayer (1932), and design values generated by these tests are still in use today. However, yield behavior in dowel-type connections was not explicitly investigated until 1949, when Johansen introduced the Yield Model, which linked the behavior of single-fastener joints to the dowel's bending strength and to the wood's crushing strength (Johansen, 1949). The NDS adopted the Yield Model in 1991 and defined four yield modes applicable to dowels in shear. The yield modes for single-shear cases are shown in Figure 2.1.

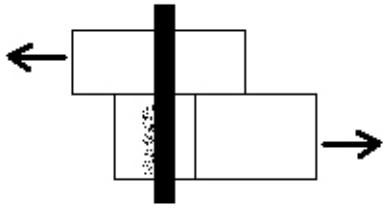

MODE I_m

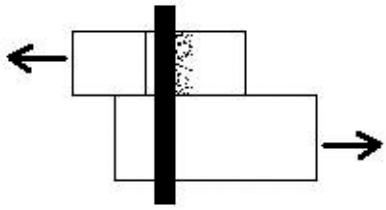

MODE I_s

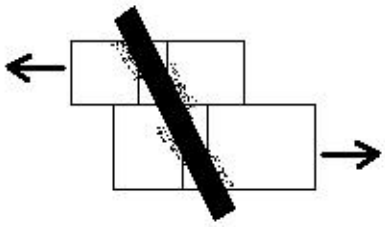

MODE II

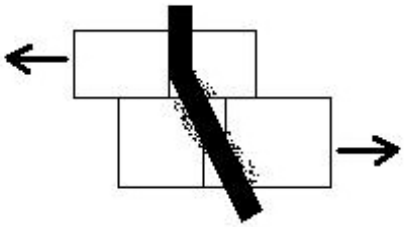

MODE III_m

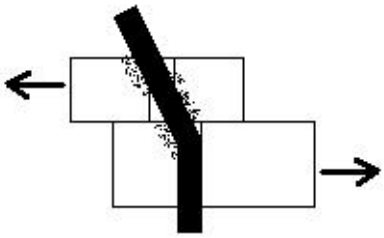

MODE III_s

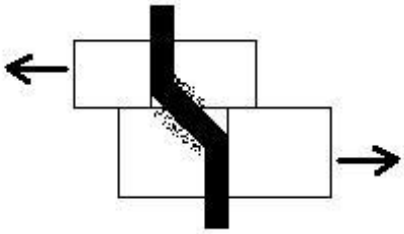

MODE IV

Figure 2.1: Yield Modes for Single-Shear Connections (after AF&PA, 2001).

Since their introduction, the NDS yield limit equations (shown in Table 2.1) have been used to predict the yield strength and behavior of single fastener joints as functions of the dowel diameter, dowel bending strength, dowel bearing strength, and member thicknesses. Section I1 of NDS Appendix 1 describes yield mode I as a "bearing-dominated yield of the wood fibers in contact with the fastener." This mode occurs rarely and is difficult to replicate consistently. Mode II represents the "pivoting of the fastener at the shear plane" with local "crushing of wood fibers near the faces of the wood members." Mode III describes "fastener yield in bending at one plastic hinge point per shear plane." Finally, mode IV represents "fastener yield in bending at two plastic hinge points per shear plane" (AF&PA, 2001).

Table 2.1: Yield Limit Equations for Single-Shear (after AF&PA, 2001)

Yield Mode	Single Shear
I_m	$Z = \frac{Dl_m F_{em}}{R_d}$
I_s	$Z = \frac{Dl_s F_{es}}{R_d}$
II	$Z = \frac{k_1 Dl_s F_{es}}{R_d}$
III_m	$Z = \frac{k_2 Dl_m F_{em}}{(1+2R_e)R_d}$
III_s	$Z = \frac{k_3 Dl_s F_{em}}{(2+R_e)R_d}$
IV	$Z = \frac{D^2}{R_d}\sqrt{\frac{2F_{em}F_{yb}}{3(1+R_e)}}$

Where

$$k_1 = \frac{\sqrt{R_e + 2R_e^{\,2}(1+R_t+R_t^{\,2}) + R_t^{\,2}R_e^{\,3}} - R_e(1+R_t)}{(1+R_e)}$$

$$k_2 = -1 + \sqrt{2(1+R_e) + \frac{2F_{yb}(1+2R_e)D^2}{3F_{em}l_m^{\,2}}}$$

$$k_3 = -1 + \sqrt{\frac{2(1+R_e)}{R_e} + \frac{2F_{yb}(2+R_e)D^2}{3F_{em}l_s^{\,2}}}$$

Where

D = diameter, in.
F_{yb} = dowel bending strength, psi
R_d = zero for parallel to grain
$R_e = F_{em}/F_{es}$
$R_t = l_m/l_s$
l_m = main member dowel bearing length, in.
l_s = side member dowel bearing length, in.
F_{em} = main member dowel bearing strength, psi
F_{es} = side member dowel bearing strength, psi

2.2.2 Multiple-Fastener Connections

For many years it was assumed that the behavior of multiple fastener connections could be approximated by multiplying the strength of a single fastener by the total number of fasteners present. Experimentation by Lantos (1969) and others has since disproved this assumption by showing that the strength of a multiple fastener connection is not simply proportional to the number of fasteners. Currently, the NDS includes an additional safety factor for multiple bolt connections in order to account for this disparity. However, this "group action factor" is applied only in design, and does not factor into the yield limit equations (see Appendix A and Table 2.1). Additionally, Wilkinson (1980) and others have noted various limitations of the Lantos method, which provides the basis for the group action calculation found in NDS. First, Lantos assumed linear elastic joint behavior, though this is rarely the case for wood connections. Second, Lantos does not account for load redistribution and variable load-slip behavior among fasteners. These limitations of the group action factor and its absence from the yield limit equations called for further research into the behavior of multiple fastener connections.

2.2.3 Dynamic Loading

Much previous experimentation related to wood structures has employed monotonic loading to replicate static situations. However, instances of natural hazards have raised interest in the response of timber elements and joints to dynamic loading. This increased interest led the Consortium of Universities for Research in Earthquake Engineering (CUREE) to develop a testing protocol aimed at wood structures under reverse-cyclic loading (Krawinkler, et. al., 2000). Reverse-cyclic loading is deflection-controlled and involves cycling loads through zero in order to test specimens in both tension and compression. The order and magnitudes of the cycles are defined in the CUREE test protocol and are described in detail in section 3.3.7. With the CUREE protocol in place, recent research has been devoted to understanding the effects of reverse-cyclic loading on multiple-fastener connections.

2.2.4 Multiple-Bolt Connections Subject to Reverse-Cyclic Loading

Early research by Gutshall (1994) employed reverse cyclic loading to investigate the NDS load duration factor as applied to wood joints with dowel-type fasteners. In addition, he studied the influence of prior cyclic loading on connection ductility and capacity. Gutshall's final objective was to "investigate and quantify" certain "characteristics of the cyclic response of a dowel type mechanical fastener," such as hysteretic energy dissipation, stiffness, and damping (Gutshall, 1994). His work on this final objective, in particular, helped provide a foundation for some of the more recent research.

While he did not work with reverse cyclic loading, Jorissen (1998) did address Johansen's Yield Model in his study of various failure mechanisms in multiple-bolt, double-shear wood connections. Jorissen suggests that the capacities predicted by Johansen's model are unconservative in the case of stiff dowels, which tend to cause timber splitting rather than embedment. In his thesis Jorissen notes a linear relationship between density and embedment strength. Thus, his decision to test specimens of varying density was, in effect, a way of proving the limited role embedment plays in capacity. After much testing, Jorissen found no connection between the timber density and the load carrying capacity. On the other hand, the number of bolts per row, the slenderness ratio of the bolts, and the bolt spacing proved influential. In particular, Jorissen concluded that the "load carrying capacity of multiple fastener connections is lower for small spacings than for high spacings," with the influence decreasing "if the spacing is increased" (Jorissen, 1998). These findings were addressed in later research by Billings (2004).

In 2001 Heine developed a model to describe the role of oversized bolt holes and slack behavior in wood connections subjected to reverse-cyclic loading. His model was later validated by Anderson in 2002. In addition, testing by both Heine and Anderson challenged the in-row, between-bolt spacing recommended by NDS. Both concluded that the recommended spacing of four bolt diameters (4D) could lead to premature connection failure with respect to calculated yield limits. In agreement with Heine, Anderson

suggests that "an increase in bolt spacing from 4D to 7D would enhance multiple-bolt connection performance by allowing more redistribution of bolt forces by limiting the likelihood of premature brittle failure" (Anderson, 2002).

Anderson's research also served to affirm Jorissen's previous conclusions regarding the influence of the number of bolts on connection strength. Anderson noted a decrease in the maximum load-per-fastener as the number of fasteners increased. However, this drop-off was much more dramatic between one-bolt and three-bolt specimens than it was between three-bolt and five-bolt specimens. In response to this finding Anderson proposed a stair-step group action factor for multiple-bolt connections.

In addition to his work on group action, Anderson offered an important conclusion regarding fastener yielding in wood connections. He tested various different arrangements in order to develop yield modes II, III, and IV for analysis. Anderson easily developed yield mode II using two 2x6's and ½-in. (1.27 cm) diameter bolts, as well as yield mode IV using two 4x6's and 3/8-in. (0.95 cm) diameter bolts, but he had trouble developing yield mode III consistently. His connections aimed at creating yield mode III consisted of ¼-in. (0.64 cm) thick steel side members, 4x6 Southern pine main members, and 3/8-in. (0.95 cm) diameter bolts. However, the single-bolt connections yielded according to mode IV, and the three and five-bolt connections displayed various yield modes ranging from II to IV. These results prompted Anderson to suggest that bolts "yield by migrating through the yield modes from mode II to mode IV" (Anderson, 2002). He argued that the brittle splitting failures in his test specimens prevented some of the bolts from completing this migration to the higher yield modes.

Billings' work in 2004 followed from Heine's and Anderson's skepticism regarding the 4D in-row spacing recommended by NDS. Billings employed a one-row, single-shear test setup similar to Anderson's in her search for the optimal bolt spacing under reverse-cyclic loading. She tested spacings of 3D, 5D, 6D, 7D, and 8D in three different connection configurations designed to develop yield modes II, III, and IV. She concluded that the 7D spacing recommended by Anderson was indeed best because it

offered the highest values for both yield load and E.E.P. energy. In other words, the 7D spacing was found to maximize the duration of yield strength and maintain "longer periods of yielding before failure finally occurred" (Billings, 2004). However, this conclusion contains an important caveat. Dimensional constraints of the testing machine limited Billings to the recommended minimum end distance of 7D, even in the connections featuring 8D between-bolt spacings. Thus, the 7D end distance may have controlled the behavior of the 8D connections, limiting their capacity. Further research should be conducted to examine this possibility.

Additionally, Billings had trouble developing yield modes III and IV with consistency. Billings employed ¼-in. (0.64 cm) thick steel side members, 4x6 Southern pine main members and ½-in. (1.27 cm) diameter bolts in efforts to produce mode III yielding. Her arrangements predicted to yield according to mode IV contained two 2x6 Southern pine members with 3/8-in. (0.95 cm) diameter bolts. In both cases the connections tended to yield according to mode II. Citing Anderson's hypothesis regarding the "migration" of bolts through yield modes, Billings suggested that her specimens failed to reach the stresses required for the upper yield modes due to premature splitting failures. This conclusion was supported by her material tests, which revealed lower-than-expected specific gravity in the wood members, and higher-than-expected bending yield strengths in the bolts. Billings had assumed specific gravities of 0.55 for the Southern Yellow Pine 2x6's, and 0.51 for the Mixed Southern Pine 4x6's. In addition, she assumed a bolt bending yield strength of 45,000 psi in her yield mode predictions, according to NDS Appendix I.4. By comparison, Billings' measurements indicated that the 4x6's used in the mode III tests had an average specific gravity of 0.25 and the ½-in. (1.27 cm) diameter bolts had an average bending yield strength of approximately 61,000 psi. The 2x6's used in the mode IV tests had a respectable average specific gravity of 0.59, but the 3/8-in. (1.91 cm) diameter bolts exhibited a high average bending yield strength of approximately 69,000 psi. These deviations from predicted material values likely played a large part in the brittle connection behavior that hindered the development of modes III and IV.

To investigate this possibility, Billings substituted the actual values for specific gravity and bolt yield strength into the yield mode equations. With the actual values included in the predictions, both the mode III and mode IV arrangements were instead predicted to behave according to mode II. These new predictions were consistent with test results and suggest that using actual values for specific gravity and bolt bending yield strength produces more accurate yield mode predictions. In addition to these recalculations, Billings tested a series of alternative connection configurations in both monotonic and reverse-cyclic loading in efforts to determine which variable most affected the yield modes.

To test the influence of specific gravity, Billings constructed a glue-laminated 4x6 using planed 2x6's with approximate specific gravities of 0.55. To isolate the influence of specific gravity, Billings again used a ¼-in. (0.64 cm) thick steel side member and five ½-in. (1.27 cm) diameter bolts, the same combination she had used in the bulk of her mode III testing. Using a 6D bolt spacing, she observed "slight bolt bending," but noted that "behavior was mostly in accordance with Yield Mode II" (Billings, 2004). Thus, while her calculations indicated that low specific gravity played a part in the failure to reach mode III, testing demonstrated that this variable has a limited influence on its own. Billings concluded that "better 4x6 material may not produce the Yield Mode III as predicted" (Billings, 2004). This finding supported Jorissen's assertion that wood density alone has a limited influence on connection capacity.

To test the influences of side member thickness and bolt diameter, Billings replaced the ¼-in. (0.64 cm) steel plate with a ½-in. (1.27 cm) plate and the ½-in. (1.27 cm) diameter bolts with five 3/8-in. (0.95 cm) bolts. She retained a 4x6 main member of low specific gravity and a 6D bolt spacing in order to isolate the effects of her other changes. Despite the modifications, the connection still behaved according to yield mode II. Next, a 2x6 of normal specific gravity was attached to a 4x6 of low specific gravity using five ½-in. (1.27 cm) diameter bolts. This connection also displayed mode II behavior.

Finally, Billings tested a combination of these variables by using thicker side members, denser 4x6 main members, and bolts of smaller diameter. Her connections featured 2x6 Southern Yellow Pine side members of normal specific gravity, 4x6 Mixed Southern Pine main members of normal specific gravity, 3/8-in. (0.95 cm) diameter bolts, and 6D bolt spacings. Connections featuring five bolts displayed a combination of mode II and mode III yielding, while connections featuring one bolt and three bolts each displayed mode II yielding exclusively. Billings' success in generating mode III with this configuration affirms the importance of various parameters on yield behavior. In addition, this configuration can be tested more extensively to assess the optimum bolt spacing in a connection subject to true mode III behavior.

2.3 Dowel Bearing Strength

As noted in section 2.2.1, the yield limit equations are useful for predicting connection behavior. These equations consider both the bending yield strength of the dowels (F_{yb}) and the dowel bearing strength (F_e). The dowel bearing strength, also called the dowel embedment strength, is a measure of the yield strength of the wood under the pressure of the dowels. NDS Table 11.3.2 includes a list of dowel bearing strengths as functions of specific gravity. These values pertain exclusively to bolts in parallel-to-grain loading, and are based on a linear relationship developed through testing by Wilkinson (1991). Wilkinson's relationship between dowel bearing strength and specific gravity is included below as Equation 2.1.

$$F_e = 11200*G \qquad (2.1)$$

A general relationship between wood strength and specific gravity was verified by Billings (2004), when her connections split prematurely as the result of low specific gravities, among other factors. However, upon measuring bearing strengths directly, both Billings and Anderson (2002) demonstrated that Equation 2.1 sometimes fails to accurately predict bearing strength.

In their measurements, Anderson and Billings used a full-hole setup similar to the one described in section 10.2 of ASTM D 5764-97a, Standard Test Method for Evaluating Dowel Bearing Strength of Wood and Wood-Based Products. This method is characterized by applying load to a dowel inserted through a full hole in the center of the embedment specimen (see Figure 2.2), and thereby differs from the half-hole method described in section 10.1 ASTM D 5764-97a, and illustrated in Figure 2.3.

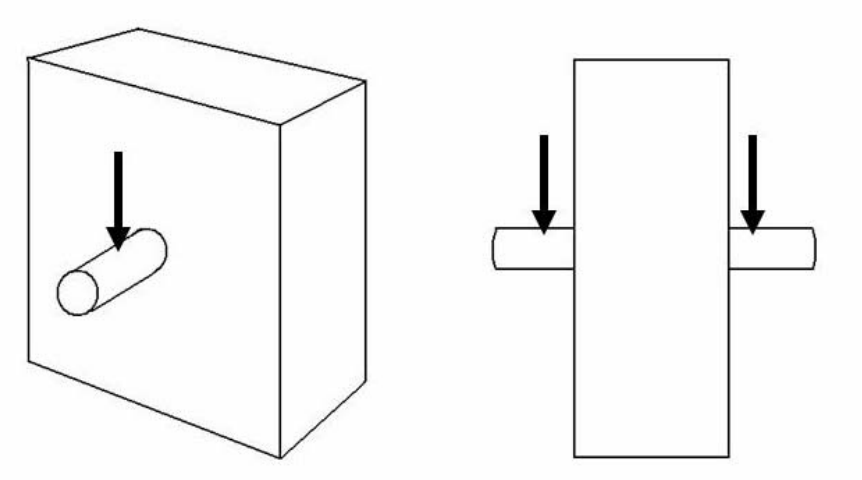

Figure 2.2: Illustration of Full-Hole Setup for Dowel Bearing Strength

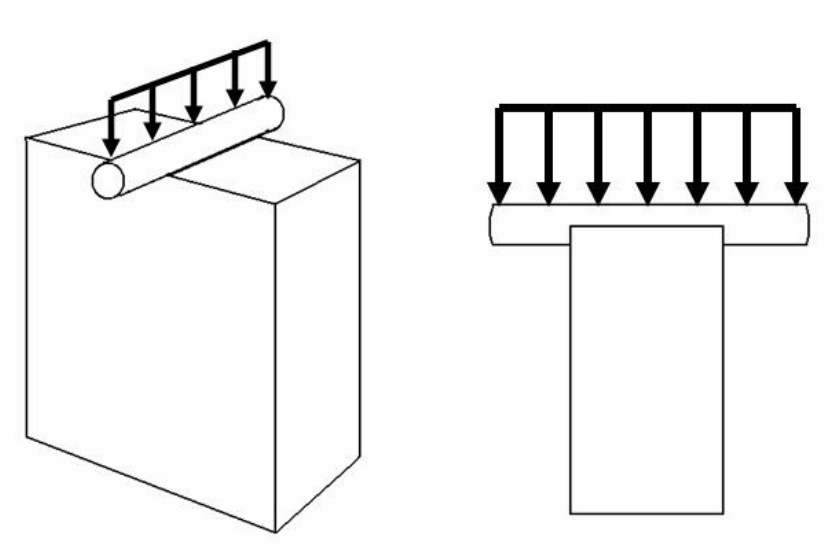

Figure 2.3: Illustration of Half-Hole Setup for Dowel Bearing Strength

The only difference between the setup used by Anderson and Billings and the full-hole setup depicted in Figure 2.2 was in the location of the load application. Instead of applying two point loads directly to the bolt, the load was applied uniformly to the top of the specimen. In this setup, the dowel passed through two fixed steel plates on either side of the specimen in addition to passing through the specimen itself. This setup involved a simple flat loading head as opposed to the more complicated loading apparatus required to apply the point loads depicted in Figure 2.2.

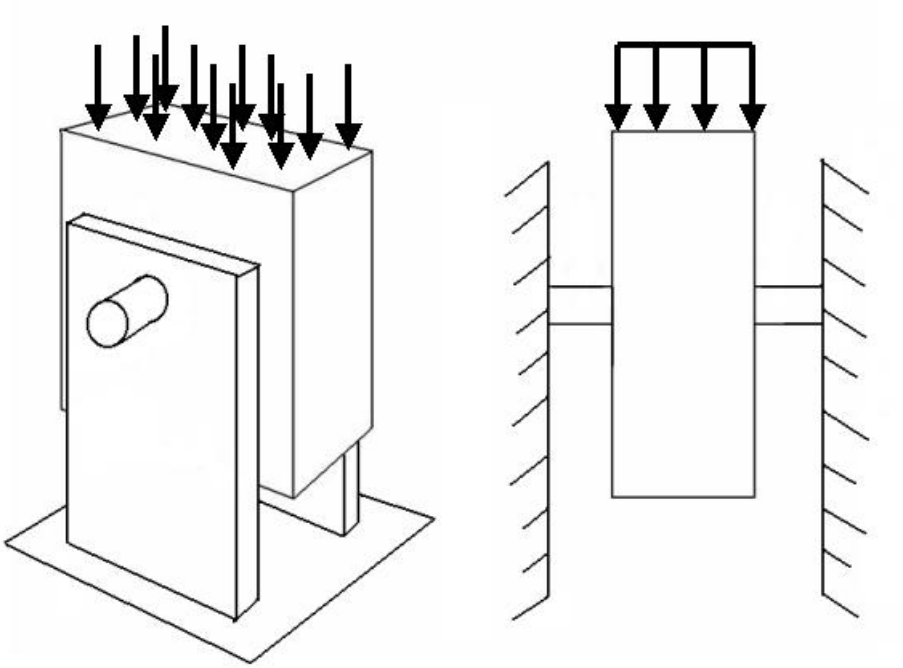

Figure 2.4: Illustration of Modified Full-Hole Setup Used by Anderson (2002) and Billings (2004)

Upon testing, both Anderson and Billings measured different average bearing strengths than those predicted by Equation 2.1. Two of the experimental averages are listed below in Table 2.2 along with the specific gravities and the bearing strengths predicted by Equation 2.1.

Table 2.2: Experimental vs. Predicted Bearing Strengths

	Wood Species	# of Tests	Listed SG	Average Measured SG	Average Experimental F_e	Predicted F_e (from Eqn. 2.1)
Anderson (2002)	Southern Yellow Pine	100	0.55	0.54	5634 psi	6048 psi
Billings (2004)	Mixed Southern Pine	50	0.51	0.25	4076 psi	2800 psi

Testing specimens of normal specific gravity at a load rate of 0.08 in./min (2.03 mm/min), Anderson measured bearing strengths whose average was 7% lower than the bearing strength predicted by the NDS equation. However, testing specimens of low specific gravity at the same load rate, Billings measured bearing strengths whose average was 46% higher than the bearing strength predicted by the NDS equation. These findings suggest that bearing strength does not always vary linearly with specific gravity. Instead, bearing strength may vary non-linearly with specific gravity, or it may depend on other factors as well. These factors could include the slope of grain in the specimen and the size of the specimen, among others. Whatever the factors, these findings indicate that the bearing strength used in the yield limit equations to predict connection behavior should be based on preliminary testing rather than Equation 2.1 whenever it is possible.

2.4 Bolt Bending

2.4.1 General

The bending yield strength (F_{yb}) of fasteners is another important component in Johansen's Yield Model and in the yield limit equations describing yield mode III and yield mode IV (see Table 2.1). However, despite its necessity in predicting yield modes, the bending yield strength of fasteners has been the subject of little study and is only lightly addressed by the NDS. This has led to questions regarding the accurate measurement of this property. Before discussing the measurement of bending yield strength in bolts, however, it is necessary to understand how processes used in the manufacture of bolts might affect their mechanical behavior.

2.4.2 Bolt Manufacture

Structural bolts tend to be made of steel, an alloy consisting primarily of iron and carbon (Young, et. al., 1998). The various grades of structural steel bolts are based on mechanical properties such as strength, hardness, and ductility. These mechanical properties are dependent on the presence and percentage of different elements in the steel alloy, and on the processes used to form and treat the bolts.

Steel has a maximum carbon content of approximately 2.0%, and structural steels typically have carbon contents around 0.3% (Young, et. al., 1998). Carbon is useful for adding strength to the alloy, but high-carbon alloys are also less ductile. Steel alloys used in bolt manufacture fall into two categories of carbon content. Lower grade bolts tend to feature low carbon contents of less than 0.25%, and are therefore low in strength and high in ductility. These low-carbon steel bolts are sometimes referred to as "mild"-carbon bolts. Higher grade bolts tend to feature medium carbon contents (0.25-0.60%), which result in higher strength and lower ductility (Fastenal, 2000). Some of the ductility lost with higher carbon contents can be added back after manufacture through various treatment processes. Other elements commonly added to steel alloys include manganese, chromium, nickel, and molybdenum (Young, et. al., 1998). Like carbon, these elements are added to increase strength.

Once the steel alloy has been formulated, it is ready to be manufactured into bolts. Most structural bolts are manufactured according to one of two methods: heat forging or cold forming (McBain, et. al., 1982). Both of these processes begin with long strands of steel which have been rolled into a round bar or wire. Smaller lengths, sufficient for forming individual bolts, are then cut off from the wire strand. These smaller lengths are referred to as "blanks" or "pins" (McBain, et. al., 1982). At this point the methods of manufacture diverge.

In heat forging, the end of the pin which will be shaped into the bolt head is heated. This end is then impacted by a circular "punch" in order to create a temporary cylindrical head, referred to as a "cheese" (McBain, et. al., 1982). A closed die is used to support the

opposite end of the pin during impact. Even with a pliable, heated steel pin, one impact is often insufficient, and two are needed to form the cheese without buckling the end of the pin (McBain, et. al., 1982). In these cases, the first impact is made by a cone-shaped punch, and the second is made by the circular punch. Next, the cheese is hot trimmed or "stripped" by another machine to form a hexagonal head (McBain, et. al., 1982). Finally, the threads are cut by rotating cutting dies.

In cold forming, a cheese is also formed through impact from punches. In this case, however, the impacted end of the pin is not heated. The formation of this unheated end requires more powerful blows from the punches, and, therefore, more energy than is used in heat forging (McBain, et. al., 1982). Following the formation of the cheese, the bolt is punched into an extrusion and trimming die like the one depicted below in Figure 2.5.

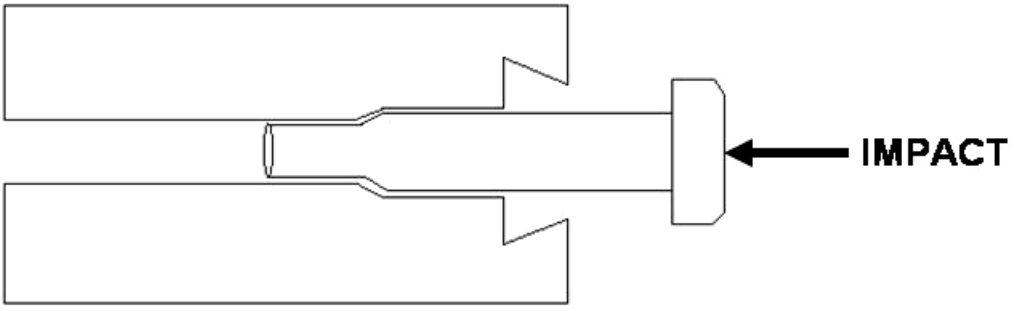

Figure 2.5: Illustration of Extrusion and Trimming Die (after McBain, et. al., 1982)

This die serves to trim the cheese into a hexagonal head and to straighten and shape the body into the desired dimensions. The cross-section of the body reduces as it is "extruded" into the die (McBain, et. al., 1982). This compressed cross-section undergoes strain hardening, and thereby increases in strength. Strain hardening, sometimes referred to as work hardening, is an increased resistance to plastic deformation caused by the high density of dislocations present in the compressed cross-section (Shackelford, 2000).

Finally, the threads are formed either by cutting or by thread rolling, a cold-working process.

Once the bolts are shaped, they are frequently treated in order to add strength by increasing resistance to yielding. Yielding occurs under stress and is enabled by the formation and movement of dislocations in the crystalline steel microstructure. Treatments designed to strengthen steel work by producing changes in microstructure that act to impede these dislocations (Young, et. al., 1998). The three primary methods used for adding strength to structural steels are (1) alloying, in which atoms are inserted or substituted into the microstructure, (2) strain hardening, which serves to generate networks of dislocations to limit the movement of other dislocations, and (3) heat treatment, which produces additional grain boundaries, necessary for blocking the movement of dislocations (Young, et. al., 1998).

Alloying takes place at the beginning of manufacture and involves the introduction of elements such as those described previously in this section. Strain hardening occurs through cold-working processes like the extrusion employed in the cold formation of bolts. Heat treatments involve the heating and cooling of solid state steel in order to obtain the desired mechanical properties. The temperature to which the steel is heated before the onset of cooling determines its final microstructure (Young, et. al., 1998). This temperature is carefully controlled, as it directly influences the final strength, hardness, and ductility of the steel.

Medium-carbon steel bolts are frequently heat treated. This, combined with the higher carbon content, serves to produce high strengths when compared to the low-carbon bolts, which cannot be heat-treated (Fastenal, 2000). Instead of heat treatment low-carbon bolts rely exclusively on alloying and the strain hardening associated with cold-working.

During their experimentation, both Anderson (2002) and Billings (2004) used low-carbon steel bolts exclusively in order to replicate the bolted wood connections typically encountered in the field. These included SAE J429 Grade 2 bolts and ASTM A 307A

bolts. Due to the factors described above, these bolts likely featured low yield strengths and high ductility.

2.4.3 Bolt Bending

The bending yield strength (F_{yb}) of fasteners is another important component in Johansen's Yield Model and in the yield limit equations describing yield mode III and yield mode IV (see Table 2.1). However, despite its necessity in predicting yield modes, the bending yield strength of fasteners has been the subject of little study and is only lightly addressed by the NDS. This has led to questions regarding the accurate measurement of this property.

Section 11.3.5 of the NDS states that the dowel bending yield strengths "shall be based on yield strength derived using methods provided in ASTM F 1575 or the tensile yield strength derived using procedures of ASTM F 606" (AF&PA, 2001). In addition, NDS Appendix I.4 describes each of these methods and explains when each should be used. NDS recommends using the three-point loading method, described ASTM F1575, except in the cases of "short, large diameter fasteners," for which "direct bending tests are impractical" (AF&PA, 2001). It is for these special cases, that NDS recommends using "test data from tension tests such as those specified in ASTM F606" (AF&PA, 2001). Making the link between tensile tests and bending yield strength, NDS Appendix I.4 goes on to state the following: "Research indicates that F_{yb} for bolts is approximately equivalent to the average of bolt tensile yield strength and bolt tensile ultimate strength," and that it normally falls between 48,000 psi and 140,000 psi for "various grades of SAE J429 bolts" (AF&PA, 2001). Despite this wide range, NDS recommends using 45,000 psi for "commonly available bolts" (AF&PA, 2001). While this value represents a conservative design parameter, research by Billings (2004) suggests that it complicates yield mode predictions. Accurate predictions depend on specific and accurate measurements of bending yield strength according to the testing procedures outlined in ASTM F 606 and ASTM F 1575.

2.4.4 Tensile Test

ASTM F 606 contains the Standard Test Methods for Determining the Mechanical Properties of Externally and Internally Threaded Fasteners, Washers, and Rivets. The tensile test procedure described in ASTM F 606 is the same one used to grade all ASTM bolts, and is similar to the test used for grading SAE J429 bolts. Both tests employ a threaded fixture similar to the one depicted in Figure 2.6 to apply a direct tensile force to the specimen. For structural bolts, ASTM recommends leaving at least four exposed threads.

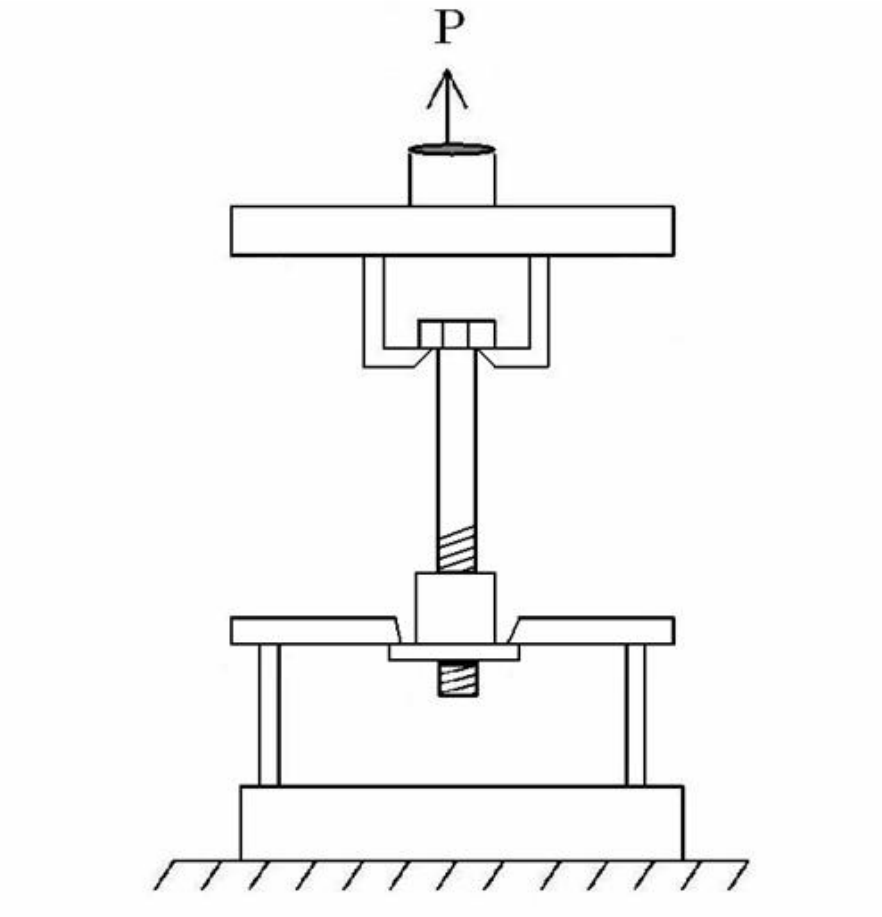

Figure 2.6: Threaded Tensile Test Fixture

After testing to failure, the yield load is normally determined using the offset method described in section 3.6.3.1 of ASTM F 606-02. This offset method is used to interpret results from various other ASTM material property tests and is described in detail in the next section. The tensile yield stress (F_y) is then equal to the yield load divided by the thread stress area (A_s) of the bolt, where A_s comes from Equation 2.2.

$$A_s = 0.7854 * [D - (0.9743)/n]^2 \quad (\text{in.}^2) \tag{2.2}$$

where: D = nominal bolt diameter (in.)
n = number of threads per inch

2.4.5 3-Point Bending Test

ASTM F 1575 contains the Standard Test Method for Determining the Bending Yield Moment of Nails. While this method applies specifically to nails, NDS section 11.3.5 indicates that it may also be used in the measurement of bolt bending yield strength. The method involves a three-point loading procedure, in which the load is applied at the midspan of the simply supported specimen (see Figure 2.7) at a rate less than or equal to 0.25 in./min (6.35 mm/min).

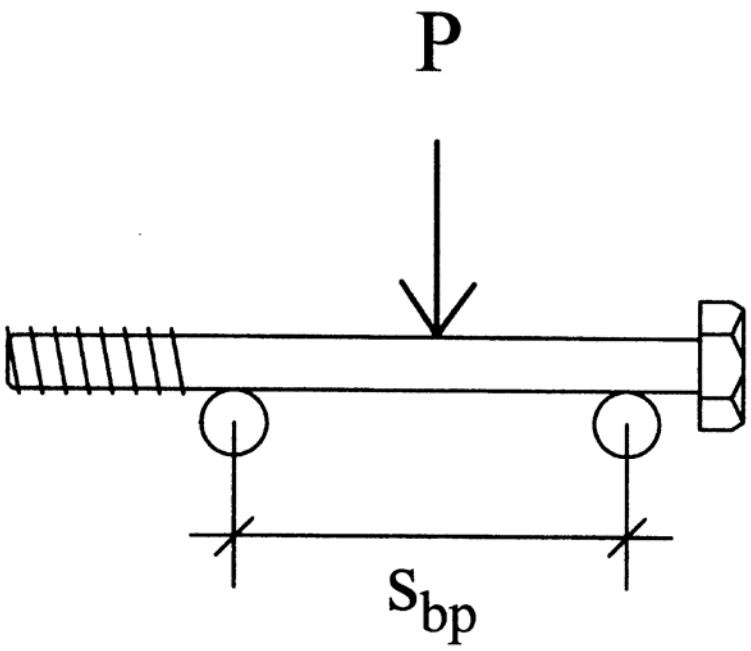

Figure 2.7: Schematic of 3-Point Loading Procedure

NDS Appendix I.4 states that the "fastener bending yield strength (Fyb) shall be determined by the 5% diameter (0.05D) offset method of analyzing load-displacement curves" (AF&PA, 2001). According to this method, the 5% offset yield load is determined by "fitting a straight line to the initial linear portion of the load-deformation curve, offsetting this line by a deformation equal to 5% of the [fastener] diameter, and selecting the load at which the offset line intersects the load-deformation curve" (Section 10.1 of ASTM F 1575-03). See Figure 2.8 below for details.

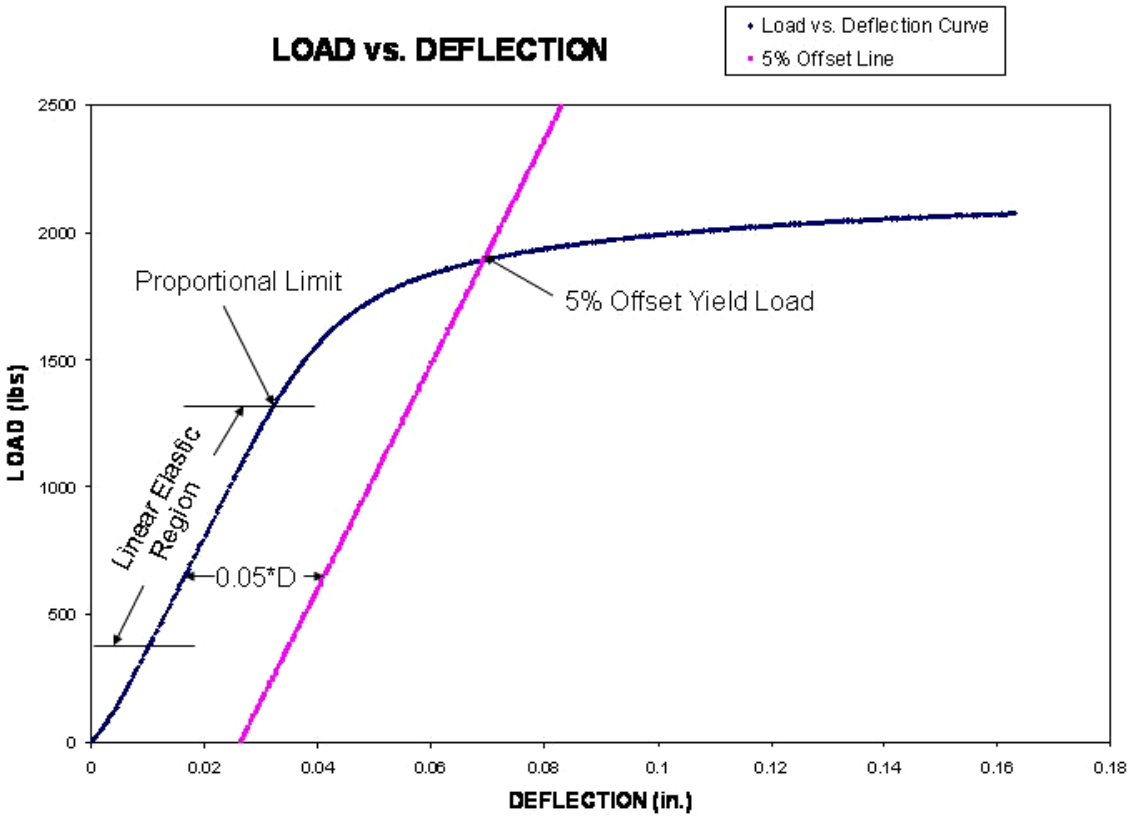

Figure 2.8: Load vs. Deflection Plot Illustrating 5% Offset Yield Load

Next, the 5% offset yield load is used in the following calculation to determine the bending yield moment (M_y):

$$M_y = \frac{P * s_{bp}}{4} \qquad (2.3)$$

where: s_{bp} = spacing between supports

P = 5% offset yield load

Finally, the bending yield stress (F_{yb}) is calculated using Equation 2.4:

$$F_{yb} = \frac{M_y}{S} \tag{2.4}$$

where: S = the section modulus = $\frac{D^3}{6}$

D = dowel diameter

According to F 1575-01, the spacing between the supports (s_{bp}) is taken to be 3.75-in. (9.53 cm) when the dowel diameter exceeds 0.25-in. (0.64 cm). However, for large diameter bolts this fixed spacing tends to produce small span-to-depth ratios, which could prevent pure bending by introducing shear effects. In 2003, the test method was changed to allow for longer spans equal to 11.5*D for D ≥ 0.190 in. (0.48 cm). This method has its own limitations, however, as bolts with large diameters cannot always bridge the recommended spacing. Aside from the ASTM spacing recommendation, Dodson (2003) cites testing conducted by the USDA Forest Products Laboratory, in which researchers introduced their own 5-in. (12.70 cm) spacing to test 1-in. (2.54 cm) diameter bolts. However, even this precedent is inapplicable in the cases of shorter bolts whose unthreaded lengths are less than 5-in. (12.70 cm).

2.4.6 Cantilever Bending Test

This issue was addressed by both Anderson (2001) and Billings (2004), as they each turned to a cantilever method to measure bending yield strength. The cantilever method features a cantilevered bolt inserted into a hole in the support fixture (see Figure 2.9). The load (P) is applied at a known distance (x) from the face of the support.

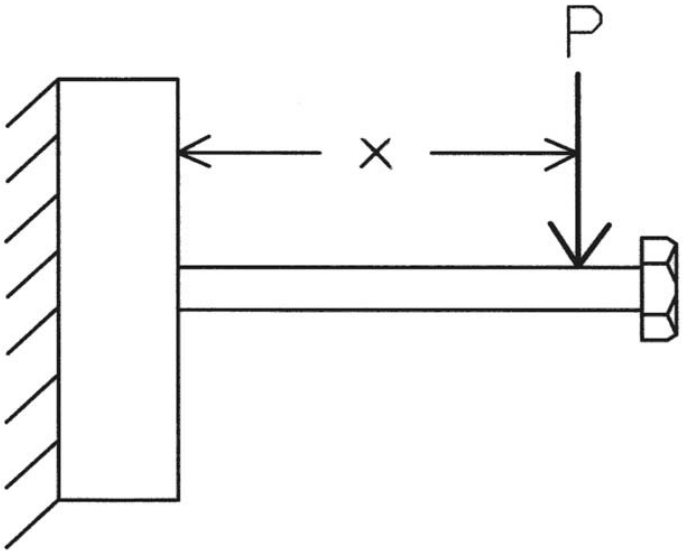

Figure 2.9: Schematic of Cantilever Loading Procedure

The bending yield strength (F_{yb}) again equals the bending yield moment (M_y) divided by the section modulus (S). This time, M_y comes from Equation 2.5:

$$M_y = P * x \tag{2.5}$$

where: P = 5% offset yield load

x = distance from the point of load application to the face of the support

Using the cantilever method, Billings measured bending yield strengths that greatly exceeded the yield strength recommended in NDS Appendix I.4. Her mean yield strengths for 3/8-in. (0.95 cm) diameter bolts and ½-in. (1.27 cm) diameter bolts were approximately 61,000 psi and 69,000 psi, respectively. Billings concluded that she had underestimated the bending yield strengths in her yield mode predictions by using the NDS recommended strength of 45,000 psi. This underestimate undoubtedly contributed to the predominance of the mode II behavior when modes III and IV were expected, and confirms the importance of using measured values of F_{yb} to predict yield behavior.

Chapter 3: Methods and Materials

3.1 Introduction

The behavior of bolted, single-shear wood connections is predicted by the yield limit equations described in Chapter 2. This project involved the isolation and examination of yield modes III and IV, in which the bolts bend prior to wood splitting failures. Two vital components in the yield limit equations are the dowel bearing strength of the wood and the bending yield strength of the bolts. Preliminary dowel bearing measurements were performed according to the procedure outlined in section 3.4.1, and the average values were used in the yield limit equations in order to verify that the designed connections would actually exhibit the desired yield modes (see also Appendix A). Bolt bending yield strength was more difficult to measure, however, for the reasons described in section 2.4. Thus, the three different test methods described in section 3.2 were performed on various sets of bolts for the sake of comparison between methods and in an effort to arrive at the most reliable approach for measuring bending yield strength. To make sure that the bolts would yield in the connection tests, the highest values for bending yield strength recorded during cantilever and three-point bend testing were used as input in the yield limit equations (see Appendix A). When the yield limit equations still predicted mode III and IV yielding, it was considered safe to proceed with testing.

Multiple-bolt, single-shear tests were performed on the connections whose designs were predicted by the yield limit equations to produce yield modes III and IV. A single row of five bolts was used in each configuration, and bolt spacings of 7D and 8D were tested under reverse-cyclic loading in search of a recommendable spacing. The reverse-cyclic loading pattern followed the CUREE testing protocol, detailed 3.3.7. This protocol required a deflection parameter measured through the preliminary monotonic testing described in section 3.3.6. The optimization of bolt spacing was based on the seven strength and serviceability criteria employed in previous testing by Billings (2004). These included maximum load, failure load, E.E.P. yield load, 5% offset load, elastic stiffness, E.E.P. energy, and ductility ratio. These values are defined in section 3.5.

3.2 Bolt Tests

3.2.1 General

Bolts of various sizes were tested using three different test methods in order to investigate the relationship between the tensile yield strength, the 3-point bending yield strength, and the cantilever bending yield strength. In addition, the maximum bending yield strengths of the 3/8”x6” and 3/8”x8” bolts were used to predict the yield mode behavior of the connections tested in the other phase of the project**.**

While all bolts were made of low-carbon steel, they did vary in length and diameter in order to make sure that a broad spectrum of common dimensions was considered. It was intended that ten samples of each bolt size be tested according to each test method. The intended schedule of bolt testing, including test methods, dimensions, and sample sizes for all bolt tests is shown in Table 3.1.

Table 3.1: Intended Schedule for Bolt Testing

Bolt Diameter (in.)	Bolt Length (in.)	Test Method	Number of Replications
3/8	4	Tensile	10
		3-Point Bend	10
		Cantilever	10
	6	Tensile	10
		3-Point Bend	10
		Cantilever	10
	8	Tensile	10
		3-Point Bend	10
		Cantilever	10
1/2	4	Tensile	10
		3-Point Bend	10
		Cantilever	10
	6	Tensile	10
		3-Point Bend	10
		Cantilever	10
	8	Tensile	10
		3-Point Bend	10
		Cantilever	10
3/4	4	Tensile	10
		3-Point Bend	10
		Cantilever	10
	6	Tensile	10
		3-Point Bend	10
		Cantilever	10
	8	Tensile	10
		3-Point Bend	10
		Cantilever	10

Various constraints surfaced during testing, however, and the schedule indicated in Table 3.1 was modified. While all ninety of the planned cantilever tests were performed, only eighty of the 3-point tests were performed due to the limited capacity of the load cell, which could not have accommodated the high loads expected from the ¾"x4" test set. In addition, all tensile testing was terminated when it was determined that the test method and available equipment were not sufficient for accurate measurements of tensile yield strength. Details of these findings are included in section 4.4, and a summary of all bolt tests actually performed is included below in Table 3.2.

Table 3.2: Actual Schedule for Bolt Testing

Bolt Diameter (in.)	Bolt Length (in.)	Test Method	Number of Replications Performed
3/8	4	3-Point Bend	10
		Cantilever	10
	6	3-Point Bend	10
		Cantilever	10
	8	3-Point Bend	10
		Cantilever	10
1/2	4	3-Point Bend	10
		Cantilever	10
	6	3-Point Bend	10
		Cantilever	10
	8	3-Point Bend	10
		Cantilever	10
3/4	4	3-Point Bend	---
		Cantilever	10
	6	3-Point Bend	10
		Cantilever	10
	8	3-Point Bend	10
		Cantilever	10

3.2.2 Materials

Various sizes of low-carbon steel, hex-head bolts were tested. These included both ASTM A 307A and SAE J429 Grade 2 bolt types, as well as bolts from multiple manufacturers. The minimum tensile yield strength is listed as 74,000 psi for the SAE bolts and 60,000 psi for the ASTM bolts. During testing it was determined that the yield strength of the bolts was also slightly influenced by the bolt manufacturer. Thus, the bolt type and manufacturer were kept constant between test methods for a particular specimen size. For example, every ½"x6" bolt tested for all three test methods was an SAE J429 Grade 2 bolt, and featured a manufacturer's stamp that read "HKT." The bolt types and manufacturer's markings for each specimen size are included in Table 3.3.

Table 3.3: Bolt Types and Manufacturer's Markings

Specimen Size	Bolt Type	Manufacturer's Marking
3/8"x4"	SAE J429 Grade 2	BL
3/8"x6"	SAE J429 Grade 2	HKT
3/8"x8"	SAE J429 Grade 2	BL
1/2"x4"	SAE J429 Grade 2	HKT
1/2"x6"	SAE J429 Grade 2	HKT
1/2"x8"	SAE J429 Grade 2	HKT
3/4"x4"	ASTM A 307A	QB
3/4"x6"	SAE J429 Grade 2	HKT
3/4"x8"	ASTM A 307A	CYI

In addition, flat washers and hex-head nuts were used in the tensile tests. The washers and nuts were made of zinc-plated steel and were pre-packaged in sets of 25 according to the size of the bolt they were made to fit. The 3/8-in. (0.95 cm) diameter nuts were made to fit a 3/8-in. (0.95 cm) diameter bolt with 16 threads per inch. The ½-in. (1.27 cm) diameter nuts were made to fit a ½-in. (1.27 cm) diameter bolt with 13 threads per inch. The ¾-in. (1.91 cm) diameter nuts were made to fix a ¾-in. (1.91 cm) diameter bolt with 10 threads per inch.

3.2.3 Sample Size Determination

The sample size of ten replications was determined using the following equation (Heine, 2001):

$$n = \frac{2 * Z_{\alpha/2}^2 * COV^2}{e^2} \tag{3.1}$$

where: COV=σ/mean

e=Δ/mean

COV=coefficient of variance, unitless

σ=the standard deviation, same unit as mean

mean=population mean, any unit

e=the relative error, %

Δ=the absolute error, same unit as mean

$Z_{\alpha/2}$=the area under the curve associated with a 100(1-α)% confidence interval

The coefficient of variance was taken to be 13.67 percent, the average COV value recorded by Billings (2004) during her bolt bending tests. $Z_{\alpha/2}$ equals 1.645 for a 90 percent confidence level. Thus, a sample size of ten assures with 90 percent confidence that the estimated mean is within 10 percent of the true mean.

3.2.4 Specimen Identification

All of the bolts tested are classified by a combination of four identifiers. The first identifier is a letter denoting the bolt diameter. Three-**E**ighths inch diameters are represented by the letter "E." One-**H**alf inch diameters are represented by the letter "H." Three-**F**ourths inch diameters are represented by the letter "F." The second identifier is a number denoting the bolt length in inches. The third identifier is a letter indicating the test method used. Tensile tests are represented by the letter "t." 3-point bending tests involve simply-supported specimens and are thereby represented by the letter "s." Cantilever tests are represented by the letter "c." The fourth and final identifier is the specimen's number within its sample set. This number will range from 1 to 10, as ten specimens were tested from each sample set. As an example, the bolt identified as E4c7 has a 3/8-inch diameter, is four inches long, was tested according to the cantilever method, and represents the seventh bolt tested in its sample set.

3.2.5 Tensile Tests

Tensile tests were based on the standard test methods published by ASTM and by the Society of Automotive Engineers (SAE). The first standard is contained in ASTM F 606-02, Standard Test Methods for Determining the Mechanical Properties of Externally and Internally Threaded Fasteners, Washers, Rivets (ASTM, 2003a). The second standard is contained in the SAE standards for SAE J429 bolts (SAE, 1999). One deviation from

these standard methods was related to the test fixture. Instead of using a threaded fixture like the one depicted in Figure 2.6, an assembly featuring nuts and washers was employed. The tensile test setup is shown in Figure 3.1.

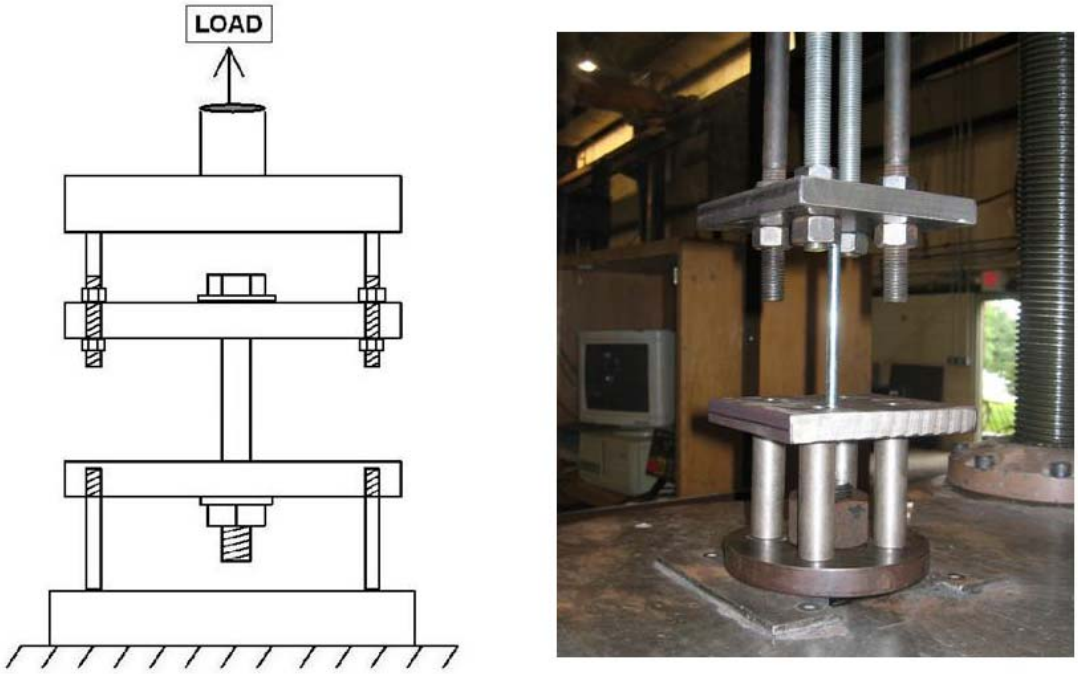

Figure 3.1: Diagram and Photograph of Tensile Test Setup

It was intended that the elongation of the bolts be measured using an extensometer, and that the yield point would be determined by the 5% offset method described in section 2.4.5. However, elongation proved difficult to measure and tension testing was subsequently aborted. For a discussion of the initial tension tests and the problems associated with measuring elongation see section 4.4.2.

3.2.6 3-Point Bending Tests

Three-point bending tests followed the ASTM F 1575-03 Standard Test Method for Determining Bending Yield Moment of Nails. The load (P) was applied at midspan ($s_{bp}/2$) of the simply supported specimen depicted in Figure 3.2. The threaded portion of the bolt was excluded from all tests.

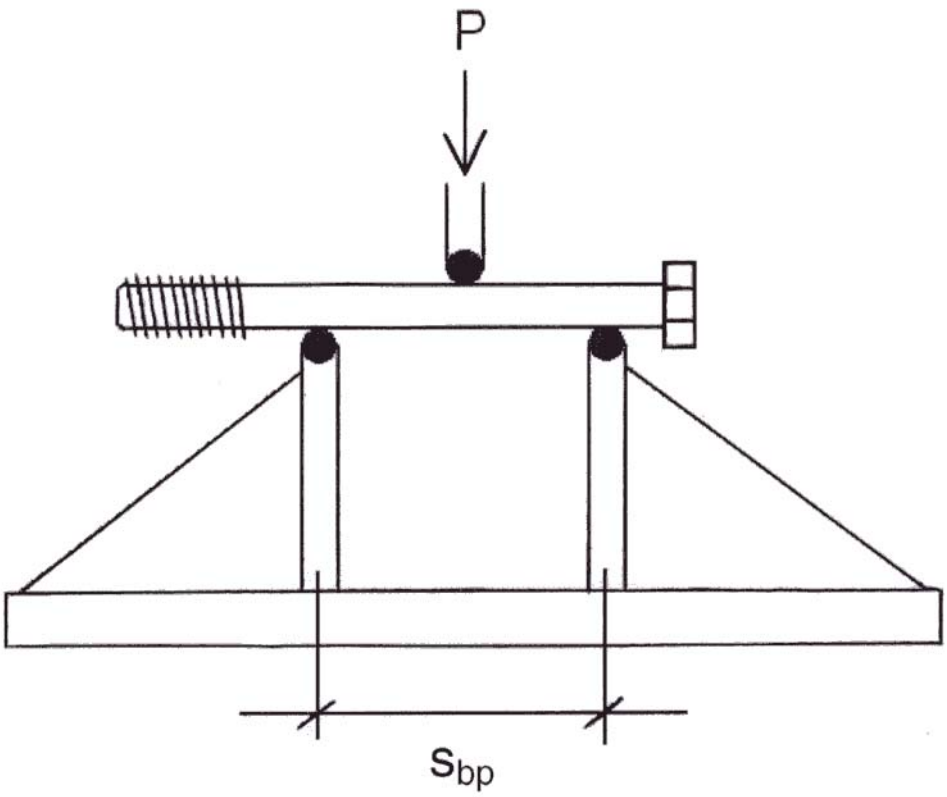

Figure 3.2: Schematic of 3-Point Test Fixture

Both supports featured welded steel angles for improved stability, and could slide toward or away from each other in order to accommodate various spans. Both the supports and the loading head featured 3/8-in. (0.95 cm) diameter, grade 8 bolts at the points of contact with the test specimens. These high-strength bolts were used in order to ensure that the test specimens were the only components deflecting. During testing, the supports were tightly bolted to the steel base-plate, and the base-plate was bolted to the surface of the testing machine in order to prevent lateral translation of the fixture. The load was applied at a rate of 0.1 in./min (2.54 mm/min) by an MTS testing machine. The machine used a 10,000 pound load cell. See Figure 3.3 for details of the 3-point test setup.

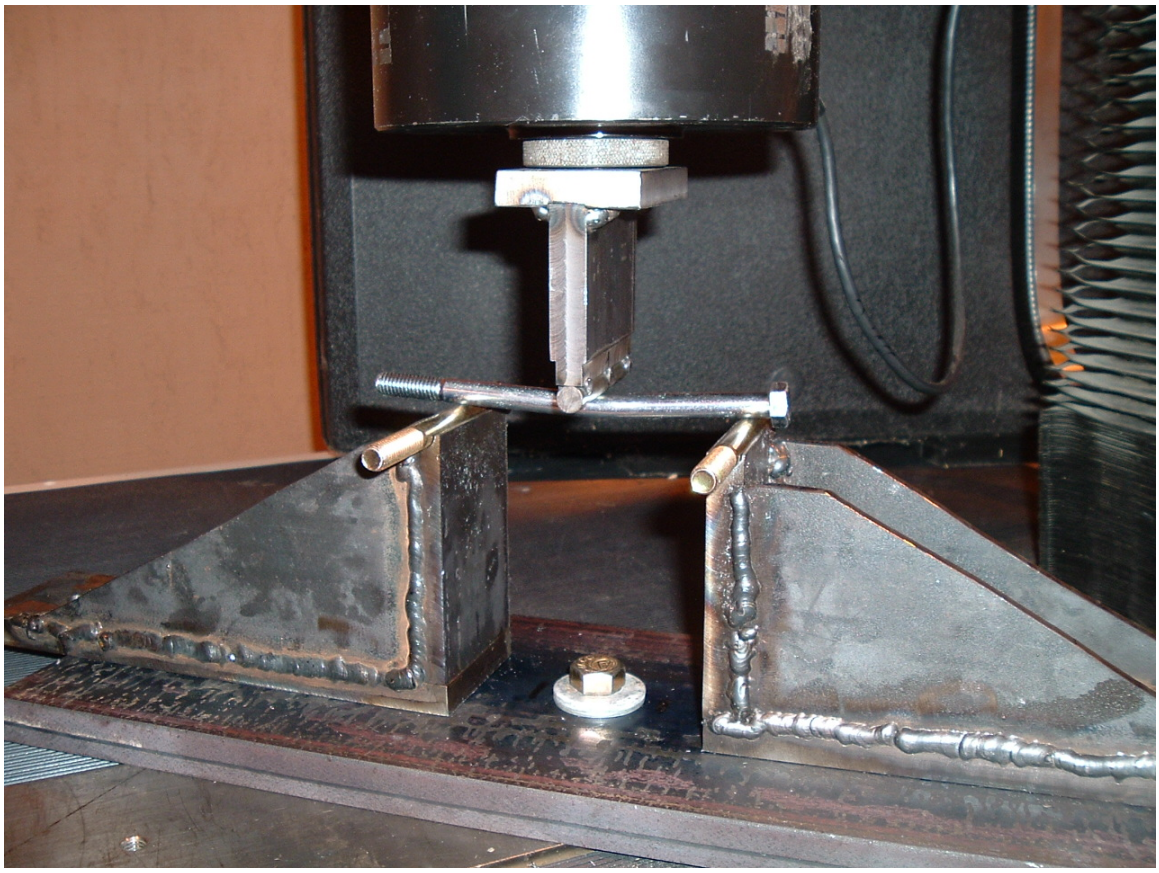

Figure 3.3: 3-Point Test Setup

The span lengths (s_{bp}) were taken from a formula included in Table 1 of ASTM F 1575-03. For dowels of diameter larger than 0.190-in. (0.48 cm), ASTM recommends a span of 11.5 times the dowel diameter rounded to the nearest tenth of an inch. This resulted in recommended spans of 4.3-in. (10.92 cm) for 3/8-in. (0.95 cm) diameter bolts, 5.8-in. (14.73 cm) for ½-in. (1.27 cm) diameter bolts, and 8.6-in. (21.84 cm) for ¾-in. (1.91 cm) diameter bolts. In some cases these recommended spans were longer than the specimens themselves. In these cases the span was set as long as possible, with the threads of each specimen still being excluded. Table 3.4 contains the experimental span lengths (s_{bp}) for each specimen diameter (D) and length (L). The ¾"x4" specimens were not subjected to

this test, as the yield load would have exceeded the maximum load of 10,000 pounds allowed by the load cell.

Table 3.4: Span Lengths for 3-Point Bend Tests

D (in.)	L (in.)	s_{bp} (in.)
3/8	4	2.25
3/8	6	4.30
3/8	8	4.30
1/2	4	2.25
1/2	6	4.00
1/2	8	5.80
3/4	4	N.A.
3/4	6	3.50
3/4	8	5.00

The bending yield load (P) was taken at an offset equal to 5% of the bolt diameter according to section 10.1 of ASTM F 1575-03. This load was then multiplied by s_{pb} and divided by 4 to determine the bending yield moment (M_y). Finally, M_y was divided by the section modulus (S) to determined the bending yield stress (F_{yb}). These calculations are described in detail in section 2.4.5 of chapter 2.

3.2.7 Cantilever Bending Tests

Cantilever bending tests were conducted in accordance with similar tests performed by Billings (2004). For these tests a point load was applied to a cantilevered bolt at a specified distance (x) from the face of the support fixture (see Figure 3.4). The bolts fit tightly in the fixture and the threads were excluded from all tests.

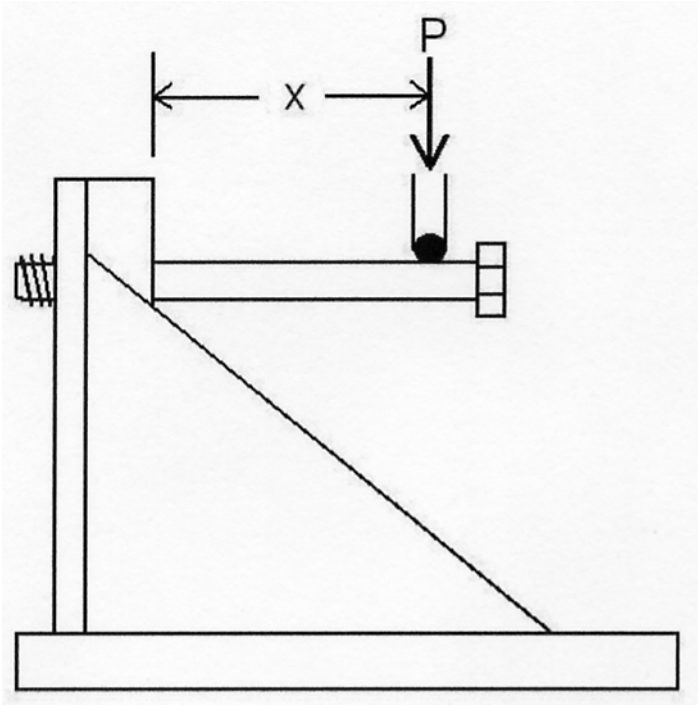

Figure 3.4: Schematic of Cantilever Test Fixture

The fixed elements of the support included a vertical, steel rear-plate welded to a steel base-plate, and two steel angles welded between the rear-plate and base-plate for added stability. The rear-plate featured a 1-in. (2.54 cm) diameter hole designed to allow bolts of all diameters to pass through. This feature allowed for the threaded portions of the bolts to be placed well away from the bearing point. Additional sets of vertical plates featuring holes cut to the same diameters as the test specimens were bolted to the fixed rear-plate during testing. These sets of plates provided the fixity required for the cantilever setup, as the bolts fit snuggly into their respective sets. The ability to exchange these plates enabled testing of all three specimen diameters without a need for three entirely separate fixtures. During testing the base-plate of the fixture was bolted to the surface of the testing machine in order to prevent lateral translations and to keep the fixture from rocking. In addition, dial gauges were employed at various times and locations during testing in order to verify that the fixture did not move. The load was applied at a rate of 0.1 in./min (2.54 mm/min) by an MTS testing machine. The machine

used a 10,000 pound load cell. See Figure 3.5 for a detailed photograph of the cantilever test setup.

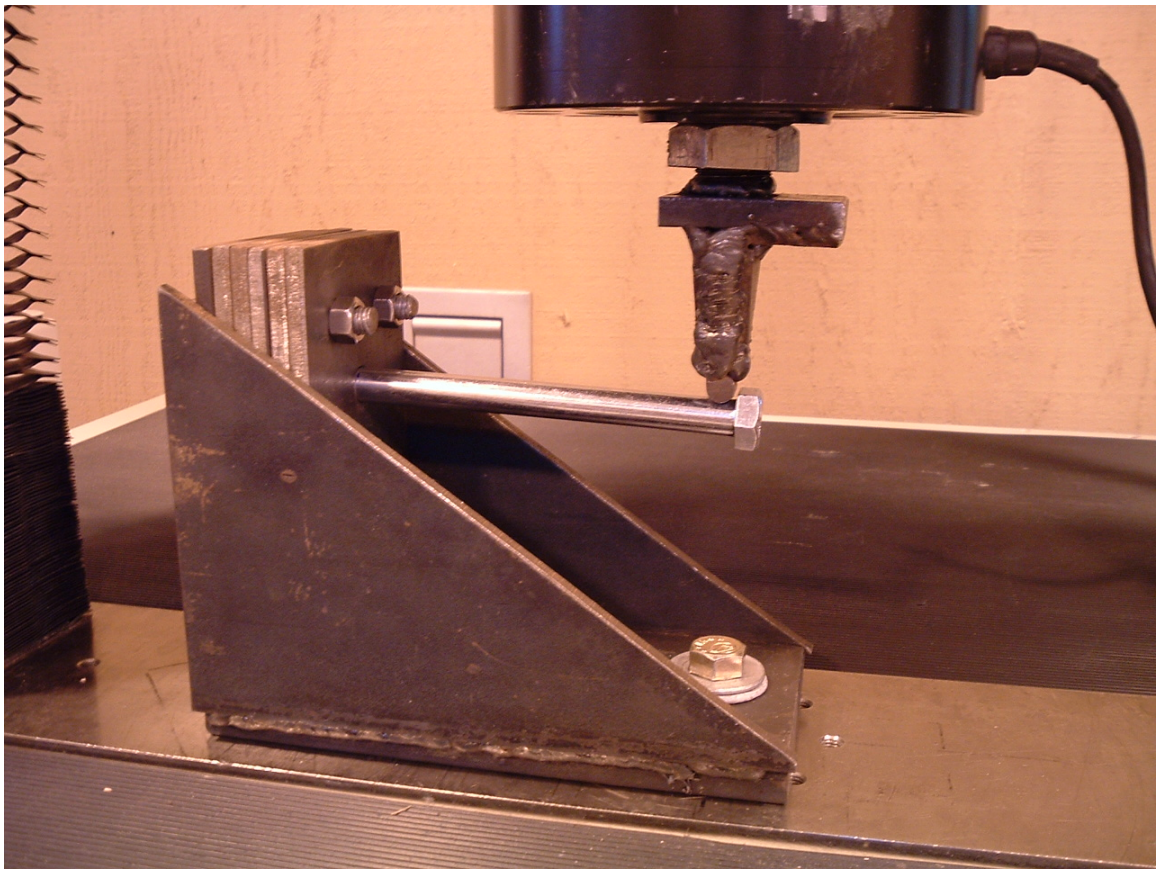

Figure 3.5: Cantilever Test Setup

The distance (x) from the point of load application to the face of the support was influenced by the length of the specimen being tested. The specimens were inserted into the plates such that the threads were roughly ½-in. (1.27 cm) or more beyond the face of the support. The load was then applied near the end of the specimen's shaft (see Figure 3.5) in order to maximize the span-to-depth ratio and limit shear effects. Table 3.5 contains the experimental moment arms (x) for each specimen diameter (D) and length (L).

Table 3.5: Moment Arms for Cantilever Tests

D (in.)	L (in.)	x (in.)
3/8	4	2.00
3/8	6	3.50
3/8	8	5.00
1/2	4	2.00
1/2	6	3.50
1/2	8	5.00
3/4	4	1.25
3/4	6	3.00
3/4	8	4.00

The bending yield load (P) was taken at an offset equal to 5% of the bolt diameter. This load was then multiplied by the moment arm (x) to determine the bending yield moment (M_y). Finally, M_y was divided by the section modulus (S) to determined the bending yield stress (F_{yb}). These calculations are described in detail in section 2.4.6 of chapter 2.

3.3 Connection Tests

3.3.1 General

Multiple-bolt, single-shear wood connections subject to yield modes III and IV were tested parallel to grain under monotonic and reverse-cyclic loading to determine a recommendable between-bolt spacing. Tested connections featured a single shear plane and five bolts spaced at two different distances: seven times the bolt diameter (7D), and eight times the bolt diameter (8D). The 4D spacing recommended by NDS was previously tested by Anderson (2002) and resulted in early splitting failures. In addition, spacings of 3D, 5D, and 6D were tested and ruled out by Billings (2004) due to early splitting failures. Billings showed that 7D and 8D spacings consistently outperformed

the smaller spacings for each of her three connection designs, and concluded that the 7D spacing was best for connections subject to mode II yielding.

The connections in this project were designed using the yield limit equations found in section 11.3.1 of the NDS (see also Table 2.1), and were designed to yield according to modes III and IV, which were not covered by Billings' conclusions. Yield mode III is characterized by bolt bending at one plastic hinge location, while yield mode IV is characterized by bolt bending at two plastic hinge locations. See Figure 2.1 for a visual representation of these yield modes. The connections designed to display mode III yielding were comprised of a 4x6 main member, a 2x6 side member, and five 3/8"x6" bolts. The connections designed to display mode IV yielding were comprised of a 4x6 main member, a 4x6 side member, and five 3/8"x8" bolts. See Appendix A for the preliminary yield mode analysis that influenced these designs.

Three connections of each sample set were tested under monotonic loading prior to the reverse-cyclic loading. Deflection data from the monotonic tests were used to determine the loading pattern of the reverse-cyclic tests. The reverse-cyclic loading pattern adhered to the CUREE test protocol described in section 3.3.7. Ten connections of each sample set were tested under reverse-cyclic loading. See Table 3.6 for a detailed listing of the proposed member layouts, test methods, and sample sizes.

Table 3.6: Summary of Connection Testing

Expected Yield Mode	Bolt Diameter	Bolt Length	Design Components	Number of Rows	Bolts Per Row	Loading Method	Number of Replications	Bolt Spacing
III	3/8-in.	6-in.	2x6 Side Member	1	5	Monotonic	3	7D 8D
			4x6 Main Member			Cyclic	10	7D 8D
IV	3/8-in.	8-in.	4x6 Side Member	1	5	Monotonic	3	7D 8D
			4x6 Main Member			Cyclic	10	7D 8D

3.3.2 Materials

All wood members used in the connection testing were Southern pine, and were equilibrated to approximately 12% moisture content in a conditioning room for 2.5 to 3 months prior to testing. All 2x6 members were Grade 2 Southern Yellow Pine, with a published specific gravity of 0.55 (AF&PA, 2001). All 4x6 members were Grade 2 Mixed Southern Pine, with a published specific gravity of 0.51 (AF&PA, 2001). All of the wood members were cut from lumber donated by Morgan Lumber Company of Red Oak Virginia and Amelia Lumber Company of Amelia Virginia. Efforts were made to exclude as many knots and other imperfections from the tested members as possible. Grade stamps from wood members of both sizes are shown in Figures 3.6 and 3.7.

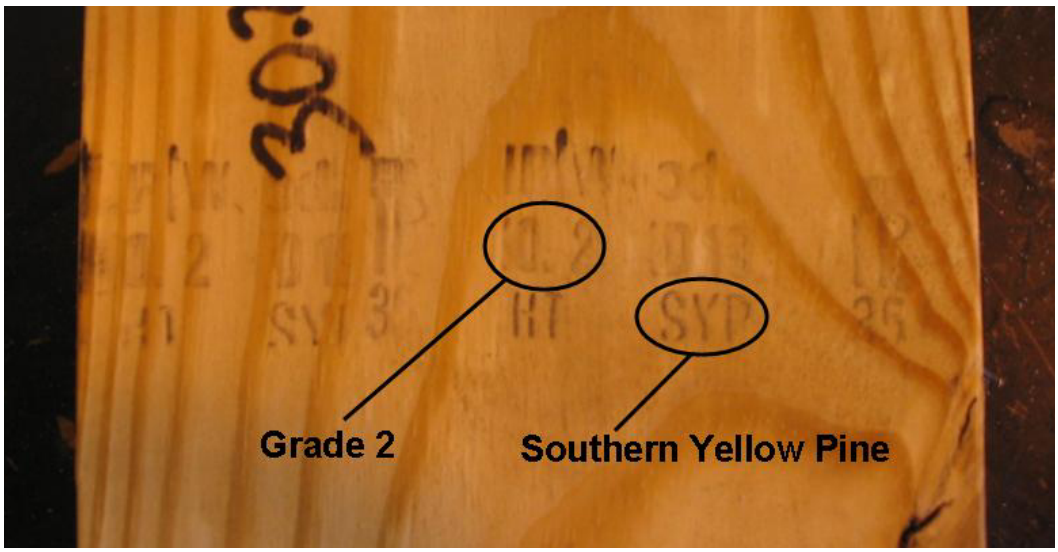

Figure 3.6: Grade Stamp from 2x6 Member

Figure 3.7: Grade Stamp from 4x6 Member

All bolts used in the connection tests were low-carbon steel, hex-head bolts. These included both ASTM A 307A and SAE J429 Grade 2 bolts. Bolt types and manufacturers were homogeneous within individual connection specimens, but were occasionally mixed between specimens in a sample set. This was necessary because it was difficult to obtain enough bolts at a particular size from the same manufacturer without having ordered them all at the same time. The bolt type and manufacturer was recorded for each specimen in case differences in connection behavior resulted.

3.3.3 Sample Size Determination

The sample size of ten replications for the cyclic loading tests was taken from Heine (2001), and was determined using Equation 3.1 from section 3.2.3. Using a sample COV of 16.4 percent based on single-bolt, single-shear tests by Gutshall, Heine determined that

a sample size of ten assures with 90 percent confidence that the estimated mean is within 12 percent of the true mean (Heine, 2001).

3.3.4 Specimen Identification

All of the connection tests are classified by a combination of four identifiers. The first identifier is a number denoting the expected yield mode. The second identifier is a number denoting the bolt spacing in inches. In this case the number "7" represents a spacing equal to seven times the bolt diameter (7D), and the number "8" represents a spacing equal to eight times the bolt diameter (8D). The third identifier is a letter indicating the test method used. Monotonic tests are represented by the letter "m." Reverse-cyclic tests are represented by the letter "c." The fourth and final identifier is the specimen's number within its sample set. This number will range from 1 to 10, as ten specimens were tested from each sample set. As an example, the connection identified as 47c2 is expected to yield according to yield mode IV, has a 7D bolt spacing, was tested according to the reverse-cyclic method, and represents the second connection tested in its sample set.

In addition, dowel bearing strength, moisture content, and specific gravity were measured for each member of each connection. This demanded that both members of every connection be distinguished from each other with a fifth identifier. This identifier was a letter representing each member's position in the connection. Side members were loaded into the top fixture of the test setup, and were therefore distinguished with the letter "t." Main members were loaded into the bottom fixture and were distinguished with the letter "b." For example, the member identified as 47c2t was the side member of the connection described in the previous paragraph.

3.3.5 Connection Layout and Fixture Details

The connection layout is illustrated in Figure 3.8. The term "connection bolts" was given to the five bolts used to connect the wood members to each other. These 3/8-in. (0.95 cm) diameter bolts were always aligned vertically in a single-row. The connection bolt

holes were oversized by 1/16-in. (0.16 cm) and were pre-drilled on a drill press using a 7/16-in. (1.11 cm) drill bit.

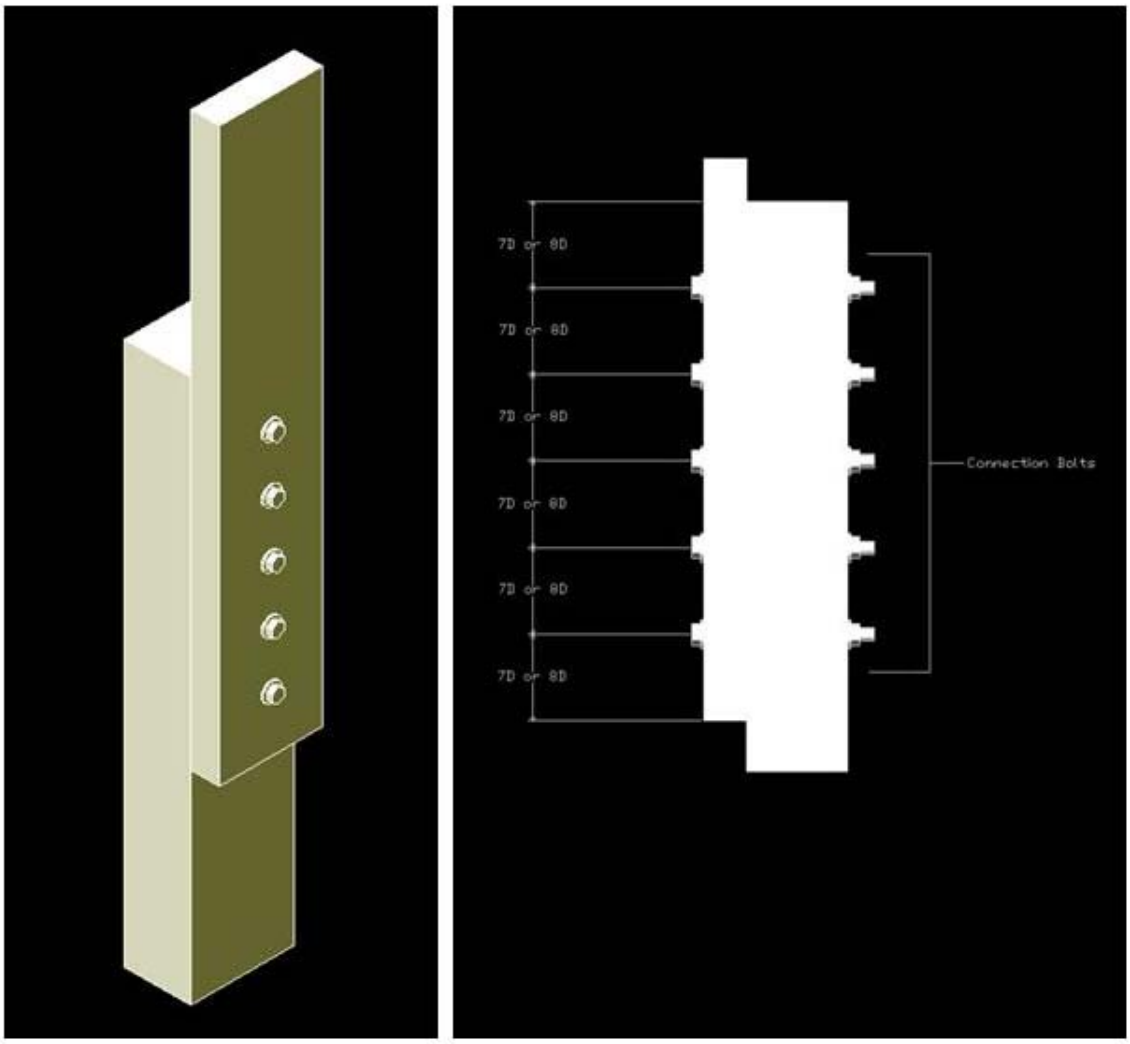

Figure 3.8: Connection Layout

The term "fixture bolts" was given to the bolts that connected the wood members to the top and bottom fixtures. These fixture connections were vital to holding the test specimens in place. Most of the fixtures employed were the same as those used by

Billings (2004). The bracing system differed slightly, but performed the same function as the one she used. Photographs of the fixture assembly are shown below in Figure 3.9.

Figure 3.9: Connection Test Setup

The bottom fixture consisted of two sides. Each side consisted of a welded steel right angle and two steel stiffening elements between the legs of the angles. Each bottom leg was 10-in. (25.40 cm) long by 12-in. (30.48 cm) wide by 1-in. (2.54 cm) thick. The vertical legs were 10.75-in. (27.31 cm) high, 12-in. (30.48 cm) wide, and ½-in. (1.27 cm) thick. The bottom legs featured slotted holes at 10-in. (25.40 cm) on-center for attachment to the testing apparatus and were able to slide to accommodate main members of varying thickness. Five staggered fixture bolts were used to secure the test specimens in the fixture. These bolts were all ¾-in. (1.91 cm) diameter, SAE J429 Grade 8 bolts. Potentiometers were attached to both sides of the bottom fixture and were used to measure the deflections of each wood member. While the deflection measurements for the side members were critical for analyzing the data, the deflection measurements for the

main members were taken in order to verify that they did not move significantly during testing. A photograph of the bottom fixture is included as Figure 3.10.

Figure 3.10: Bottom Fixture and Potentiometer

The top fixture featured two angled sides fixed to a top plate. The steel angles were oriented with their long legs back to back and featured two steel stiffeners between the legs. The top legs were 5-in. (12.70 cm) long, 12-in. (30.48 cm) wide, and ½-in. (1.27 cm) thick, and featured slotted holes for ¾-in. (1.91 cm) diameter bolts. The slotted holes allowed the angles to slide, enabling the wood members to be installed or removed easily. The vertical legs were 10.25-in. (26.04 cm) high, 12-in. (30.48 cm) wide, and 1.25-in. (3.18 cm) thick. One of the two vertical legs featured two ¾-in. (1.91 cm) diameter,

threaded holes on either side used to accommodate the ¾-in. (1.91 cm) diameter bolts in the side bracing system described below. The top plate measured 10.125-in. by 12.125-in. by 2-in. (25.72 cm by 30.80 cm by 5.08 cm) for the mode III tests, and 12.25-in. by 13.25-in. by 2-in. (31.11 cm by 33.66 cm by 5.08 cm) for the mode IV tests. The top plate for the mode III tests featured threaded holes spaced 6.5-in. (16.51 cm) apart. This spacing enabled the top fixture to accommodate the 2x6 side members. The top plate for the mode IV tests featured threaded holes spaced 8-in. (20.32 cm) apart. This spacing enabled the top fixture to accommodate the 4x6 side members. Both plates featured a threaded 1.5-in. (3.81 cm) diameter hole for the connection to the load cell. Five staggered fixture bolts were used to secure the test specimens. These bolts were all ¾-in. (1.91 cm) diameter, SAE J429 Grade 8 bolts. A photograph of the top fixture is included as Figure 3.11.

Figure 3.11: Top Fixture

The side bracing system was employed to limit the moment placed on the load cell by any joint eccentricities. The bracing system consisted of two welded steel braces. Each brace was comprised of a ¾-in. (1.91 cm) thick steel base-plate and two L5x5x3/4 angles featuring slotted holes in the vertical legs. The slotted holes were greased in order to limit the effects of friction. Two ¾-in. (1.91 cm) diameter bolts ran through the slotted hole of each side brace and into the top fixture. These bolts transferred the moment caused by joint eccentricities and acted to keep the loading head and top fixture level. Photographs of the bracing system are shown below in Figure 3.12.

Figure 3.12: Side Bracing System

Loads were applied by an MTS testing machine at the Brooks Forest Products Laboratory at Virginia Tech. The machine was equipped with a 50,000 pound load cell and was

capable of applying loads in both vertical directions. The specifics of the loading procedures are described in sections 3.3.6 and 3.3.7.

3.3.6 Monotonic Tests

Three monotonic tests were performed for each of the four data sets (see Table 3.6). Having been predrilled for the connection bolts, the specimens were loaded into the fixtures described in section 3.3.6. Side members were loaded into the top fixture and main members were loaded into the bottom fixture. For monotonic specimens expected to yield according to mode III, a strip of Teflon was included between the members to limit friction during testing. Monotonic tests for the mode IV specimens had already been performed when this feature was first introduced. All of the reverse-cyclic tests described in the next section featured the Teflon strip as well.

Next, the main and side members were temporarily connected by running two extra 3/8-in. (0.95 cm) diameter bolts through a couple of the predrilled connection holes. The members were then clamped together and positioned such that their centerlines matched up with the centerlines of the fixtures. The specimens were also checked to make sure they were level vertically. These steps helped to ensure that the load was applied parallel to grain and along the bolt-lines of the specimens.

Once they were positioned, the specimens were fastened to the top and bottom fixtures. The top fixture was clamped tightly to the wood side member, and an electric drill with a ¾-in. (1.91 cm) diameter bit was used to drill the five bolt holes required by the fixture bolts. Once the five Grade 8 bolts (described in section 3.3.5) were inserted in the top fixture, the bottom fixture was drilled and bolted in the same manner. Lock washers and nuts were then added to the threaded ends of the fixture bolts. These nuts were tightened using a pneumatic air wrench.

Next, the potentiometers described in section 3.3.5 were set up on each side of the specimen. Finally, the preliminary bolts that were inserted into the connection prior to drilling were removed, and five 3/8-in. (0.95 cm) diameter test bolts with flat washers

were inserted into the connection. Washers and nuts were added to the threaded ends of the test bolts, and they were tightened manually. Manual tightening was employed to replicate field installation. Connection bolts were then labeled "a" through "e," with bolt "a" at the bottom of the row, and bolt "e" at the top. Labeling was useful for examining the bolts after testing. This step concluded the installation of each specimen.

With the specimens in place, the monotonic load was applied by the MTS testing machine described in section 3.3.5. The load was applied in tension at a rate of 0.0714 in./min (1.81 mm/min). This was the same load rate employed by Anderson (2002) and Billings (2004) in order to satisfy the conditions of ASTM D 1761-88 (2000)e1, *Standard Test Methods for Mechanical Fasteners in Wood* (ASTM, 2003). Section 28.4 of this test standard specifies that maximum loads should occur between 5 and 20 minutes into the test. Tests were run until the load dropped below 80% of the maximum load.

Data pertaining to the mode III connections were recorded every 0.08 seconds by a data acquisition system, while mode IV data were recorded every 1.0 seconds. These data were then compiled into load versus deflection plots. The deflection at which the load first dropped below 80% of the maximum load was calculated for each specimen. These deflections were then averaged for each monotonic sample set. The resulting averages represented monotonic deformation capacities (Δ_m), described in the CUREE protocol and detailed in the next section (Krawinkler, et. al., 2001).

3.3.7 Reverse-Cyclic Tests

Ten reverse-cyclic tests were performed for each of the four data sets (see Table 3.6). All reverse-cyclic specimens were loaded into the test fixture and prepared for testing in the same way that the monotonic specimens had been loaded and prepared. This procedure is described in the previous section.

With the specimens in place, a reverse-cyclic loading pattern was applied by the MTS testing machine described in section 3.3.5. The load was applied at a rate of 4.724 in./min (119.99 mm/min). This load rate matched the rate employed by Anderson (2002)

and Billings (2004). Data were recorded every 0.08 seconds by a data acquisition system.

The loading pattern was deflection-controlled and employed the deflection parameters outlined in the CUREE test protocol for reverse-cyclic loading (Krawinkler, et. al., 2001). The CUREE protocol begins with a reference deformation (Δ). This reference deformation is a fraction of the monotonic deformation capacity (Δ_m), and is dependent on deflections revealed through prior monotonic testing (see section 3.3.6). CUREE recommends the following value for the reference deformation: $\Delta = 0.6*\Delta_m$ (Krawinkler, et. al., 2001).

Once Δ was calculated, it was used as a reference in determining the magnitudes of the deflection cycles. The CUREE protocol involves three types of cycles: initiation cycles, primary cycles, and trailing cycles. Initiation cycles are executed at the beginning of the loading history, and "serve to check loading equipment, measurement devices, and the force-deformation response at small amplitudes" (Krawinkler, et. al., 2001). Primary cycles are cycles whose amplitude is greater than any preceding cycle. Trailing cycles follow primary cycles, and their amplitudes are equal to 0.75 times the amplitude of the preceding primary cycle. All cycles are symmetric, featuring both a positive and a negative amplitude. For the experimental tests, the positive deflections corresponded with tensile forces caused by raising the loading head, and the negative deflections corresponded with compression forces caused by lowering the loading head. A typical CUREE loading pattern illustrating the three types of cycles is included below in Figure 3.13.

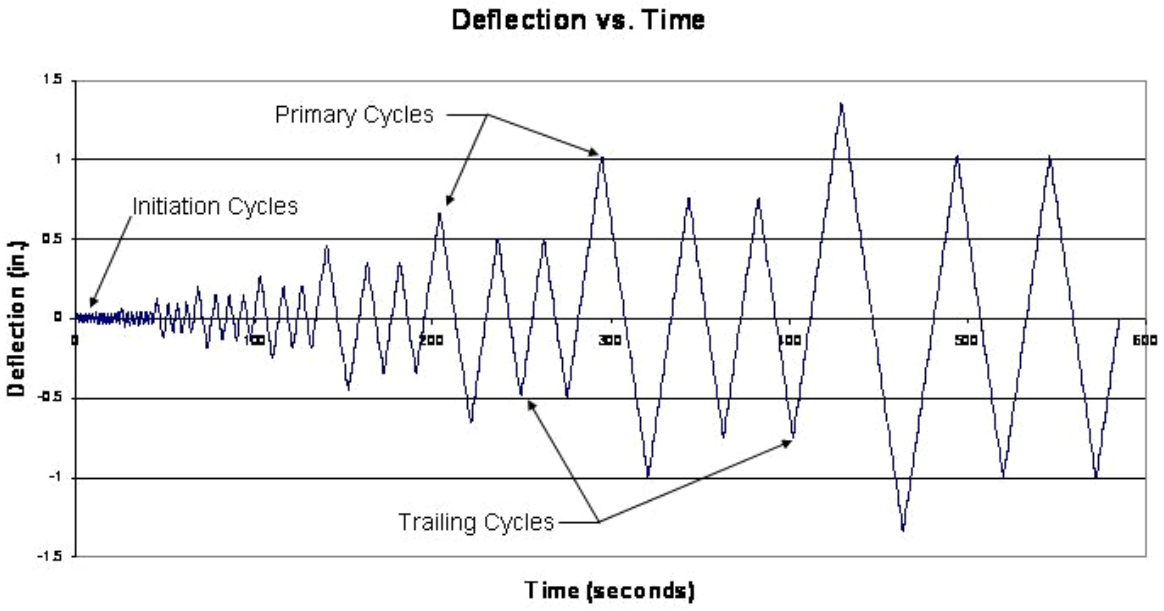

Figure 3.13: Graphical Representation of CUREE Reverse-Cyclic Protocol

The order and amplitude of the cycles are also detailed in the CUREE protocol (Krawinkler, et. al., 2001). The loading pattern described below was taken from the CUREE protocol and was used for all reverse-cyclic testing. This same pattern was followed by Anderson (2002) and Billings (2004) as well.

- Six initiation cycles with an amplitude of 0.05Δ
- A primary cycle with an amplitude of 0.075Δ
- Six trailing cycles
- A primary cycle with an amplitude of 0.1Δ
- Six trailing cycles
- A primary cycle with an amplitude of 0.2Δ
- Three trailing cycles
- A primary cycle with an amplitude of 0.3Δ
- Three trailing cycles
- A primary cycle with an amplitude of 0.4Δ

- Two trailing cycles
- A primary cycle with an amplitude of 0.7Δ
- Two trailing cycles
- A primary cycle with an amplitude of 1.0Δ
- Two trailing cycles

The CUREE protocol states that subsequent primary cycles should increase in amplitude by 0.5Δ with each step, and that each of these primary cycles should be followed by two trailing cycles. For example, the next three primary cycles would have amplitudes of 1.5Δ, 2.0Δ, and 2.5Δ, and each of these primary cycles would be followed by two trailing cycles. Testing should continue well past the point at which the maximum load is registered. For this project the tests were allowed to continue for two or three primary cycles beyond the maximum load. In most cases the tests were stopped after the two trailing cycles that followed the primary cycle of amplitude 2.0Δ. Occasionally a specimen would fail early or late with respect to average. In these cases the amplitude of the final primary cycle varied between 1.5Δ and 3.0Δ.

3.4 Wood Material Tests

3.4.1 Dowel Bearing Strength

Dowel bearing strength was measured using the method employed by Anderson (2002) and Billings (2004), and was similar to the full-hole test described in section 10.2 of ASTM D 5764-97a, Standard Test Method for Evaluating Dowel Bearing Strength of Wood and Wood-Based Products. Specimens 4-in. (10.16 cm) long, 3-in. (7.62 cm) wide, and 1.5-in. (3.81 cm) thick were cut from all wood members subjected to connection testing and were taken as close to the bolt locations as possible. These specimen dimensions satisfied the range of dimensions recommended by ASTM and were similar to the dimensions used by Billings, whose specimens measured 4.5-in. by 3-in. by 1.5-in (11.43 cm by 7.62 cm by 3.81 cm). Most specimens were taken from the region between the connection bolt holes and the fixture bolt holes, as shown below in

Figure 3.14. If splitting or knots in this region prevented a reasonably clear specimen from being cut, then the dowel bearing specimen was taken from the end of the member beyond the fixture bolt holes. In all cases the 4-in. (10.16 cm) length of the specimen corresponded with the longitudinal axis of the source member, the 3-in. (7.62 cm) width corresponded with the 5.5-in. (13.97 cm) wide face of the source member, and the 1.5-in. (3.81 cm) thickness corresponded with the remaining depth of the source member. See Figure 3.14 for details.

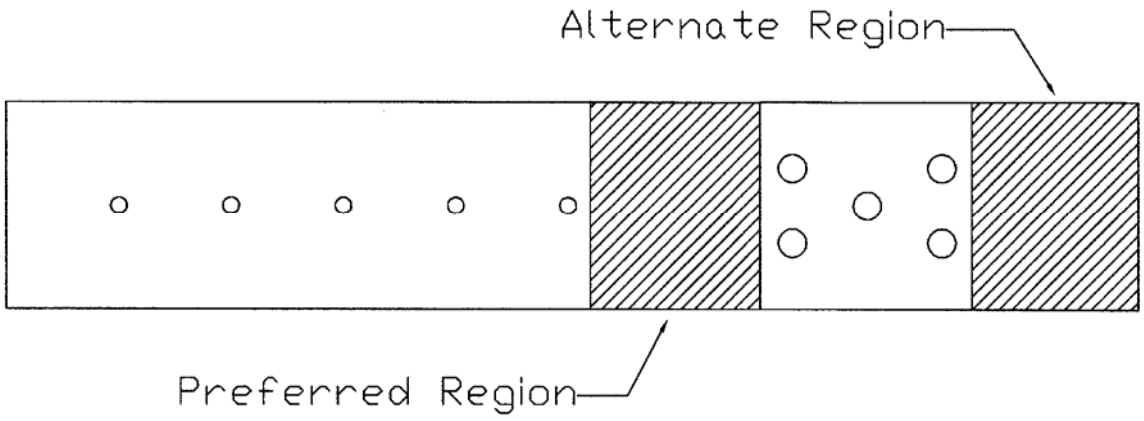

Figure 3.14: Source Regions for Dowel Bearing Specimens

Each specimen was predrilled in the center of its wide face (see Figure 3.15) using a 7/16-in. (1.11 cm) drill bit and a drill press. This hole diameter was 1/16-in. (0.16 cm) larger than the 3/8-in. (0.95 cm) diameter bolts used, and corresponded with the oversized holes used in the connection tests.

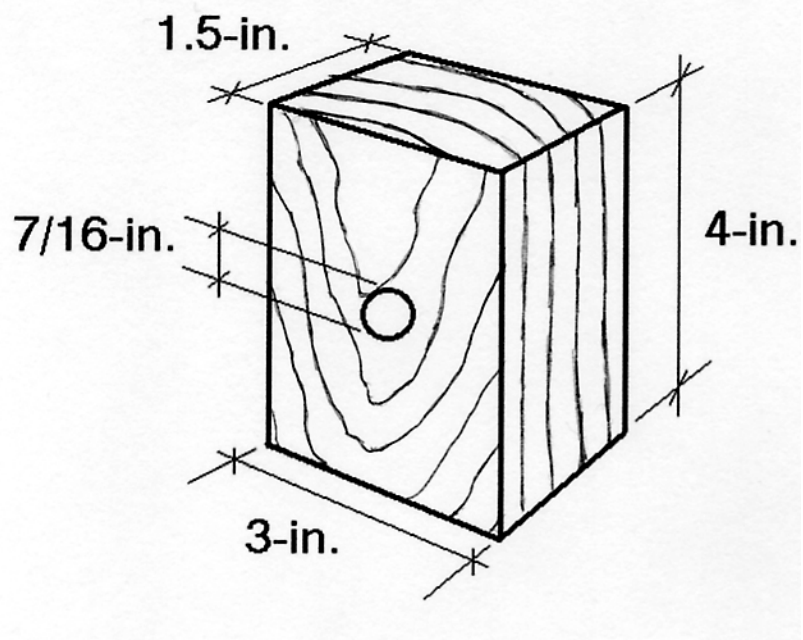

Figure 3.15: Dowel Bearing Specimen

The dowel bearing specimens were loaded into the fixture shown below in Figure 3.16 by running a bolt between the fixture walls and through the specimen. An SAE J429 grade 8 bolt was used in order to prevent any bolt bending from occurring before failure occurred in the wood specimens. The fixture itself was constructed with steel plates for rigidity.

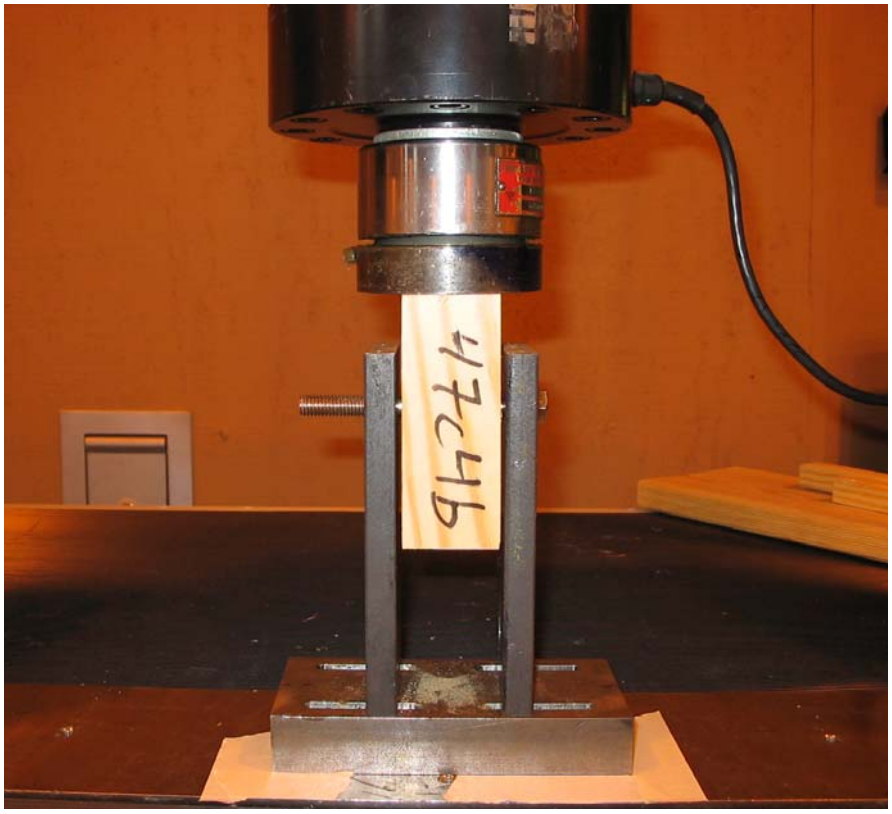

Figure 3.16: Dowel Embedment Test Setup

The load was applied in compression to the end of each specimen by an MTS testing machine and the loading head depicted in Figure 3.17. The construction of the loading head included a spherical seat, which allowed the flat plate to adjust to any eccentricities on the face of the wood specimen. The MTS machine used a 10,000 pound load cell. The load was applied at a rate of 0.08 in./min (2.03 mm/min). This was the same rate used by Anderson and Billings to produce failures occurring between 1 and 10 minutes, the duration specified in section 10.4 of ASTM D 5764-97a.

The interpretation of results followed from section 11 of ASTM D 5764-97a. The dowel bearing strength was taken to be equal to the 5% offset yield load determined by the 5% offset method described in section 2.3.2.

In addition to measuring the dowel bearing strength of the tested members from each connection, this same procedure was used on sample specimens prior to connection testing. The average dowel bearing strengths measured in these preliminary tests were used in the yield limit equations in order to accurately predict the yield mode for each connection design. This was a critical step toward insuring mode III and IV yielding. The load rate for the preliminary tests was 0.08 in./min (2.03 mm/min). This tended to produce failures occurring just before the 1 to 10 minute range recommended by ASTM. Despite this discrepancy, this same load rate was kept for all subsequent dowel bearing tests in order to ensure continuity with the testing performed by Anderson and Billings.

3.4.2 Moisture Content

The moisture content was measured for all wood members tested according to ASTM D4442-92, Standard Test Methods for Direct Moisture Content Measurement of Wood and Wood-Base Materials. Once a connection had been tested, small specimens (roughly 1"x1"x1") were cut from both wood members. The specimens were taken from locations between the connection bolt holes. After they were cut, the specimens were weighed on a digital balance and placed in a drying oven set to approximately 215°F (102° C). This preliminary weight is referred to as the wet weight (W_o). The specimens were left in the oven for approximately 24 hours until they were entirely dry. After 24 hours they were removed from the oven and weighed again. This weight is referred to as the oven-dry weight (W_d). The moisture content (MC) is expressed as a percentage and was calculated using Equation 3.2:

$$MC(\%) = \frac{W_0 - W_d}{W_d} * 100 \qquad (3.2)$$

3.4.3 Specific Gravity

The specific gravity was measured for all wood members tested according to section 10.2.2 of ASTM D2395, Standard Test Methods for Specific Gravity of Wood and Wood-Based Materials. These measurements were made using the same specimens cut

for the moisture content measurements. Following the oven-dry weight measurement described in the previous section, the specimens were coated with paraffin wax by submerging them in a wax bath. The coated specimens were then submerged in a small tub of water resting on a digital balance. The weight added to the balance by submerging a specimen was equal to the weight of the water displaced by the specimen, which, in turn, was equal to the volume (V) of the specimen. The specific gravity (SG) was calculated using Equation 3.3.

$$SG = \frac{W_d}{V} \tag{3.3}$$

3.5 Methods of Data Analysis

3.5.1 General

Following connection testing, the monotonic and reverse-cyclic test data were analyzed and compared according to the seven strength and serviceability parameters described in section 1.2. These parameters included: maximum load, failure load, E.E.P. yield load, 5% offset load, elastic stiffness, E.E.P. energy, and ductility ratio. The methods used to calculate these parameters from the monotonic data are described in section 3.5.2, and the methods used to analyze the reverse-cyclic data are described in section 3.5.3.

3.5.2 Monotonic Connection Tests

Monotonic test data were analyzed using a Microsoft Excel program called "Ana." This program was used by Billings in 2004 and was based on a methodology proposed by Dolan in a 1999 draft standard entitled "Standard Test Method for Evaluating Dowel-Bearing Strength for Wood and Wood-Based Products" (ASTM, 1999). In this document Dolan proposes an analysis based on a bilinear approximation of the load-deflection curve. The bilinear curve represents an idealized elastic-plastic relationship, and is called the "equivalent energy elastic-plastic" (E.E.P.) curve. The development of the E.E.P. curve is described below and is illustrated in Figure 3.17.

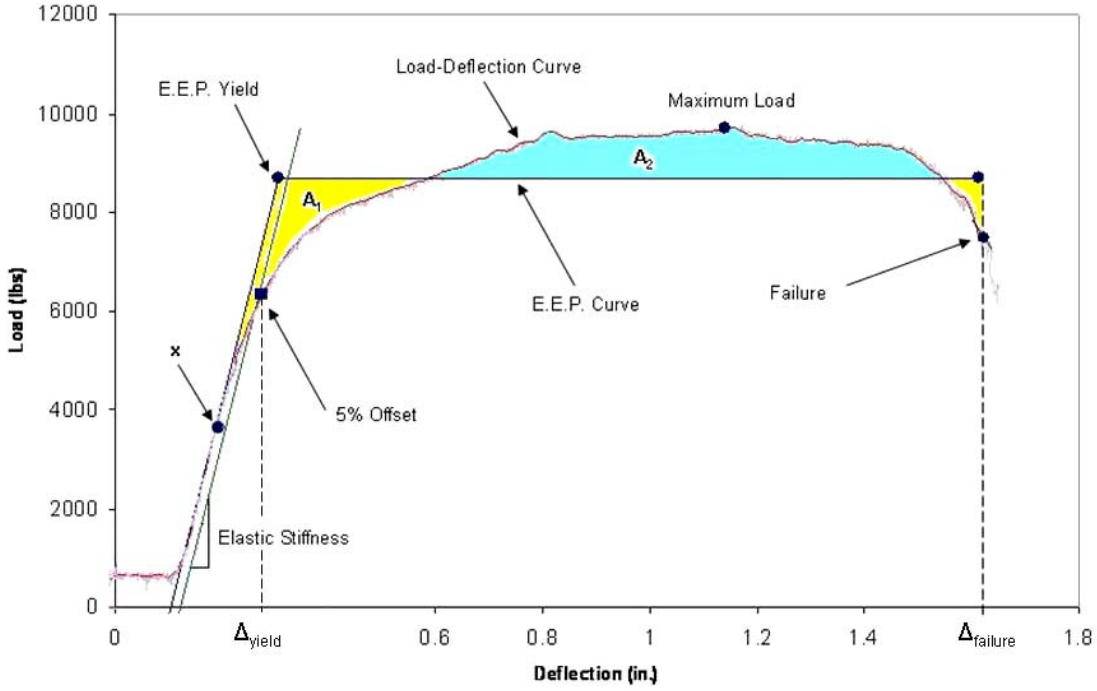

Figure 3.17: E.E.P. Curve for Monotonic Loading

First the slack in the data is subtracted out and the origin is relocated. Next, the elastic portion of the curve is generated by drawing a line through the origin and through the point "x." Point "x" is the point along the load-deflection curve at which the load is equal to 0.4 times the maximum load ($0.4*F_{max}$). The failure point is then located at a load equal to $0.8*F_{max}$. The deflection at this point is called $\Delta_{failure}$. Next, the plastic portion of the E.E.P. curve is drawn such that the areas A_1 and A_2 are equal. This measure is designed to make sure that the area under the E.E.P. curve, also called E.E.P. energy, is equal to the area under the original load-deflection curve. The point at which the plastic line segment intersects the elastic line segment is defined as the E.E.P. yield point, and the deflection at this point is called Δ_{yield}. Finally, the ductility ratio can be calculated using Equation 3.4.

$$Ductility\ Ratio = \Delta_{failure} / \Delta_{yield} \quad (3.4)$$

The "Ana" program was designed by Anderson (2002) to follow this procedure, and it was also used at various stages during the data analysis for this project. Once the load and deflection values were pasted into the spreadsheet, the program modeled the data with an approximated load-deflection curve. The operations described by Dolan were then performed, generating values for the maximum load, failure load, $0.4*F_{max}$, E.E.P. yield load, 5% offset load, and their corresponding displacements. Values for the slack, elastic stiffness, E.E.P. energy, and ductility ratio were also generated. One significant change was made to the program in order to correct a faulty formula used to calculate the E.E.P. yield load. For this reason the E.E.P. yield load, Δ_{yield}, and the ductility ratio cannot be compared to the values reported by Billings or Anderson. However, all other values are comparable. Results of the monotonic testing are included in section 4.3.

3.5.3 Reverse-Cyclic Connection Tests

Analysis of the reverse-cyclic tests required a simplification of the load-deflection data. Piece-wise, linear curves were formed by connecting the points of maximum load for each primary cycle (see Figure 3.18). Both a positive and a negative piece-wise curve were generated for each test. Both curves were then analyzed according to Dolan's method. Figure 3.19 shows a typical set of reverse-cyclic E.E.P. curves and various points of interest.

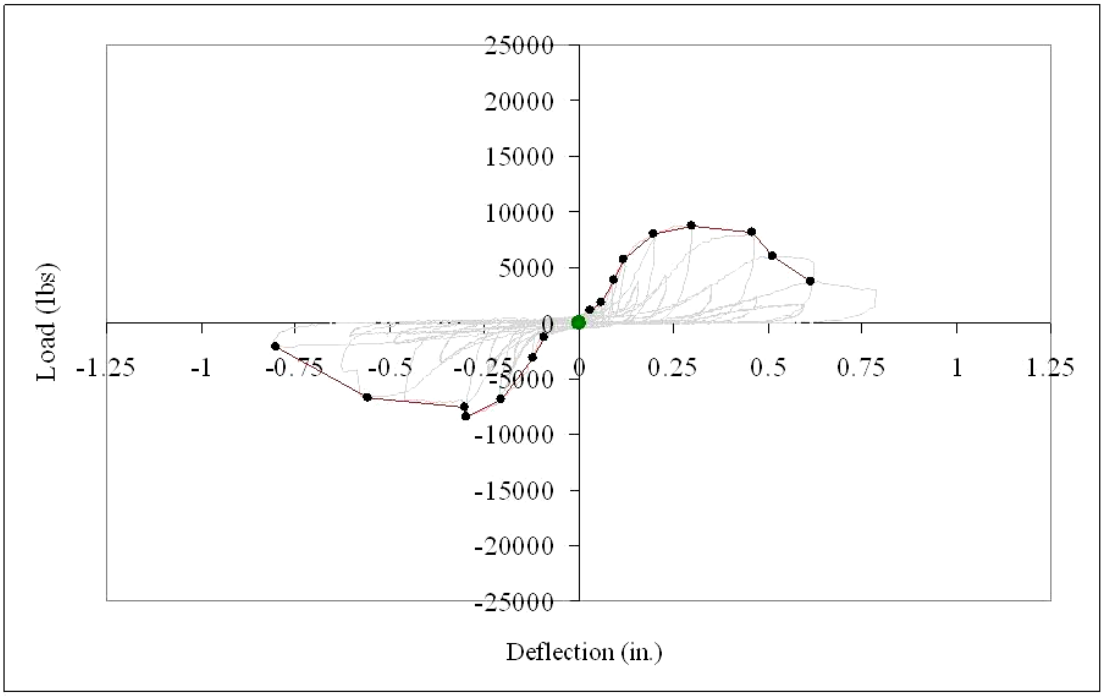

Figure 3.18: Piece-Wise Load vs. Deflection Curve for Reverse-Cyclic Data

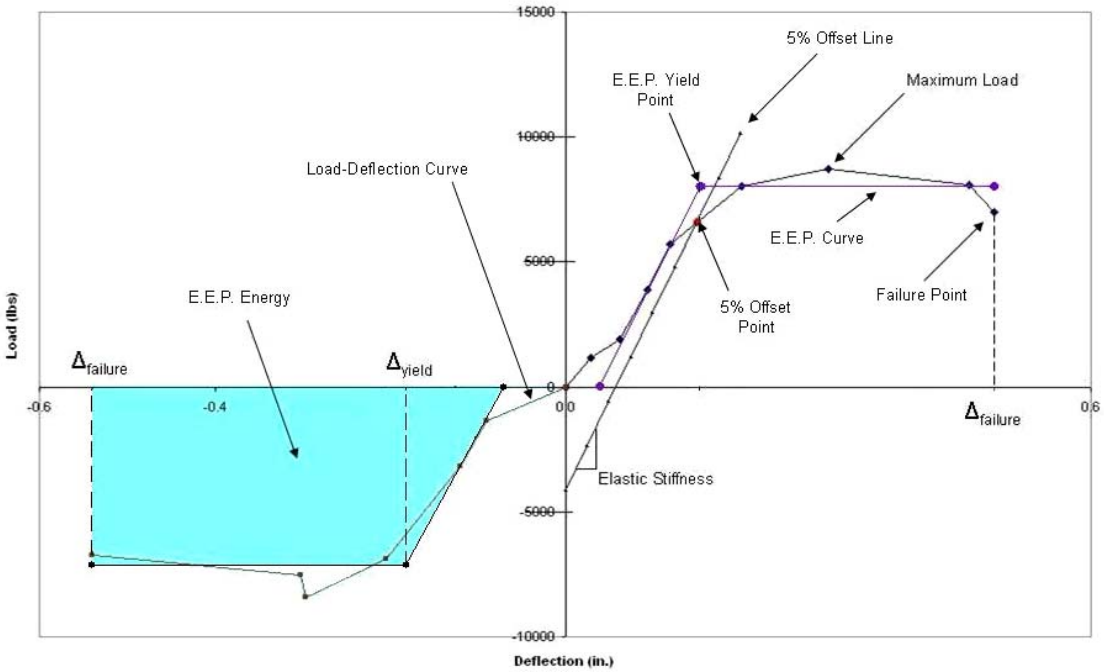

Figure 3.19: E.E.P. Curves for Reverse-Cyclic Data

The points for the piece-wise curves, including the maximum load, were calculated using a Microsoft Excel program called "LinearApprox." This program was designed by Anderson (2002) and is the same program that Billings used for this purpose. All other values and points of interest were calculated manually. This marked a departure from the work of Billings, who used "Ana" for these calculations. Once calculated, all parameters pertaining to the negative E.E.P. curve were converted to positive numbers and averaged with their counterparts from the positive E.E.P. curve.

These average values make up the reverse-cyclic test data included in section 4.3. Once again, the values for E.E.P. yield load, Δ_{yield}, and the ductility ratio are not comparable with those calculated by Billings and Anderson using the faulty version of "Ana." However, all other values are comparable.

Chapter 4: Results and Discussion

4.1 Introduction

This chapter contains both preliminary calculations and the results of all of the testing described in chapter 3. All preliminary calculations pertaining to connection yield limits and expected failure loads are discussed in section 4.2. The results of the connection tests themselves are discussed in section 4.3. Finally, the results of the bolt study are discussed in section 4.4.

4.2 Preliminary Yield Limit Calculations

4.2.1 General

Prior to connection testing, yield limit calculations were performed in order to make sure that the proposed connection configurations were predicted by NDS to yield according to modes III and IV. These calculations utilized the yield limit equations found in section 11.3 of the NDS (AF&PA, 2001). The yield limit equations required as inputs the bending yield strength of the bolts and the dowel bearing strength of the wood. These values were obtained through the testing described in sections 4.2.2 and 4.2.3. The yield mode calculations are included in section 4.2.4.

4.2.2 Bolt Bending Yield Strength

Various 3/8-in. (0.95 cm) diameter bolts were tested according to the 3-point and cantilever bending methods described in sections 3.2.6 and 3.2.7. The bolts were SAE J429 Grade 2, and both 6-in. (15.24 cm) and 8-in. (20.32 cm) lengths were tested. The grade and dimensions were the same as those proposed for the connection testing. Three bolts at each length were tested according to each method. Twelve bolts were tested in all.

Following testing, the bending yield strengths (F_{yb}) for the specimens in each sample set were calculated and averaged using the formulas from sections 3.2.6 and 3.2.7. The

diameters used in the calculations were the means of the actual diameters for each sample set. These actual diameters were measured using a digital caliper. The results of preliminary bending tests are included below in Table 4.1.

Table 4.1: Preliminary Bolt Bending Yield Strengths

	Bolt Length (in.)	Nominal Bolt Diameter (in.)	Number of Tests	Average Fyb (psi)
3-Point Bend	6	3/8-in.	3	77,700
	8	3/8-in.	3	77,100
Cantilever	6	3/8-in.	3	67,500
	8	3/8-in.	3	56,000

To be conservative in the yield mode predictions, a preliminary bending yield strength of 78,000 psi was assumed for both the 6-in. (15.24 cm) and 8-in. (20.32 cm) bolts.

4.2.3 Dowel Embedment Strength

A total of six specimens were tested according to the method described in section 3.4.1 in order to obtain average preliminary values for the dowel embedment strengths (F_e) of the wood members. Three of the specimens were cut from 2x6 Southern Yellow Pine members and three were cut from 4x6 Mixed Southern Pine members. The measured values for each sample set were averaged and are included below in Table 4.2.

Table 4.2: Preliminary Dowel Embedment Strengths

	Number of Tests	Average Specific Gravity	Average F_e (psi)
2x6	3	0.545	5970
4x6	3	0.471	3920

To be conservative in the yield mode predictions, a preliminary dowel embedment strength of 5800 psi was assumed for the 2x6 members, while a value of 3900 psi was assumed for the 4x6 members.

4.2.4 Yield Limit Calculations

The preliminary values for bending yield strength and dowel embedment strength were used as inputs in the yield limit equations included in Table 2.1. The yield limit equations were used to calculate nominal design values (Z) per bolt. According to NDS section 11.3.1, the controlling nominal design value should be taken as the "minimum computed yield mode value" (AF&PA, 2001). Thus, Z values for modes II, III_s, III_m, and IV were calculated for each proposed connection assembly and compared with one another. These calculations are included in Appendix A, and their results are included below in Table 4.3. The controlling yield modes of III_s for the first connection assembly and IV for the second connection assembly satisfied objective C of section 1.2.

Table 4.3: Nominal Design Values for Yield Limit Calculations

MAIN MEMBER	SIDE MEMBER	NOMINAL BOLT DIAMETER	Z_{II} (lbs)	Z_{IIIs} (lbs)	Z_{IIIm} (lbs)	Z_{IV} (lbs)	CONTROLLING YIELD MODE
4x6	2x6	3/8-in.	1860	1360	1890	1510	III_s
4x6	4x6	3/8-in.	2100	1880	1880	1390	IV

Following the yield limit calculations, the controlling nominal design values were used to calculate the maximum loads expected to be carried by each connection assembly. These calculations were made using the Equation 4.1, which was taken from NDS Table 10.3.1 (AF&PA, 2001).

$$Z' = Z*(C_D*C_M*C_t*C_g*C_\Delta*C_{eg}*C_{di}*C_{tn}) \quad (4.1)$$

Where

Z = the controlling nominal design value

$C_D, C_M, C_t, C_g, C_\Delta, C_{eg}, C_{di}, C_{tn}$ = Adjustment Factors

The load (Z') returned by equation 4.1 was then multiplied by the number of fasteners per connection in order to obtain the maximum expected load on each connection. Details of these calculations, including the calculations of all applicable adjustment factors, are included in Appendix A. The results are included below in Table 4.4.

Table 4.4: Maximum Loads Expected

	Spacing	Maximum Load (lbs)
MODE III_s	7D	10,600
	8D	10,500
MODE IV	7D	11,100
	8D	11,100

4.3 Connection Tests

4.3.1 General

A total of 52 connections were tested according to the methods described in section 3.3. Three connections per data set were tested using a monotonic loading procedure, for a total of twelve. Ten connections per data set were tested using a reverse-cyclic loading procedure, for a total of forty. See Table 3.6 for a summary of these tests and data sets.

Following the monotonic tests, the data were analyzed and the deflections at failure were found. These deflections were then averaged for each data set. The resulting means represented monotonic deflection capacities (Δ_m) and were used as inputs in the CUREE test protocol for the reverse-cyclic tests. See sections 3.3.6 and 3.3.7 for detailed descriptions of this protocol.

Once all connection testing was completed, the data were analyzed according to the methods described in section 3.5. Values for the seven different strength and

serviceability parameters were calculated for each test and are reported in sections 4.3.2 and 4.3.3. These parameters included: maximum load, failure load, E.E.P. yield load, 5% offset load, elastic stiffness, E.E.P. energy, and ductility ratio. The means of these values were then calculated for each data set and compared to one another using t-tests. This statistical analysis is included in section 4.3.4.

In addition, samples from all connection members were cut and subjected to dowel embedment, moisture content, and specific gravity testing. These tests were conducted in order to provide insight into the physical properties of the wood members that had made up each connection. The results of the dowel embedment tests are included in section 4.3.5, and the results of the moisture content and specific gravity tests are included in section 4.3.6.

4.3.2 Predicted Mode III_s

The connections predicted to yield according to Mode III_s consisted of a 4x6 main member, a 2x6 side member, and a single row of five bolts. All bolts were SAE J429 Grade 2, had a manufacturer's stamp of HKT, and had a nominal diameter of 3/8-in. (0.95 cm). Additional connection details are included in section 3.3.

4.3.2.1 Monotonic Tests

Six monotonic tests were performed using the mode III_s configuration described above. Three of the tests featured a bolt-spacing equal to seven times the bolt diameter (7D), while the other three tests featured a bolt-spacing equal to eight times the bolt diameter (8D). Two of the tested assemblies are shown in Figure 4.1.

Figure 4.1: Example Connections from 37m and 38m Data Sets

Following each monotonic test, the bolts were removed from the test specimens and photographed. Upon inspection, each set of bolts from the 37m and 38m data sets featured mode III yielding as its predominant yield behavior. These results satisfied the yield mode predictions described in section 4.2.4, and the mode III_s configuration was therefore approved for the reverse-cyclic tests. Two sets of the tested bolts are shown below in Figure 4.2. The single plastic hinge point indicative of mode III yielding is apparent in these photographs.

Figure 4.2: Example Groups of Tested Bolts from 37m and 38m Data Sets

A load-deflection curve was generated for each monotonic test. These curves were subsequently fitted with a 5% offset line and modeled using an equivalent energy elastic-plastic (E.E.P.) curve. These procedures followed the methods of data analysis described in section 3.5.2. An example of a typical load-deflection curve and E.E.P. curve fit from the 37m data set is shown below in Figure 4.3. See Appendix B for all other monotonic curves.

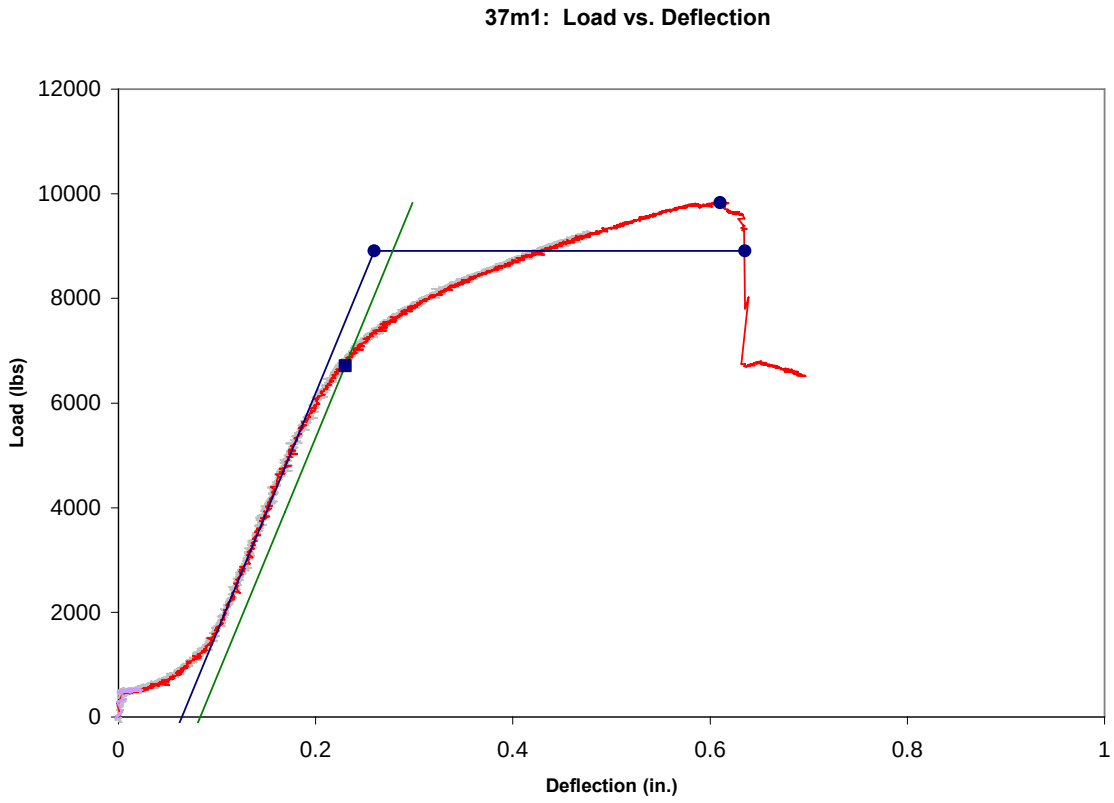

Figure 4.3: Example Load vs. Deflection Plot and E.E.P. Curve-Fit from 37m Data Set

Once the load-deflection curves, E.E.P. curves, and 5% offset lines were generated, five specific points were located and four other relevant values were calculated. The five points included: the point of maximum load, the failure point, the point at which the load equaled forty percent of the maximum load, the E.E.P. yield point, and the 5% offset yield point. The four calculated values included: the elastic stiffness, the slack, the E.E.P. energy, and the ductility ratio. These points and values are described in detail in section 3.5.2, and are included below in Tables 4.5 and 4.6. The mean values for the seven strength and serviceability parameters are included in Table 4.7.

Table 4.5: Monotonic Test Results for Mode III_s with 7D Spacing

	37m1	37m2	37m3	MEAN	STDEV	COV (%)
Max Load (lbs) =	9830	8200	7720	8583	1106	12.89
Displacement (in) =	0.61	0.60	0.44	0.55	0.10	17.36
Failure Load (lbs) =	7800	5840	3260	5633	2277	40.42
Disp. @ Failure (in) =	0.64	0.60	0.45	0.56	0.10	17.77
40% Max (lbs) =	3920	3260	3060	3413	450	13.18
Displacement (in) =	0.15	0.20	0.18	0.18	0.03	14.97
E.E.P. Yield (lbs) =	8910	7710	6960	7860	984	12.51
Displacement (in) =	0.26	0.32	0.27	0.28	0.03	12.11
5% Offset Yield Load (lbs) =	6710	5990	5050	5917	832	14.07
Displacement (in) =	0.23	0.29	0.24	0.26	0.03	13.42
Elastic Stiffness (lb/in.)=	45700	37400	43000	42033	4234	10.07
Slack (in) =	0.06	0.12	0.10	0.09	0.03	28.56
E.E.P. Energy (lb*in) =	4220	2930	1820	2990	1201	40.17
Ductility Ratio =	2.45	1.86	1.68	2.00	0.40	20.24

Table 4.6: Monotonic Test Results for Mode III_s with 8D Spacing

Max Load (lbs) =	7950	8680	6880	7837	905	11.55
Displacement (in) =	0.55	0.55	0.51	0.54	0.02	4.03
Failure Load (lbs) =	6210	5360	3920	5163	1158	22.42
Disp. @ Failure (in) =	0.55	0.80	0.52	0.62	0.15	24.03
40% Max (lbs) =	3160	3450	2730	3113	362	11.64
Displacement (in) =	0.22	0.20	0.17	0.20	0.03	13.96
E.E.P. Yield (lbs) =	7530	7780	6150	7153	878	12.27
Displacement (in) =	0.32	0.31	0.26	0.30	0.03	10.25
5% Offset Yield Load (lbs) =	5650	5740	4570	5320	651	12.24
Displacement (in) =	0.30	0.28	0.24	0.27	0.03	11.35
Elastic Stiffness (lb/in.)=	41400	42800	34600	39600	4386	11.08
Slack (in) =	0.14	0.12	0.09	0.12	0.03	24.02
E.E.P. Energy (lb*in) =	2420	4520	2130	3023	1304	43.14
Ductility Ratio =	1.71	2.61	1.98	2.10	0.46	21.89

Table 4.7: Mean Values for Strength and Serviceability Parameters, Mode III_s, Monotonic

	37m (7D)	**38m (8D)**
Max Load (lbs) =	8583	7837
Failure Load (lbs) =	5633	5163
E.E.P. Yield (lbs) =	7860	7153
5% Offset Yield =	5917	5320
Elastic Stiffness (lb/in.)=	42030	39600
E.E.P. Energy (lb*in) =	2990	3023
Ductility Ratio =	2.00	2.10

The loads and displacements included in Tables 4.5 and 4.6 were taken from actual test data points. Therefore, the failure loads and the 40% loads are not exactly equal to $0.8*F_{max}$ and $0.4*F_{max}$ respectively. They are instead the closest recorded loads. These loads and their corresponding deflections are sufficiently accurate for general post-test analysis and comparisons between spacings; however, they were not used to calculate the monotonic deformation capacities (Δ_m) needed for the CUREE loading protocol used in the reverse-cyclic tests. These deformation capacities were instead calculated using failure loads exactly equal to $0.8*F_{max}$. The deflections at these failure loads were calculated by a linear interpolation between the two nearest points. They were then averaged into two means, one for each spacing. The resulting monotonic deformation capacities were equal to 0.5430 for the 37m data set and 0.6180 for the 38m data set.

4.3.2.2 Reverse-Cyclic Tests

Twenty reverse-cyclic tests were performed using the mode III_s configuration. Ten of the tests featured a bolt-spacing equal to seven times the bolt diameter (7D), while the other ten tests featured a bolt-spacing equal to eight times the bolt diameter (8D). Two of the tested assemblies are shown in Figure 4.4.

Figure 4.4: Example Connections from 37c and 38c Data Sets

Following each reverse-cyclic test, the bolts were removed from the test specimens and photographed. Upon inspection, each set of bolts from the 37c and 38c data sets featured mode III yielding as its predominant yield behavior. These results satisfied the yield mode predictions described in section 4.2.4. Two sets of the tested bolts are shown below in Figure 4.5. The single plastic hinge point indicative of mode III yielding is apparent in these photographs.

Figure 4.5: Example Groups of Tested Bolts from 37c and 38c Data Sets

A load-deflection plot was generated for each reverse-cyclic test. Piece-wise, linear approximations were then formed by connecting the points of maximum load for each cycle. An example of a typical load-deflection plot and linear curve-fit from the 37c data set is shown below in Figure 4.6. See Appendix B for all other reverse-cyclic curve-fits.

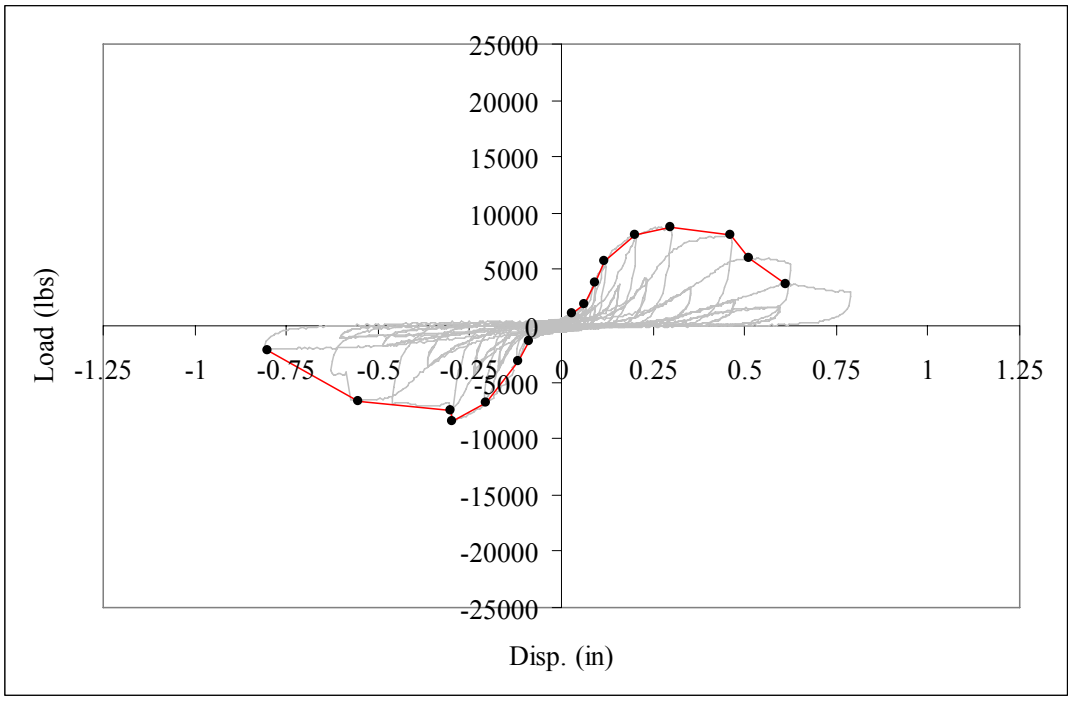

Figure 4.6: Example Load vs. Deflection Plot and Linear Curve-Fit from 37c Data Set

Once the piece-wise curves had been generated, they were modeled using E.E.P. curves and analyzed according to the methods of data analysis described in section 3.5.3. A typical set of E.E.P. curves from the 37c data set is shown below in Figure 4.7. See Appendix B for all other reverse-cyclic E.E.P. curves.

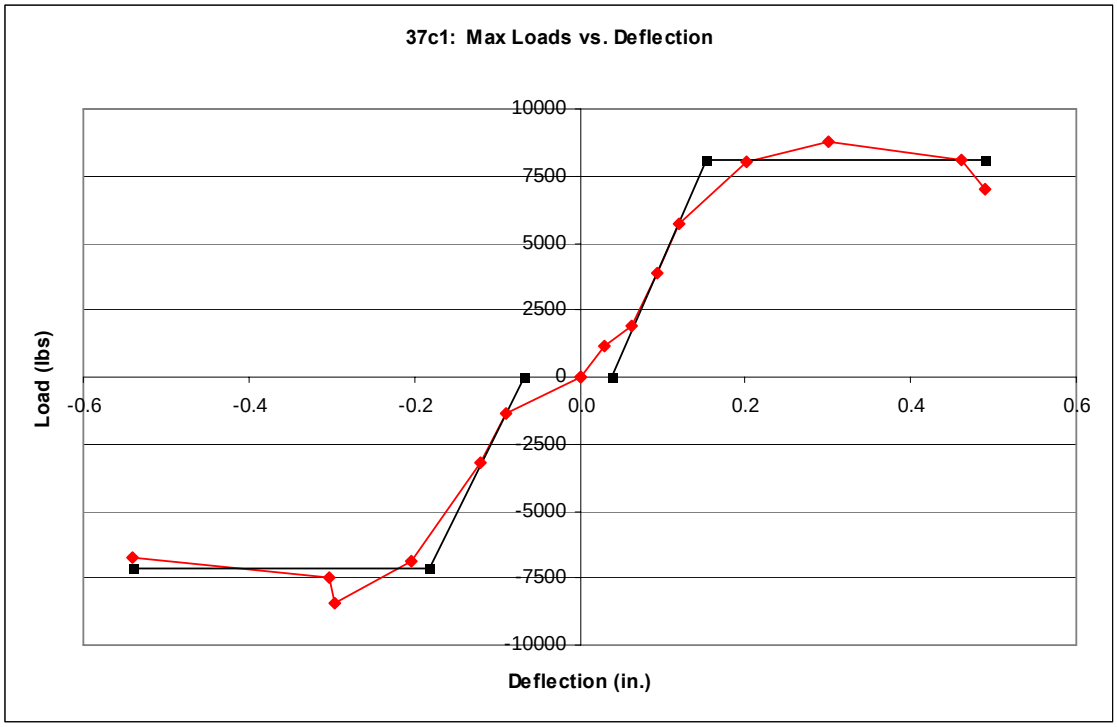

Figure 4.7: Example E.E.P. Curves from 37c Data Set

The linear, piece-wise curves and E.E.P. curves were then used to calculate the seven strength and serviceability parameters described in detail in section 3.5.3. Test values for each of these parameters are included below in Tables 4.8 and 4.9. Table 4.8 contains results from the 37c data set, while Table 4.9 pertains to the 38c data set. In addition, a direct comparison of the mean values for the seven parameters is included in Table 4.10. The test values and means for the seven parameters are also displayed graphically in Figures 4.8 through 4.14. The means are designated in each of these figures.

Table 4.8: Reverse-Cyclic Test Results for Mode III_s with 7D Spacing

	Max Load (lbs)	Failure Load (lbs)	Elastic Stiffness (lbs/in.)	5% Offset Load (lbs)	E.E.P. Energy (lbs*in.)	Ductility Ratio	E.E.P. Yield Load (lbs)
37c1	8580	6870	66900	6240	3070	4.04	7620
37c2	6850	5480	47500	5650	1110	1.95	6090
37c3	7800	6240	50900	6610	1210	1.76	6950
37c4	8880	7110	50600	6780	2510	2.47	8020
37c5	6500	5200	49400	5820	1190	2.11	5930
37c6	9030	7230	56300	7120	2110	2.35	7980
37c7	7060	5650	42900	6000	1370	1.97	6280
37c8	7600	6080	42000	5450	2100	2.40	6750
37c9	6550	5240	38400	5160	3030	3.70	6050
37c10	8430	6750	39700	5820	2590	2.36	7410
MEAN	7728	6185	48460	6065	2029	2.51	6908
STDEV	965	774	8592	619	767	0.76	812
COV %	12.48	12.52	17.73	10.20	37.81	30.10	11.75

Table 4.9: Reverse-Cyclic Test Results for Mode III_s with 8D Spacing

	Max Load (lbs)	Failure Load (lbs)	Elastic Stiffness (lbs/in.)	5% Offset Load (lbs)	E.E.P. Energy (lbs*in.)	Ductility Ratio	E.E.P. Yield Load (lbs)
38c1	6410	5130	43800	5090	1170	2.09	5730
38c2	9260	7410	42000	6010	3910	2.94	8150
38c3	9220	7380	46100	6490	2810	2.43	8160
38c4	9250	7400	55900	7540	1750	1.92	8350
38c5	7590	6070	37900	6050	1320	1.56	6800
38c6	8350	6680	38700	6640	2020	1.78	7520
38c7	8560	6850	52400	6700	2230	2.44	7710
38c8	9430	7540	53100	6480	3130	2.88	8340
38c9	7810	6250	45700	6090	1280	1.75	6860
38c10	7340	5870	43700	5940	1390	1.89	6600
MEAN	8322	6658	45930	6303	2101	2.17	7422
STDEV	1014	811	6096	638	921	0.48	889
COV %	12.18	12.18	13.27	10.13	43.84	22.28	11.98

Table 4.10: Comparison of Mean Test Values, Mode III_s, Reverse-Cyclic

	Mode III, 7D (37c)	Mode III, 8D (38c)
Max Load (lbs)	7728	8322
Failure Load (lbs)	6185	6658
5% Offset Load (lbs)	6065	6303
E.E.P. Yield Load (lbs)	6908	7422
E.E.P. Energy (lbs*in.)	2029	2101
Elastic Stiffness (lbs/in.)	48460	45930
Ductility Ratio	2.51	2.17

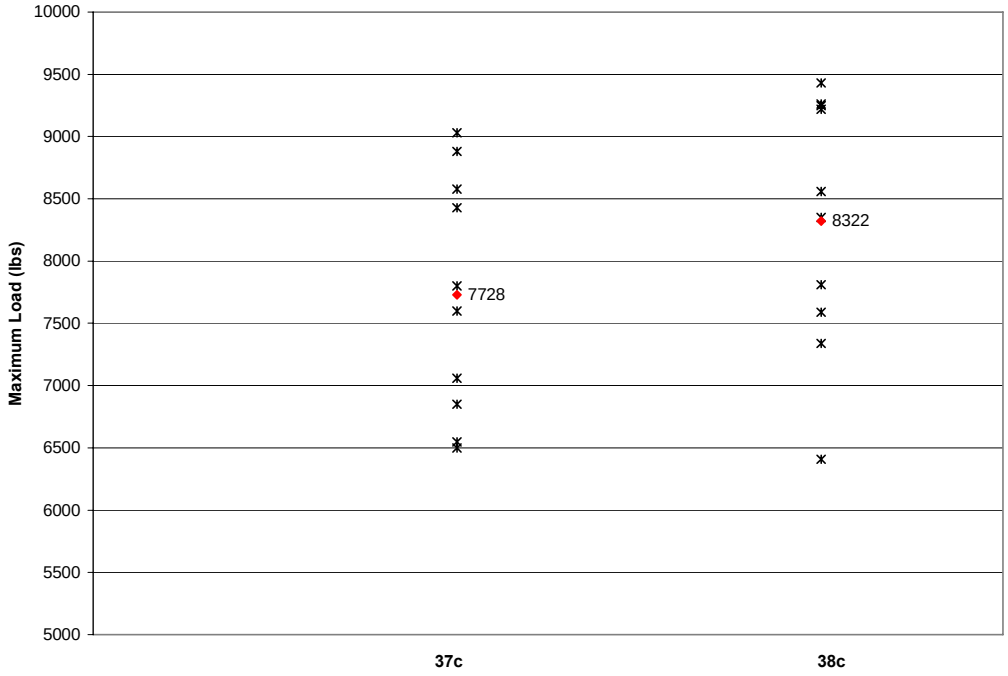

Figure 4.8: Maximum Loads, Mode III_s

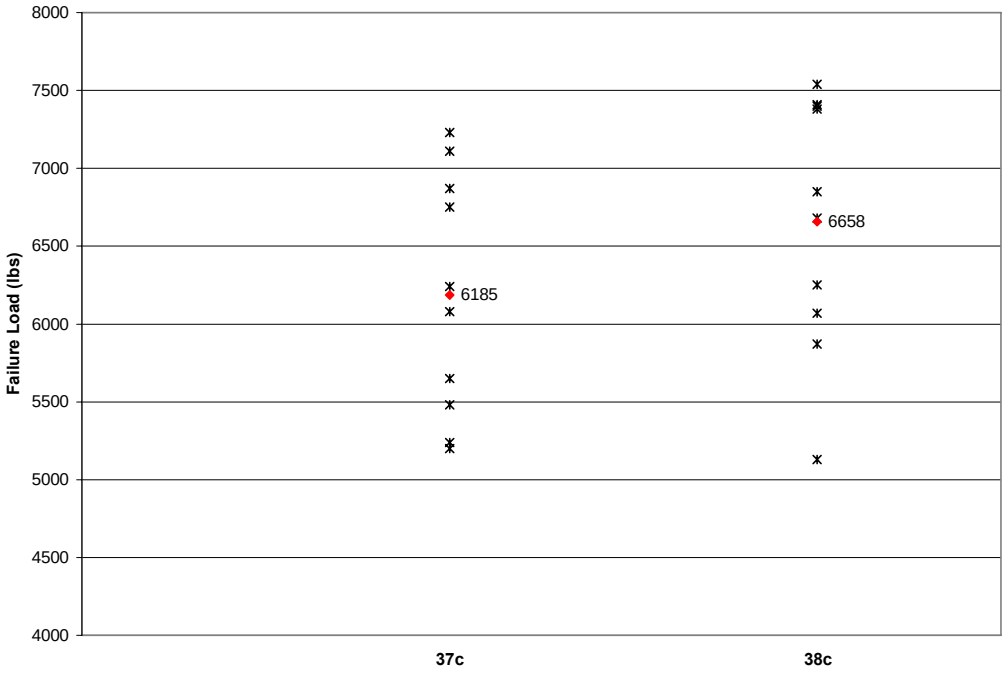

Figure 4.9: Failure Loads, Mode III_s

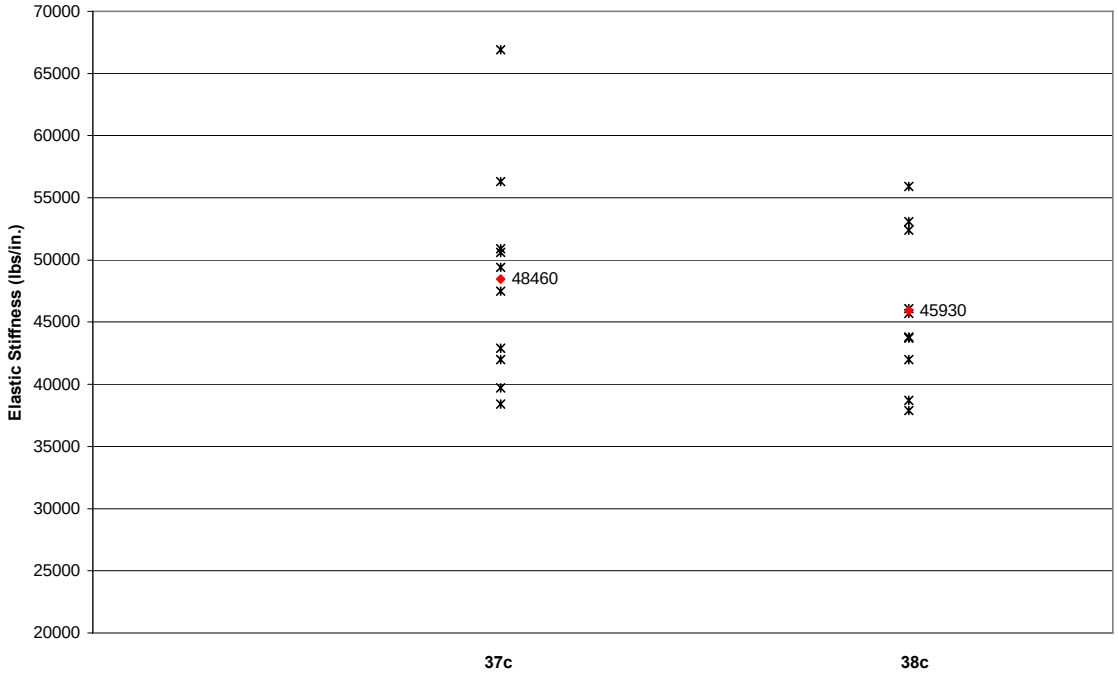

Figure 4.10: Elastic Stiffnesses, Mode III_s

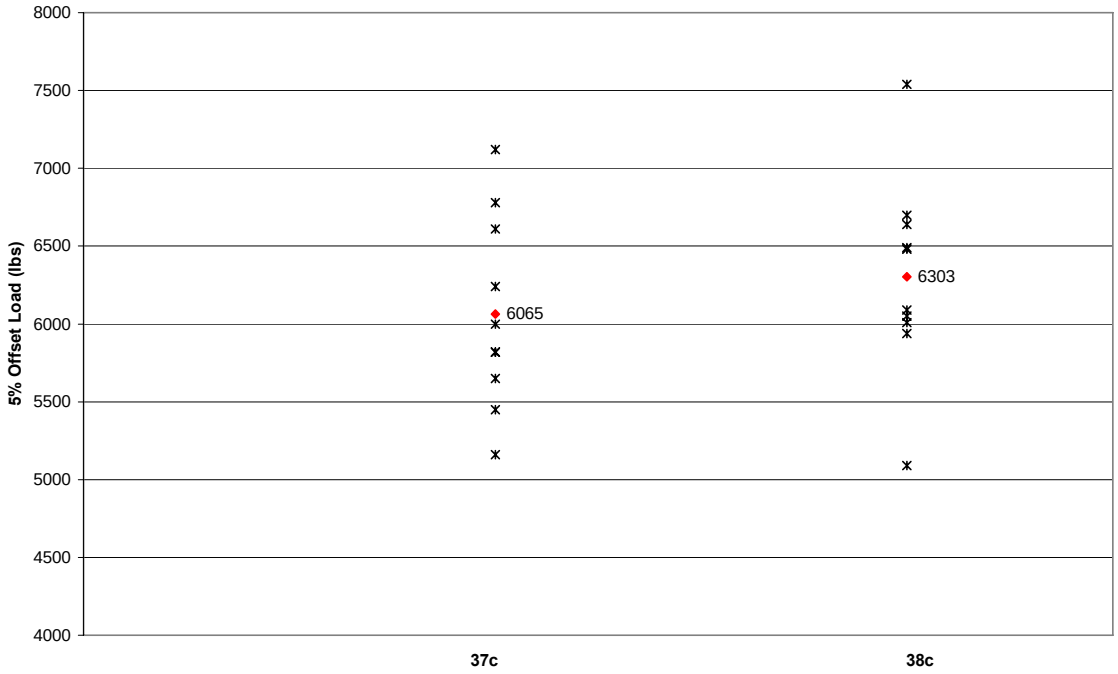

Figure 4.11: 5% Offset Loads, Mode III_s

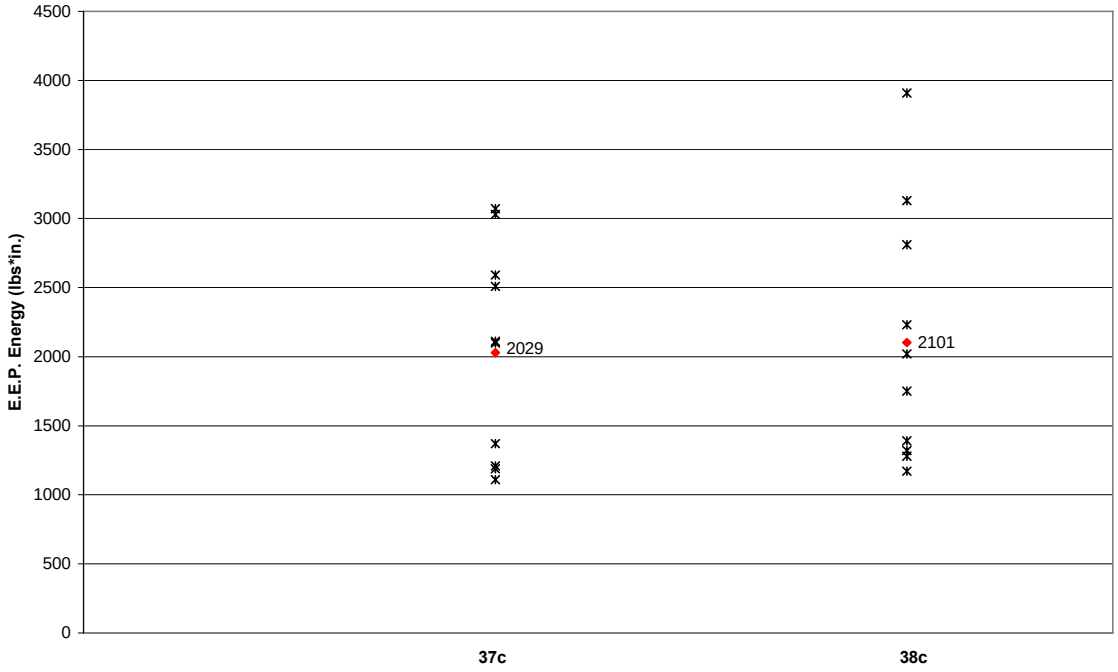

Figure 4.12: E.E.P. Energies, Mode III_s

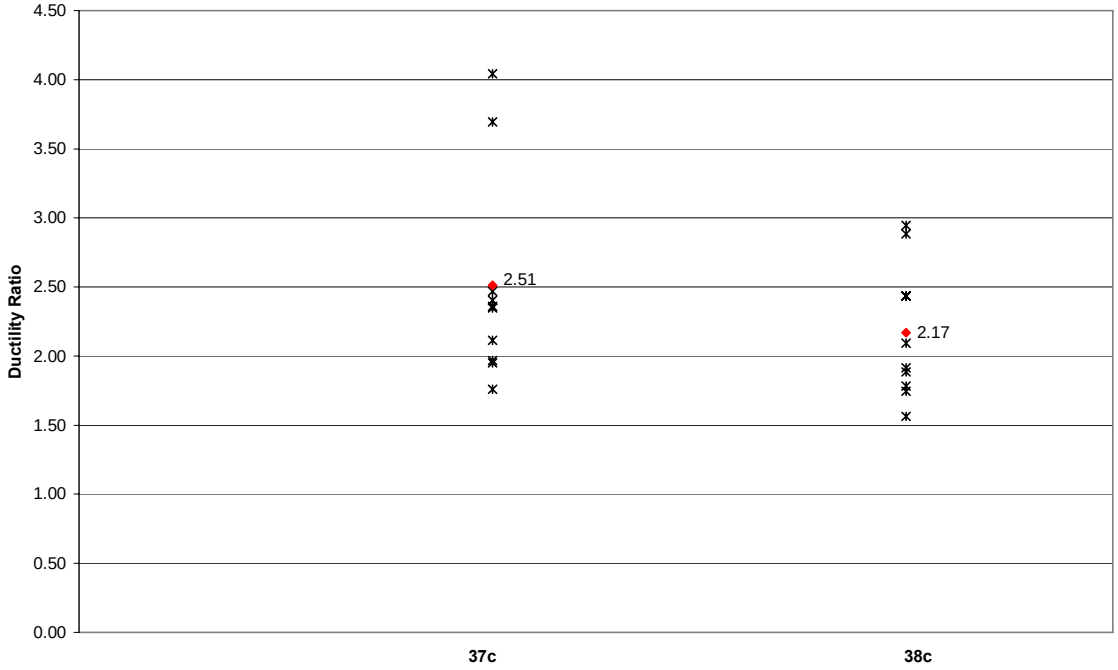

Figure 4.13: Ductility Ratios, Mode III_s

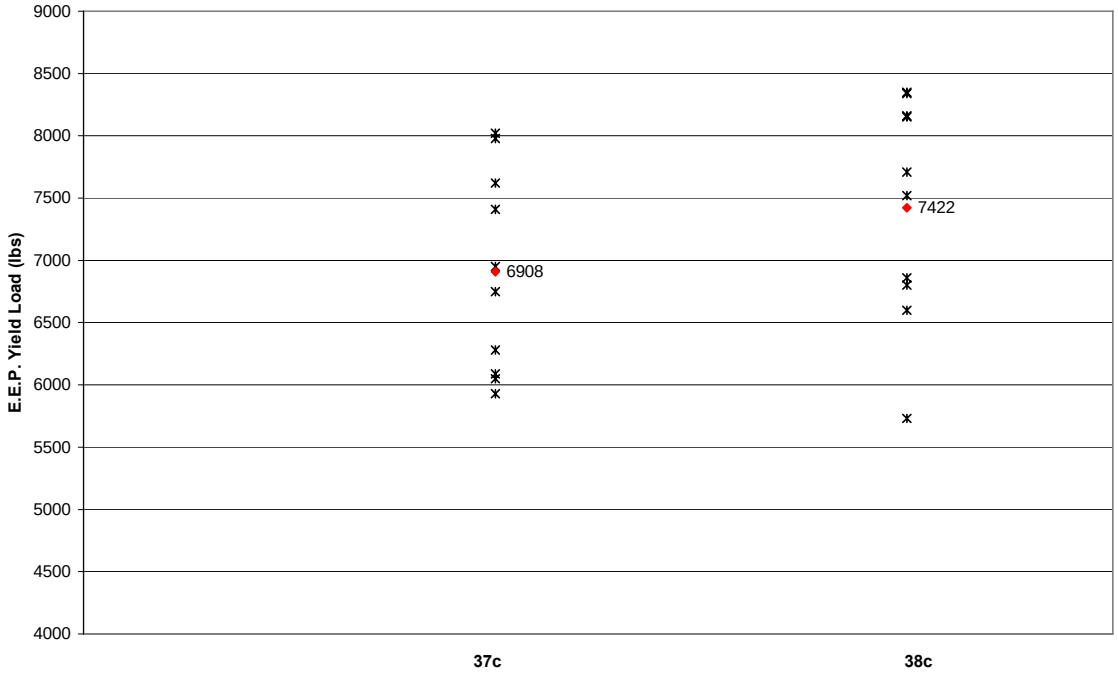

Figure 4.14: E.E.P. Yield Loads, Mode III_s

From the mode III_s data, it is apparent that the 8D spacing resulted in greater connection strengths. The mean values for maximum load, failure load, 5% offset load, and E.E.P. yield load are all higher for the 8D spacing, and the low coefficients of variation for these strength parameters validate this trend.

The results for the serviceability parameters are not as clear-cut, however. The 7D spacing resulted in higher mean values for elastic stiffness and ductility ratio, but the 8D connections absorbed more energy on average. In addition, both the energy and ductility data feature high coefficients of variation, further obscuring the serviceability comparisons.

4.3.3 Predicted Mode IV

The connections predicted to yield according to Mode IV consisted of a 4x6 main member, a 4x6 side member, and a single row of five bolts. All bolts had a nominal diameter of 3/8-in. (0.95 cm), and were made of low-carbon steel. However, limited availability resulted in a mixture of SAE J429 Grade 2 bolts and ASTM A 307A bolts. Additional connection details are included in section 3.3.

4.3.3.1 Monotonic Tests

Six monotonic tests were performed using the mode IV configuration described above. Three of the tests featured a bolt-spacing equal to seven times the bolt diameter (7D), while the other three tests featured a bolt-spacing equal to eight times the bolt diameter (8D). Two of the tested assemblies are shown in Figure 4.15.

Figure 4.15: Example Connections from 47m and 48m Data Sets

Following each monotonic test, the bolts were removed from the test specimens and photographed. Upon inspection, each set of bolts from the 47m and 48m data sets featured mode IV yielding as its predominant yield behavior. These results satisfied the yield mode predictions described in section 4.2.4, and the mode IV configuration was therefore approved for the reverse-cyclic tests. Two sets of the tested bolts are shown below in Figure 4.16. Two plastic hinge points per bolt are indicative of mode IV yielding and are visible in these photographs.

Figure 4.16: Example Groups of Tested Bolts from 47m and 48m Data Sets

A load-deflection curve was generated for each monotonic test. These curves were subsequently fitted with a 5% offset line and modeled using an E.E.P. curve. These procedures followed the methods of data analysis described in section 3.5.2. An example of a typical load-deflection curve and E.E.P. curve fit from the 47m data set is shown below in Figure 4.17. See Appendix B for all other monotonic curves.

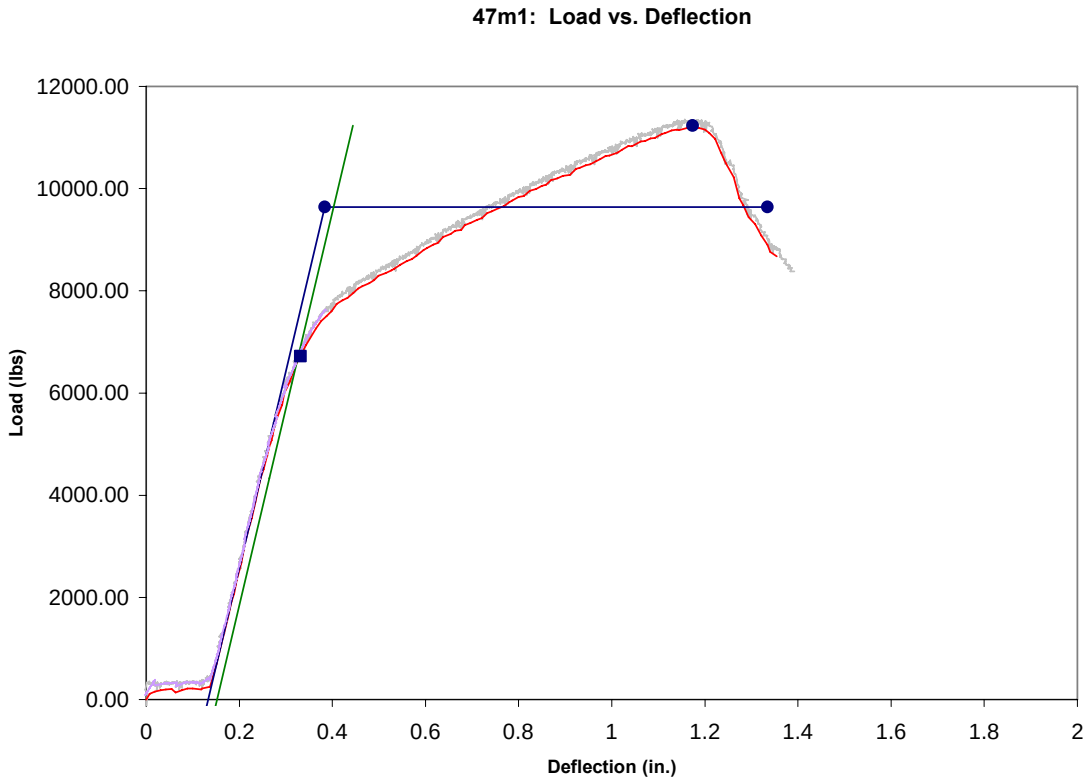

Figure 4.17: Example Load vs. Deflection Plot and E.E.P. Curve-Fit from 47m Data Set

Once the load-deflection curves, E.E.P. curves, and 5% offset lines were generated, five specific points were located and four other relevant values were calculated. The five points included: the point of maximum load, the failure point, the point at which the load equaled forty percent of the maximum load, the E.E.P. yield point, and the 5% offset yield point. The four calculated values included: the elastic stiffness, the slack, the E.E.P. energy, and the ductility ratio. These points and values are described in detail in section 3.5.2, and are included below in Tables 4.11 and 4.12. The mean values for the seven strength and serviceability parameters are included in Table 4.13.

Table 4.11: Monotonic Test Results for Mode IV with 7D Spacing

	47m1	47m2	47m3	MEAN	STDEV	COV (%)
Max Load (lbs) =	11230	9360	9920	10170	960	9.44
Displacement (in) =	1.17	0.86	1.01	1.02	0.16	15.27
Failure Load (lbs) =	8900	7220	7870	7997	847	10.59
Disp. @ Failure (in) =	1.33	0.94	1.11	1.13	0.20	17.41
40% Max (lbs) =	4330	3480	3840	3883	427	10.99
Displacement (in) =	0.25	0.20	0.18	0.21	0.03	16.29
E.E.P. Yield (lbs) =	9640	8270	8460	8790	742	8.44
Displacement (in) =	0.38	0.31	0.30	0.33	0.05	14.32
5% Offset Yield Load (lbs) =	6720	5590	5820	6043	597	9.88
Displacement (in) =	0.33	0.27	0.25	0.28	0.04	14.59
Elastic Stiffness (lb/in.)=	38500	44200	39400	40700	3064	7.53
Slack (in) =	0.13	0.12	0.08	0.11	0.03	23.92
E.E.P. Energy (lb*in) =	10370	6010	7820	8067	2190	27.15
Ductility Ratio =	3.48	3.05	3.75	3.43	0.35	10.36

Table 4.12: Monotonic Test Results for Mode IV with 8D Spacing

	48m1	48m2	48m4	MEAN	STDEV	COV (%)
Max Load (lbs) =	9710	7470	9850	9010	1336	14.82
Displacement (in) =	1.14	0.38	1.19	0.90	0.45	50.20
Failure Load (lbs) =	7520	5940	7730	7063	978	13.85
Disp. @ Failure (in) =	1.61	0.51	1.36	1.16	0.58	49.82
40% Max (lbs) =	3870	2810	3760	3480	583	16.75
Displacement (in) =	0.19	0.12	0.23	0.18	0.06	32.87
E.E.P. Yield (lbs) =	9050	6730	8400	8060	1197	14.85
Displacement (in) =	0.31	0.21	0.35	0.29	0.07	25.27
5% Offset Yield Load (lbs) =	6330	5220	5670	5740	558	9.73
Displacement (in) =	0.27	0.19	0.30	0.26	0.06	22.18
Elastic Stiffness (lb/in.)=	43300	42400	39600	41770	1930	4.62
Slack (in) =	0.10	0.05	0.14	0.10	0.04	45.79
E.E.P. Energy (lb*in) =	12710	2560	9360	8210	5172	62.99
Ductility Ratio =	5.15	2.45	3.89	3.83	1.35	35.28

Table 4.13: Mean Values for Strength and Serviceability Parameters, Mode IV, Monotonic

	47m (7D)	48m (8D)
Max Load (lbs) =	10170	9010
Failure Load (lbs) =	7997	7063
E.E.P. Yield (lbs) =	8790	8060
5% Offset Yield =	6043	5740
Elastic Stiffness (lb/in.)=	40700	41770
E.E.P. Energy (lb*in) =	8067	8210
Ductility Ratio =	3.43	3.83

The loads and displacements included in Tables 4.11 and 4.12 were again taken from actual test data points. Therefore, the failure loads and the 40% loads are not exactly equal to $0.8*F_{max}$ and $0.4*F_{max}$ respectively. They are instead the closest recorded loads. These loads and their corresponding deflections are sufficiently accurate for general post-test analysis and comparisons between spacings; however, they were not used to calculate the monotonic deformation capacities (Δ_m) needed for the CUREE loading protocol used in the reverse-cyclic tests. These deformation capacities were instead calculated using failure loads exactly equal to $0.8*F_{max}$. The deflections at these failure loads were calculated by a linear interpolation between the two nearest points. They were then averaged into two means, one for each spacing. The resulting monotonic deformation capacities were equal to 1.1373 for the 47m data set and 1.1627 for the 48m data set.

4.3.3.2 Reverse-Cyclic Tests

Twenty reverse-cyclic tests were performed using the mode IV configuration. Ten of the tests featured a bolt-spacing equal to seven times the bolt diameter (7D), while the other ten tests featured a bolt-spacing equal to eight times the bolt diameter (8D). Two of the tested assemblies are shown in Figure 4.18.

Figure 4.18: Example Connections from 47c and 48c Data Sets

Following each reverse-cyclic test, the bolts were removed from the test specimens and photographed. Upon inspection, each set of bolts from the 47c and 48c data sets featured mode IV yielding as its predominant yield behavior. These results satisfied the yield mode predictions described in section 4.2.4. Two sets of the tested bolts are shown below in Figure 4.19. Two plastic hinge points per bolt are indicative of mode IV yielding and are visible in these photographs.

Figure 4.19: Example Groups of Tested Bolts from 47c and 48c Data Sets

A load-deflection plot was generated for each reverse-cyclic test. Piece-wise, linear approximations were then formed by connecting the points of maximum load for each cycle. An example of a typical load-deflection plot and linear curve-fit from the 47c data set is shown below in Figure 4.20. See Appendix B for all other reverse-cyclic curve-fits.

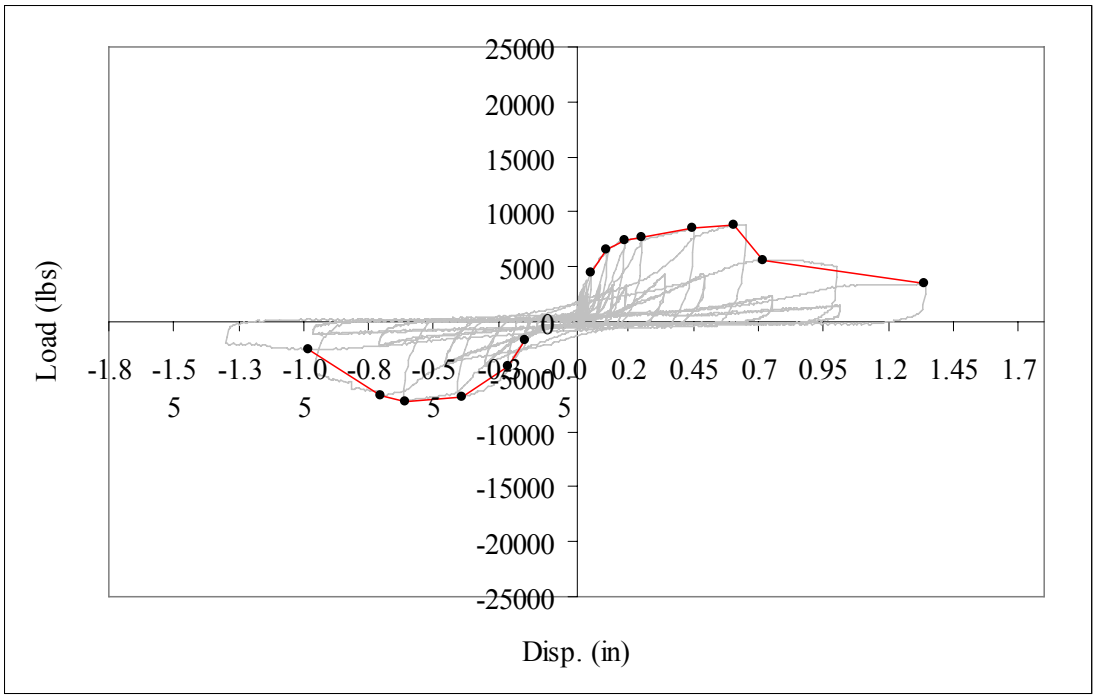

Figure 4.20: Example Load vs. Deflection Plot and Linear Curve-Fit from 47c Data Set

Once the piece-wise curves had been generated, they were modeled using E.E.P. curves and analyzed according to the methods of data analysis described in section 3.5.3. A typical set of E.E.P. curves from the 47c data set is shown below in Figure 4.21. See Appendix B for all other reverse-cyclic E.E.P. curves.

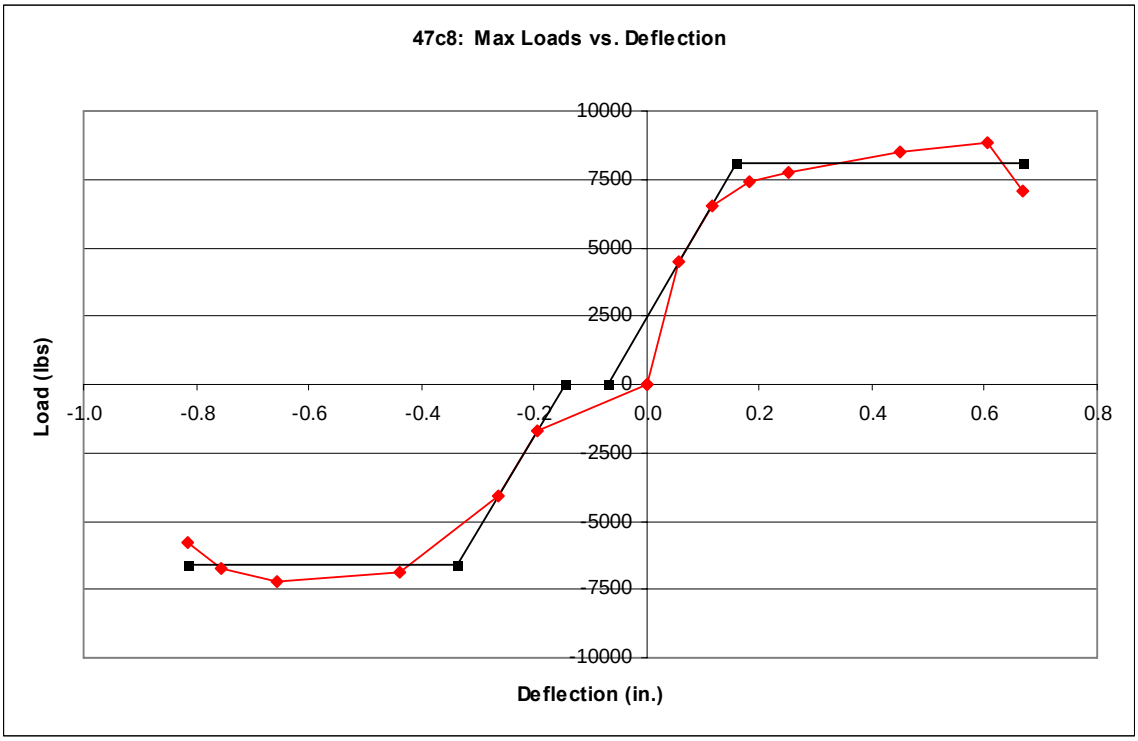

Figure 4.21: Example E.E.P. Curves from 47c Data Set

The linear, piece-wise curves and E.E.P. curves were then used to calculate the seven strength and serviceability parameters described in detail in section 3.5.3. Test values for each of these parameters are included below in Tables 4.14 and 4.15. Table 4.14 contains results from the 37c data set, while Table 4.15 pertains to the 38c data set. In addition, a direct comparison of the mean values for the seven parameters is included in Table 4.16. The test values and means for the seven parameters are also displayed graphically in Figures 4.22 through 4.28. The means are designated in each of these figures.

Table 4.14: Reverse-Cyclic Test Results for Mode IV with 7D Spacing

	Max Load (lbs)	Failure Load (lbs)	Elastic Stiffness (lbs/in.)	5% Offset Load (lbs)	E.E.P. Energy (lbs*in.)	Ductility Ratio	E.E.P. Yield Load (lbs)
47c2	6230	4990	33400	5220	1280	1.88	5610
47c3	8330	6670	36600	5800	8900	5.94	7700
47c4	5920	4740	26300	5550	2690	3.05	5410
47c5	7940	6350	37300	6110	4100	3.27	7380
47c6	8280	6630	34900	6490	3940	2.86	7500
47c7	8750	7000	42100	6990	3920	2.98	8150
47c8	8040	6430	35000	5800	4420	3.36	7360
47c9	9290	7430	36300	5840	10770	6.09	8410
47c10	7100	5680	33800	5640	1980	2.06	6430
47c11	7620	6100	32100	5930	3330	2.69	6830
MEAN	7750	6202	34780	5937	4533	3.42	7078
STDEV	1065	851	4049	499	2997	1.45	1004
COV %	13.74	13.71	11.64	8.41	66.12	42.40	14.19

Table 4.15: Reverse-Cyclic Test Results for Mode IV with 8D Spacing

	Max Load (lbs)	Failure Load (lbs)	Elastic Stiffness (lbs/in.)	5% Offset Load (lbs)	E.E.P. Energy (lbs*in.)	Ductility Ratio	E.E.P. Yield Load (lbs)
48c1	12220	9780	42800	8270	10820	4.57	10660
48c2	10130	8110	43600	7120	8600	4.83	9290
48c4	8570	6850	30800	5460	9120	5.14	7740
48c5	10030	8020	39600	7210	7170	3.95	9030
48c6	10440	8350	44600	7690	11670	5.99	9710
48c7	10250	8200	36200	6860	8500	4.07	9230
48c8	9560	7650	40100	6550	5550	3.46	8650
48c9	7570	6060	28600	6030	2490	2.02	6830
48c10	8930	7150	34900	6160	5510	3.39	8190
48c11	11490	9190	43000	7720	9300	4.20	10400
MEAN	9919	7936	38420	6907	7873	4.16	8973
STDEV	1360	1088	5590	870	2750	1.09	1175
COV %	13.71	13.71	14.55	12.60	34.93	26.14	13.09

Table 4.16: Comparison of Mean Test Values, Mode IV, Reverse-Cyclic

	Mode IV, 7D (47c)	Mode IV, 8D (48c)
Max Load (lbs)	7750	9919
Failure Load (lbs)	6202	7936
5% Offset Load (lbs)	5937	6907
E.E.P. Yield Load (lbs)	7078	8973
E.E.P. Energy (lbs*in.)	4533	7873
Elastic Stiffness (lbs/in.)	34780	38420
Ductility Ratio	3.42	4.16

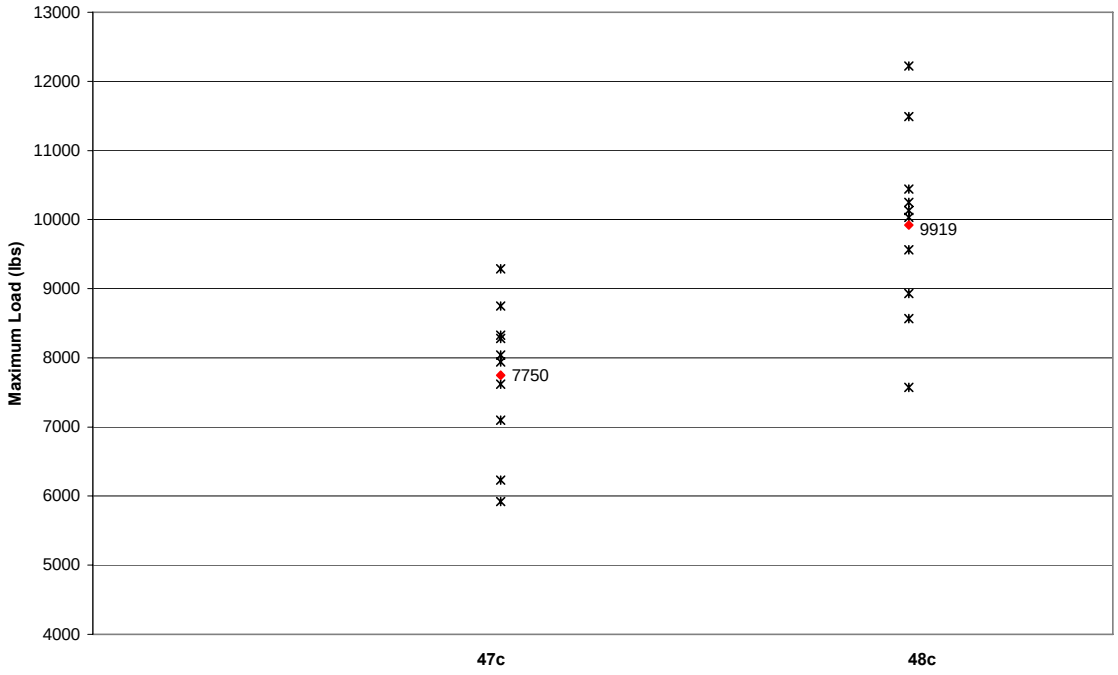

Figure 4.22: Maximum Loads, Mode IV

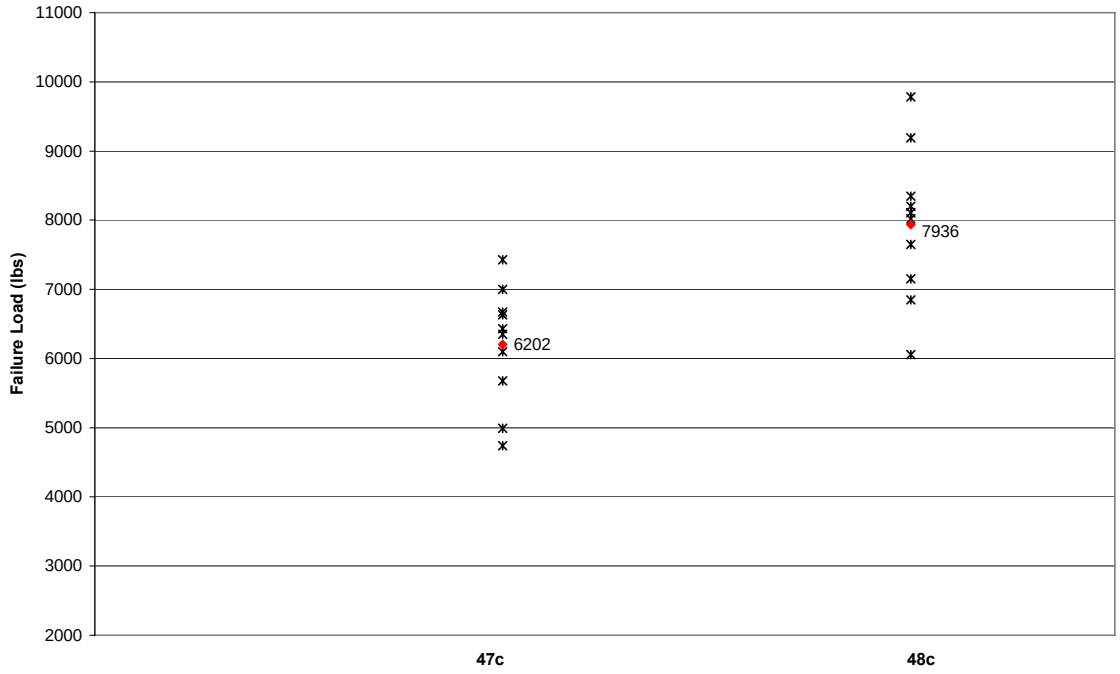

Figure 4.23: Failure Loads, Mode IV

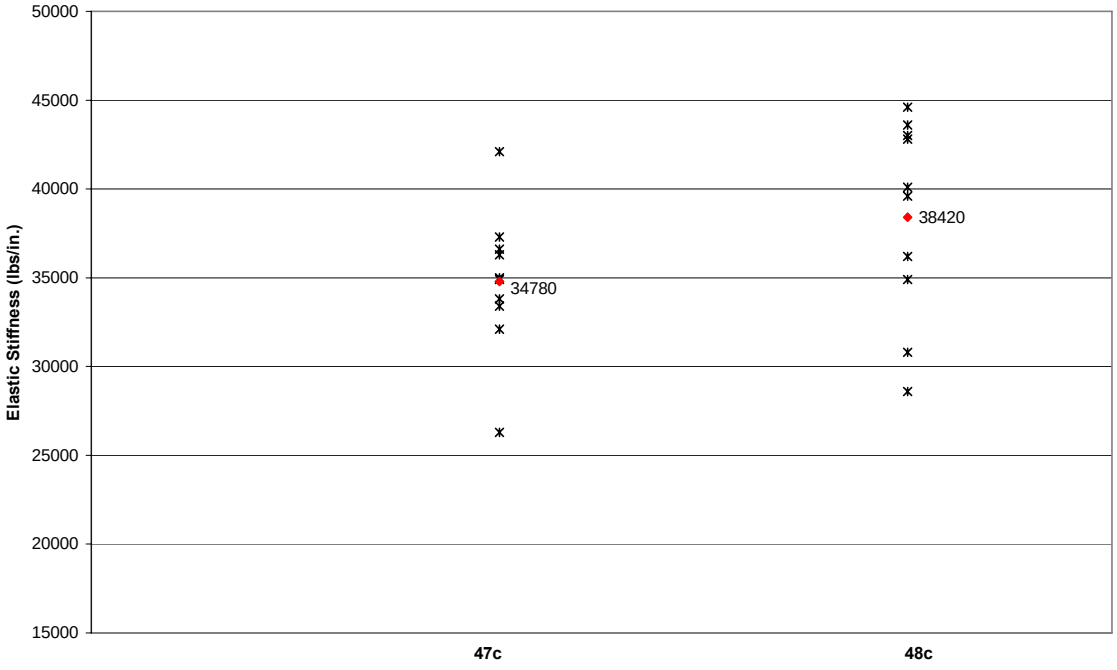

Figure 4.24: Elastic Stiffnesses, Mode IV

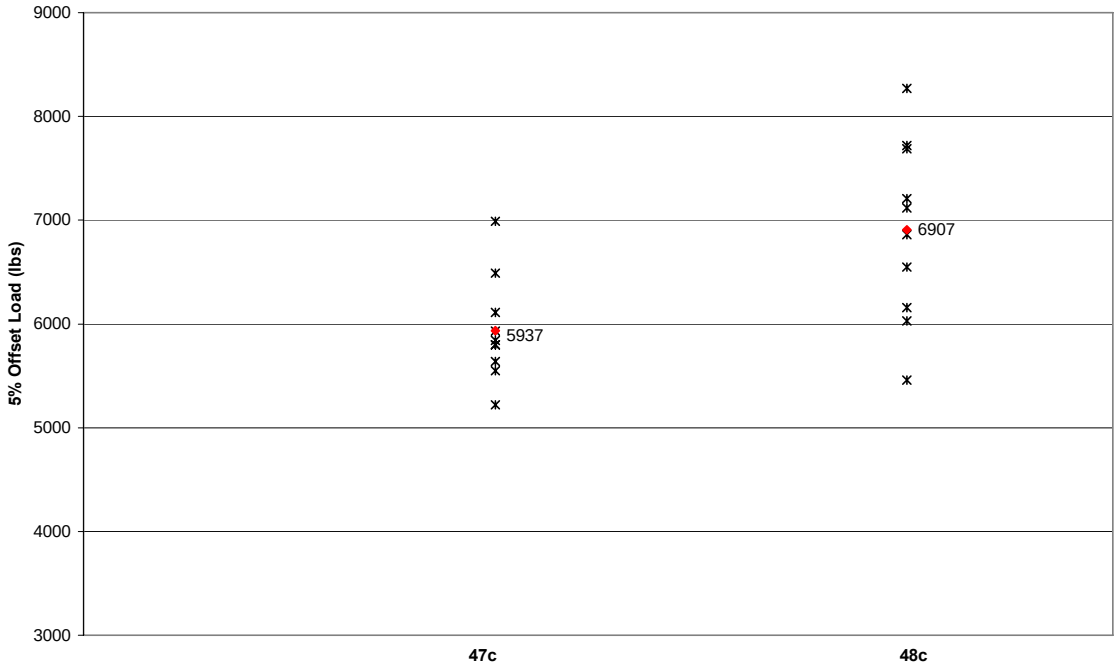

Figure 4.25: 5% Offset Loads, Mode IV

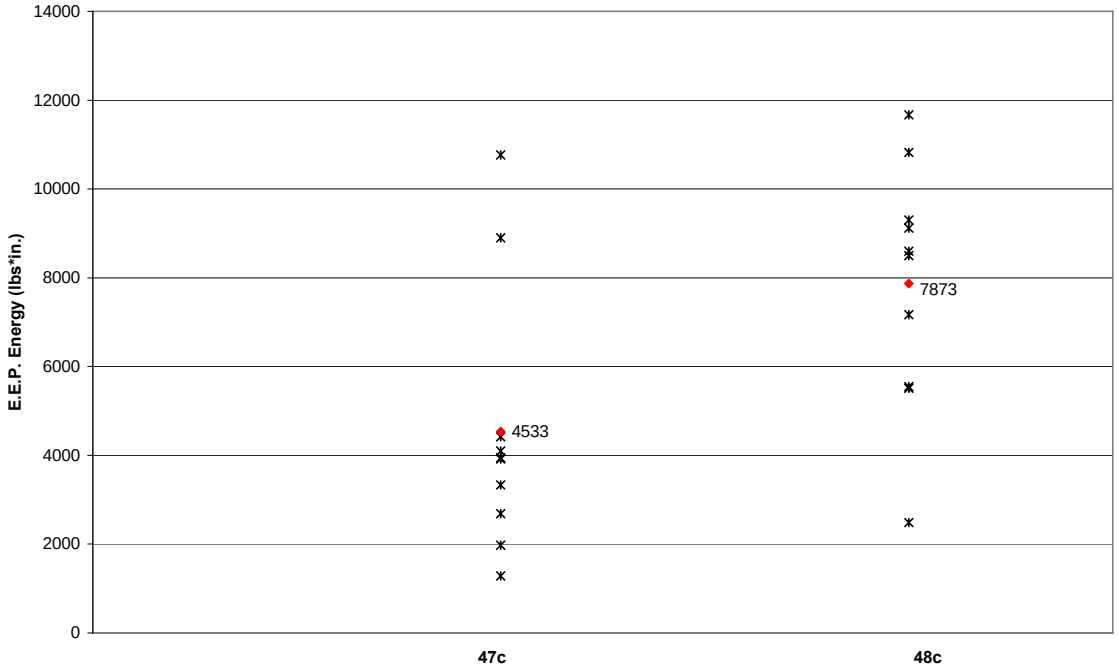

Figure 4.26: E.E.P. Energies, Mode IV

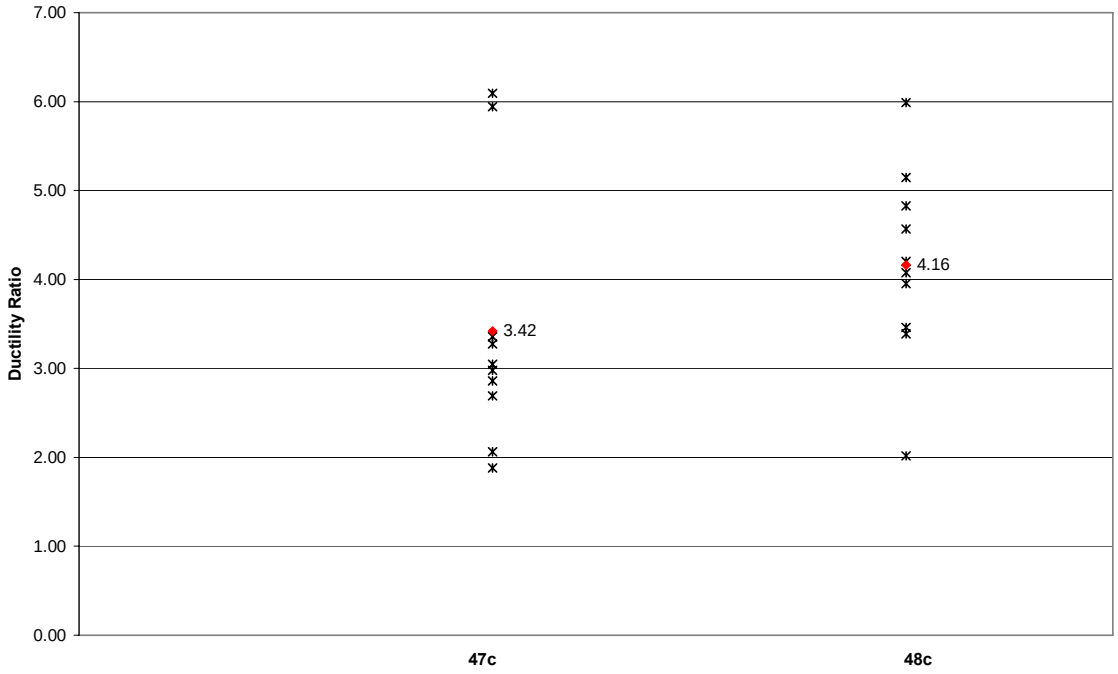

Figure 4.27: Ductility Ratios, Mode IV

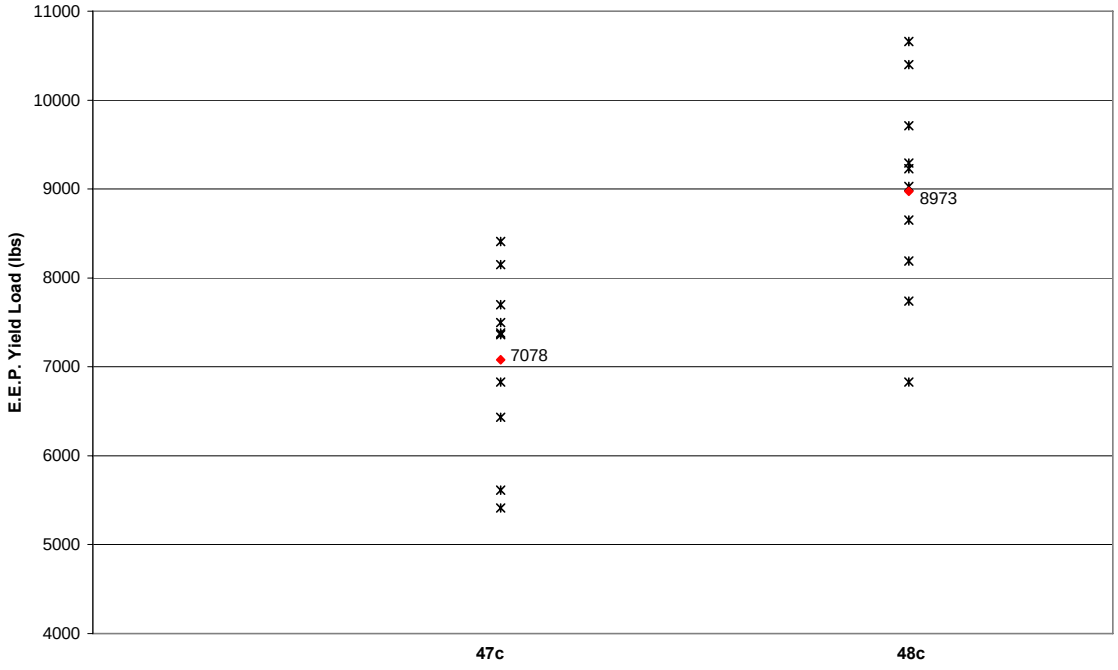

Figure 4.28: E.E.P. Yield Loads, Mode IV

From the mode IV data, it is apparent that the 8D spacing once again resulted in greater connection strengths. The mean values for maximum load, failure load, 5% offset load, and E.E.P. yield load are all higher for the 8D spacing, and the low coefficients of variation for these strength parameters validate this trend.

The results for the serviceability parameters also favor the 8D spacing. The mean values for E.E.P. energy, elastic stiffness, and ductility ratio are each higher for the 8D connections than they are for the 7D connections.

4.3.4 Statistical Analysis

T-tests were performed on the reverse-cyclic data in order to compare the mean values for each bolt spacing. Initially, it was assumed that bolt spacing had no effect on connection behavior. Therefore, the null hypothesis stated that the mean values for the 7D spacings were not statistically different than the mean values for the 8D spacings. This null hypothesis was held to be true unless the t-test returned a P value less than the α value of 0.05, in which case the null hypothesis was rejected. For each t-test it was assumed that the data were normally distributed and had equal variances. Results of the t-tests for each of the seven strength and serviceability parameters are included below in sections 4.3.4.1 and 4.3.4.2.

4.3.4.1 MODE III_s, Reverse-Cyclic

T-test results for the 37c and 38c data sets are included below in Table 4.17. The null hypothesis results are included in Table 4.18.

Table 4.17: t-Test Results for Mode III_s, Reverse-Cyclic

	MODE	α	P
Max Load (lbs)	IIIs	0.050	0.199
Failure Load (lbs)	IIIs	0.050	0.199
Elastic Stiffness (lb/in.)	IIIs	0.050	0.455
5% Offset Load (lbs)	IIIs	0.050	0.404
E.E.P. Energy (lbs*in.)	IIIs	0.050	0.859
Ductility Ratio	IIIs	0.050	0.242
E.E.P. Yield Load (lbs)	IIIs	0.050	0.193

Table 4.18: Null Hypothesis Results for Mode III_s, Reverse-Cyclic

	MODE	NULL HYPOTHESIS
Max Load (lbs)	IIIs	CAN NOT REJECT
Failure Load (lbs)	IIIs	CAN NOT REJECT
Elastic Stiffness (lb/in.)	IIIs	CAN NOT REJECT
5% Offset Load (lbs)	IIIs	CAN NOT REJECT
E.E.P. Energy (lbs*in.)	IIIs	CAN NOT REJECT
Ductility Ratio	IIIs	CAN NOT REJECT
E.E.P. Yield Load (lbs)	IIIs	CAN NOT REJECT

Table 4.18 shows that the null hypothesis could not be rejected for any of the seven parameters. Thus, it is clear that the differences in performance between the 37c connections and the 38c connections were not great enough to be statistically significant. According to the statistical analysis, the mode III_s testing was inconclusive.

4.3.4.2 MODE IV, Reverse-Cyclic

T-test results for the 47c and 48c data sets are included below in Table 4.19. The null hypothesis results are included in Table 4.20.

Table 4.19: t-Test Results for Mode IV, Reverse-Cyclic

	MODE	α	P
Max Load (lbs)	IV	0.050	0.001
Failure Load (lbs)	IV	0.050	0.001
Elastic Stiffness (lb/in.)	IV	0.050	0.112
5% Offset Load (lbs)	IV	0.050	0.007
E.E.P. Energy (lbs*in.)	IV	0.050	0.018
Ductility Ratio	IV	0.050	0.211
E.E.P. Yield Load (lbs)	IV	0.050	0.001

Table 4.20: Null Hypothesis Results for Mode IV, Reverse-Cyclic

	MODE	NULL HYPOTHESIS
Max Load (lbs)	IV	REJECT
Failure Load (lbs)	IV	REJECT
Elastic Stiffness (lb/in.)	IV	CAN NOT REJECT
5% Offset Load (lbs)	IV	REJECT
E.E.P. Energy (lbs*in.)	IV	REJECT
Ductility Ratio	IV	CAN NOT REJECT
E.E.P. Yield Load (lbs)	IV	REJECT

Table 4.20 shows that the null hypothesis was rejected for five of the seven parameters, including all four of the strength parameters. According to the t-tests, the 48c connections were strong enough and absorbed enough energy relative to the 47c connections to be statistically significant. Thus, while the results for elastic stiffness and ductility ratio were inconclusive, the 8D spacing is clearly optimal for the mode IV connections based on its higher mean values for maximum load, failure load, 5% offset load, E.E.P. yield load, and E.E.P. energy.

4.3.5 Dowel Embedment Tests

The dowel embedment strength (F_e) was measured in order to provide insight into the strength of the wood members that had made up each tested connection. The dowel embedment strengths are summarized in Tables 4.21 and 4.22. Values pertaining to monotonic members are included in Table 4.21 and values pertaining to reverse-cyclic members are included in Table 4.22. See Appendix B for the entire list of dowel embedment strengths.

Table 4.21: Dowel Embedment Strength (F_e), Monotonic Testing

2x6's

	F_e (lbs)
MEAN	2957
STDEV	504
COV %	17.0

4x6's

	F_e (lbs)
MEAN	2510
STDEV	340
COV %	13.5

Table 4.22: Dowel Embedment Strength (F_e), Reverse-Cyclic Testing

2x6's

	F_e (lbs)
MEAN	2925
STDEV	420
COV %	14.4

4x6's

	F_e (lbs)
MEAN	2493
STDEV	435
COV %	17.4

As expected, the mean values for the monotonic members were similar to those pertaining to the reverse-cyclic members. In both cases, the 4x6, Mixed Southern Pine members featured lower dowel embedment strengths than their 2x6, Southern Yellow Pine counterparts. This difference was expected based on the differing specific gravities discussed below in section 4.3.6.

4.3.6 Moisture Content and Specific Gravity

Moisture contents and specific gravities were measured in order to provide further insight into the physical properties of the wood members that had made up each tested connection. The moisture contents and specific gravities are summarized in Tables 4.23 and 4.24. Values pertaining to monotonic members are included in Table 4.23 and values pertaining to reverse-cyclic members are included in Table 4.24. See Appendix B for the entire lists of moisture contents and specific gravities.

Table 4.23: Moisture Content (MC) and Specific Gravity (SG), Monotonic Testing

2x6's

	MC	SG
MEAN	11.99	0.56
STDEV	1.53	0.06
COV %	12.73	9.86

4x6's

	MC	SG
MEAN	16.89	0.51
STDEV	0.63	0.06
COV %	3.76	10.88

Table 4.24: Moisture Content (MC) and Specific Gravity (SG), Reverse-Cyclic Testing

2x6's

	MC	SG
MEAN	13.80	0.56
STDEV	1.09	0.06
COV %	7.91	10.36

4x6's

	MC	SG
MEAN	16.86	0.50
STDEV	0.85	0.06
COV %	5.06	12.07

As expected, the mean values for the monotonic members were similar to those pertaining to the reverse-cyclic members. In both cases, the 4x6 Mixed Southern Pine members featured lower specific gravities and higher moisture contents than their 2x6, Southern Yellow Pine counterparts. The difference in specific gravities was expected based on the values listed in Table 11.3.2A of the NDS (AF&PA, 2001). The mean specific gravity of 0.56 for the 2x6 members was 1.80% higher than the listed value of 0.55, while the mean value of 0.505 was only 0.98% lower than the listed value of 0.51. The higher moisture contents for the 4x6's were the result of the larger cross-section, which necessitated a longer drying time relative to the thinner 2x6 members. While higher than the desired 12% in three out of four cases, the moisture contents were each close enough to the mark to uphold the integrity of the connection test results. In addition, all moisture contents were less than 19%, which kept the wet service factor (C_M) from being applicable (see Appendix A).

4.3.7 Summary of Connection Testing

The connection testing was performed in order to gain insight into the effect of bolt spacing on the strength and serviceability of mode III and mode IV connections subjected to reverse-cyclic loading. This "re-testing" was recommending by Billings (2004) after her tests failed to demonstrate consistent mode III or mode IV behavior. Billings' suggestions for further research also included preliminary material and connection testing to ensure the desired yield modes.

This particular recommendation was followed intently, as both the bending yield strength (F_{yb}) of the bolts and the dowel embedment strength (F_e) of the wood specimens were measured, rounded conservatively, and included in the preliminary yield limit calculations (see section 4.2). These calculations subsequently affirmed that both of the proposed connection configurations should produce their intended yield mode. The proposed mode III_s configuration included a single row of five low-carbon steel bolts, a 4x6 Mixed Southern Pine main member, and a 2x6 Southern Yellow Pine side member. Each bolt was approximately 6-in. (15.24 cm) long and 3/8-in. (0.95 cm) in diameter. The proposed mode IV configuration included a single row of five low-carbon steel bolts,

a 4x6 Mixed Southern Pine main member, and a 4x6 Mixed Southern Pine side member. Each bolt was approximately 8-in. (20.32 cm) long and 3/8-in. (0.95 cm) in diameter.

Two between-bolt spacings were tested as independent variables. The spacings were seven times the bolt diameter (7D) and eight times the bolt diameter (8D). The 7D spacing was selected because it was specifically recommended in Anderson's conclusions (2001), and because tests by Billings (2004) suggested that it was the optimal case. The 8D spacing was selected because it had not been sufficiently tested before. In her testing, Billings included a set of connections with 8D spacings between bolts, but dimensional constraints of the testing machine limited her to a 7D end-distance. Thus, her data set did not include a true 8D case.

A series of monotonic tests were first performed on the connections in order to calculate the monotonic deflection capacities (Δ_m) needed for the CUREE reverse-cyclic loading protocol. These deflection capacities were calculated by averaging the deflections at failure for each connection type, where failure was defined as the point at which the load dropped to 80% of the maximum load. In addition to contributing the deflection capacities, the monotonic tests offered some noteworthy results. For both the mode III_s and mode IV connections, the 7D spacing demonstrated superior strength and slightly inferior serviceability compared to the 8D spacing. However, these results are based on only three specimens from each data set, and further monotonic testing is needed to validate these trends.

The reverse-cyclic tests were performed using the CUREE loading protocol (see section 3.3.7), and were evaluated based on the seven strength and serviceability parameters defined by Billings (2004). These parameters included maximum load, failure load, E.E.P. yield load, 5% offset load, elastic stiffness, E.E.P. energy, and ductility ratio.

Upon testing, the 8D spacing resulted in higher strength and comparable serviceability in the case of the mode III_s connections. However, t-tests demonstrated that the differences in performance were not great enough to be statistically significant. In the case of the

mode IV connections, the 8D spacing resulted in higher strength and superior serviceability. This time, however, the statistical analysis demonstrated that the higher mean values for maximum load, failure load, E.E.P. yield load, 5% offset load, and E.E.P. energy were statistically significant. In addition, both the mode III_s connections and the mode IV connections featured bolt behavior consistent with their predicted yield modes, meaning that the test results can be accurately applied in discussions of these yield cases. Thus, from the test data, it can be stated conclusively that an 8D bolt spacing results in better performance than a 7D spacing for connections subject to reverse-cyclic loading and mode IV yielding. It can also be stated that an 8D spacing tends to result in better performance for connections subject to reverse-cyclic loading and mode III_s yielding, though these results were not conclusive.

4.4 Bolt Tests

4.4.1 General

For this part of the project, three different test methods were employed to measure the bending yield strength (F_{yb}) of low-carbon steel bolts. The three test methods included tension tests, 3-point bending tests, and cantilever bending tests, and are described in detail in section 3.2. Once the tests were completed, the data from the 3-point bending and cantilever bending tests were compared with one another. A high correlation between these data would tend to support the accuracy of both testing methods.

While all bolts were made of low-carbon steel, they did vary in length and diameter in order to make sure that a broad spectrum of common dimensions was considered. These sizes and the number of replications performed are included in Table 3.2 of chapter 3. In addition, the bolt grades and manufacturers for each sample set are included in Table 3.3.

The decision to test the bolts in tension was made based on the following statement from NDS Appendix I4: "Research indicates that F_{yb} for bolts is approximately equivalent to the average of bolt tensile yield strength and bolt tensile ultimate strength." Upon testing, however, it became apparent that the elongations required for the calculation of tensile

yield strength could not be measured accurately. As a result, the tensile testing was aborted. Details of the initial tensile tests and the problems encountered are recorded in section 4.4.2.

The remaining two test methods presented no such problems of measurement and resulted in unhindered calculations of F_{yb}. The results of the 3-point bending tests are included in section 4.4.3, and the results of the cantilever bending tests are included in section 4.4.4. Finally, a comparison between these two data sets is included in section 4.4.5.

4.4.2 Tensile Tests

The setup for the tensile tests is illustrated below in Figure 4.29, and is described in detail in section 3.2.5.

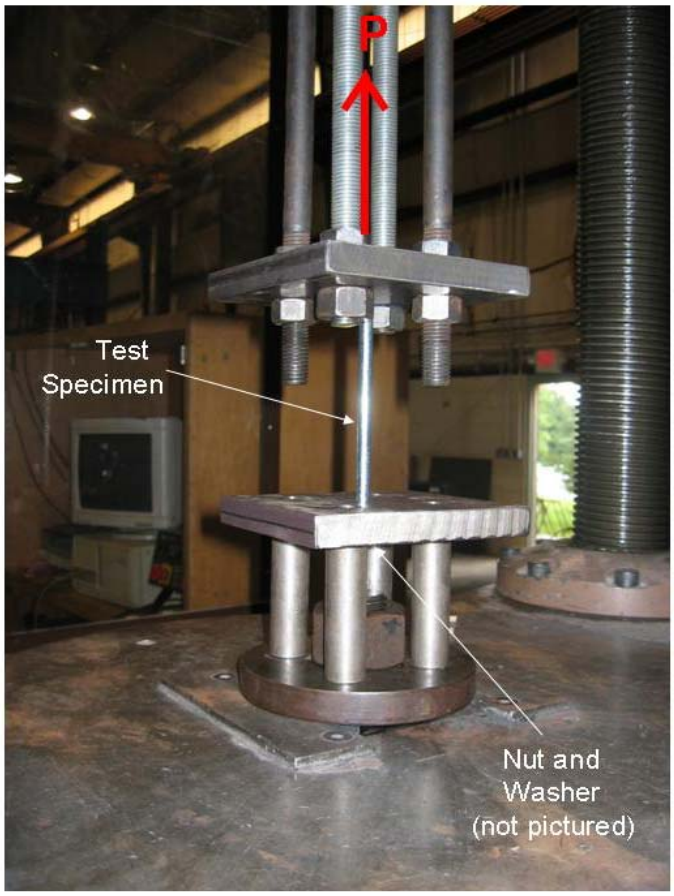

Figure 4.29: Tensile Test Apparatus

In addition to the apparatus pictured above, it was intended that an extensometer be attached to each test specimen in order to measure the elongation during testing. However, when a series of trial tests were performed without an extensometer, it was shown that the bolts failed consistently in their tapered or threaded portions (see Figures 4.30 and 4.31).

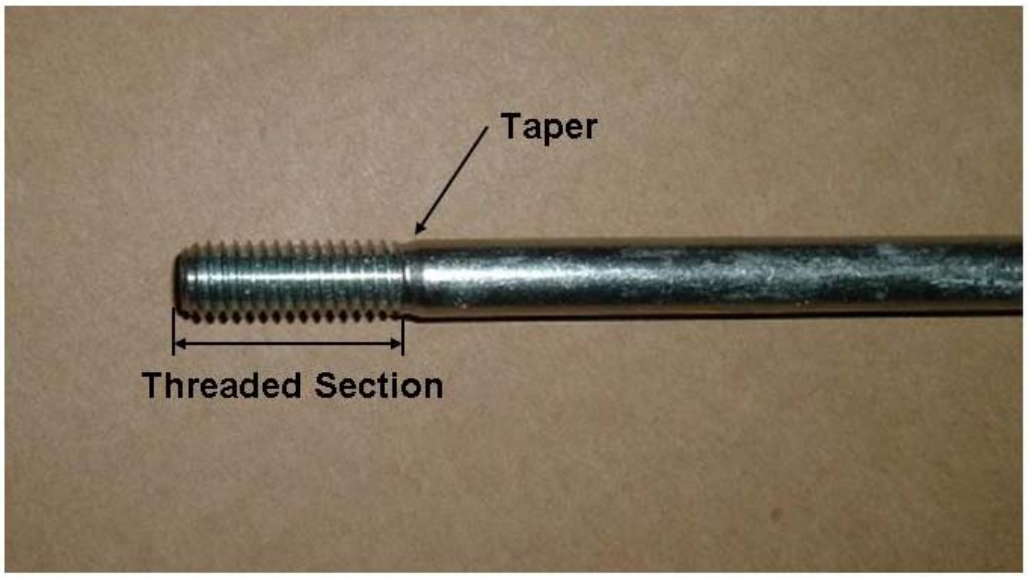

Figure 4.30: Typical Bolt Specimen

Figure 4.31: Failure in Threaded Section

The tendency to fail in the tapered or threaded regions was the result of the small cross-sectional area of these regions relative to the bolt shafts. This difference in cross-sectional area was accounted for in the yield stress calculations by the inclusion of the thread stress area (A_s) in the divisor (see section 2.4.4 and Equation 2.2), but it presented a challenge to mounting an extensometer to the bolt specimens. For effective readings, the span of the extensometer needs to include the location of failure, as this is where all critical yielding takes place (see Figure 4.32). This was not possible with the failures occurring in and around the bolt threads.

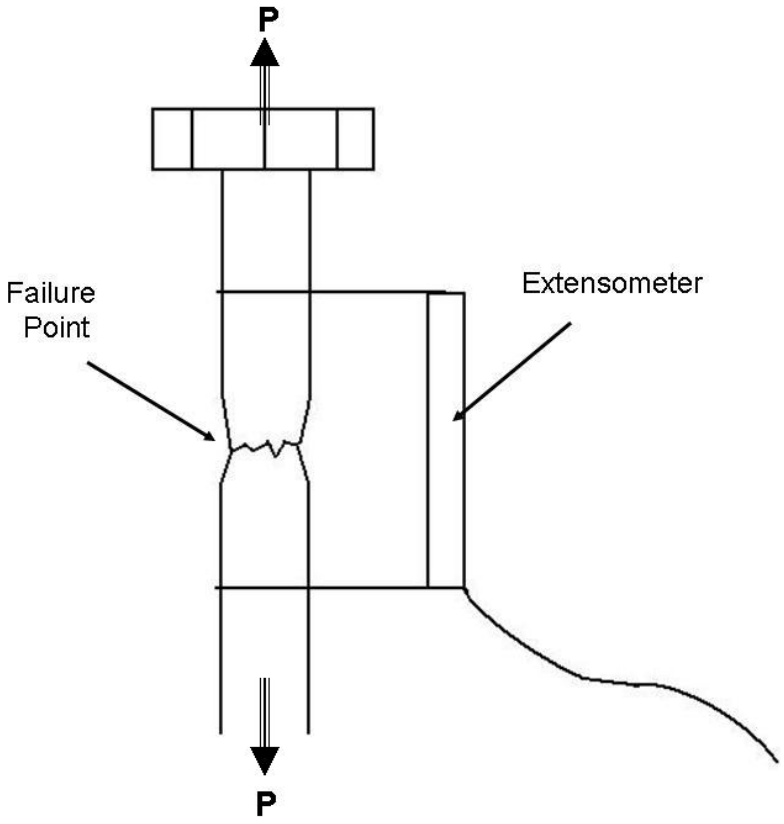

Figure 4.32: Ideal Extensometer Location

Three potential solutions presented themselves but were ultimately discounted. The first was to rely on the elongation measurements recorded by the testing machine's own LVDT. However, with so many other components to the test setup, it would have been difficult to extract the elongation of the test specimen out of the total deflection of the system. A different apparatus might have been developed, but the LVDT measurements would always be less accurate than those recorded directly by an extensometer. The second proposed solution was to try and force the failure point into the bolt shafts by adding enough nuts to completely cover the threaded portions of the bolts. This action, however, would have left the tapered section of the bolt exposed, meaning that the failure point would simply move from the threads to the taper, and not into the shaft. The third proposed solution involved the manufacture of a treaded steel sleeve to fit snuggly over

the threaded and tapered sections of each specimen. Such a sleeve would double as a nut and as a mechanism for forcing the failure point into the bolt shafts. This setup might have succeeded in forcing the shafts to yield. If it did work, however, this measure would only allow for the testing of the 6-in. (15.24) and 8-in. (20.32) bolts. The exposed shaft length of the 4-in. (10.16 cm) bolts would not have been long enough to fit the 2-in. (5.08 cm) extensometer available for use.

Additionally, correspondences with Dr. Thomas Murray, a professor of structural engineering at Virginia Tech, and Roger Hamilton of NUCOR Fasteners revealed that direct tensile measurements of bolt yield strength are almost never made, and that the listed yield strengths for bolts are based on various other test procedures such as proof loading, core hardness tests, and wedge tests. These correspondences combined with the results of the trial tests led to the termination of tensile testing as part of this project.

4.4.3 3-Point Bending Tests

A total of 80 bolts were tested using the 3-point method described in section 2.4.5. The load and the deflection were measured during each test and the relationship between these values provided the basis for analysis. In order to isolate the bending yield stresses (F_{yb}) the shear deflections (Δ_V) were calculated as functions of the load and were subtracted from the total deflections reported by the test machine. The formula for simple-span shear deflection was derived using energy equations, and is given below as Equation 4.2 (Boresi, et. al., 2003).

$$\Delta_V = \frac{PL}{3AG} \tag{4.2}$$

where: P = load (lbs)

L = s_{bp} = length between supports (in.)

A = cross-sectional area of bolt (in.^{2})

G = shear modulus = 11x10^6 psi for steel

Once the shear deflections were calculated and subtracted out, the remaining deflection values were taken to represent bending deflections (Δ_B). The loads recorded during testing were plotted against these bending deflections. In addition, a 5% offset line was generated for each sample according to the procedure described in section 2.4.5. One of the resulting plots containing a load-deflection curve and 5% offset line is shown below in Figure 4.33. This and all other data plots pertaining to the 3-point tests are also contained in Appendix C.

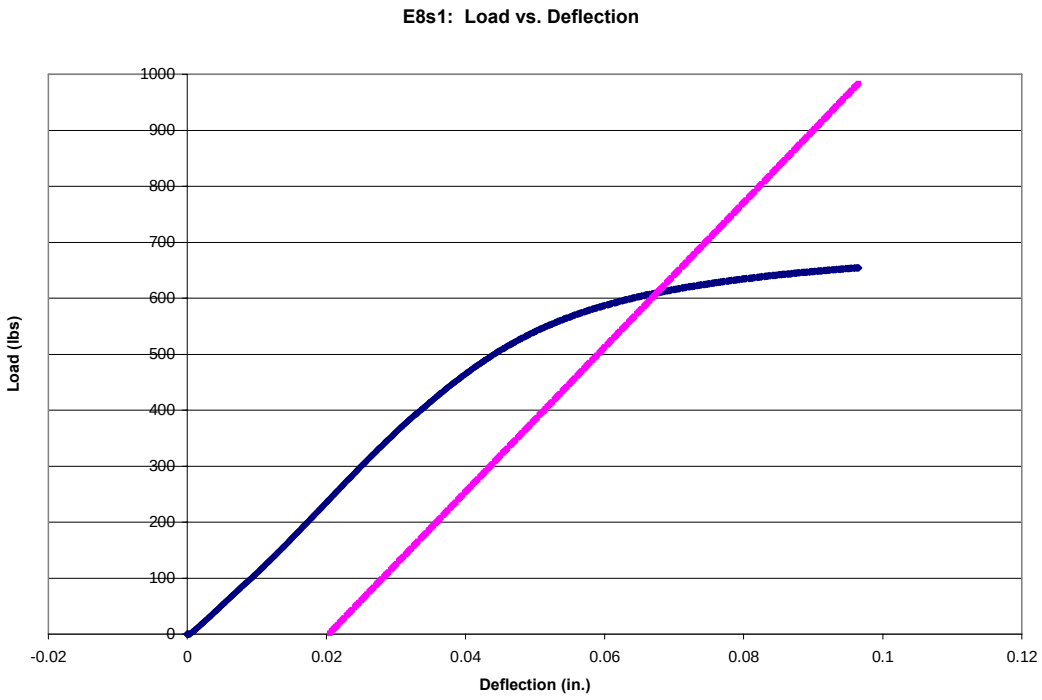

Figure 4.33: Example Load-Deflection Curve and 5% Offset Line, 3-point Method

Finally, the bending yield strengths were calculated using the 5% offset yield loads, located at the intersections of the load-deflection curves and 5% offset lines (see Figure 4.33), and Equations 2.3 and 2.4 from section 2.4.5. The mean bending yield strengths for each of the eight sample sets are recorded below in Table 4.25. The 5% offset loads for each specimen are listed in Appendix C.

Table 4.25: Bending Yield Strengths (F_{yb}) for 3-Point Tests

Nominal Diameter (in.)	Length (in.)	Span (in.)	L/D	F_{yb} (psi)
3/8	4	2.25	6.00	90,300
	6	4.30	11.47	77,500
	8	4.30	11.47	76,900
1/2	4	2.25	4.50	100,000
	6	4.00	8.00	85,900
	8	5.80	11.60	67,000
3/4	6	3.50	4.67	100,800
	8	5.00	6.67	65,000

It was expected that the bending yield strengths would be comparable between data sets. However, for each of the three bolt diameters tested, F_{yb} decreased as the L/D ratio, which is equal to the span divided by the nominal diameter, increased. One hypothesis maintained that material deflections at the point of load application and at the supports could have had an effect on these yield strength values. Such material deflections, however, could not have changed the recorded yield strengths unless the bolts were yielding at the supports prior to yielding in bending. In this case, though, one would expect greater yielding at the supports, and therefore lower yield strengths, in the cases of the shorter spans. Thus, if yielding at the supports occurred, it served only to lessen the still-large margin between the yield strengths. Further analyses of these results and their relationship to the results of the cantilever tests are included in section 4.4.5.

4.4.4 Cantilever Bend Tests

A total of 90 bolts were tested using the cantilever method described in section 2.4.6. The load and the deflection were measured during each test and the relationship between these values provided the basis for analysis. In order to isolate the bending yield stresses (F_{yb}) the shear deflections (Δ_V) were calculated as functions of the load and were subtracted from the total deflections reported by the test machine. The formula for

cantilever shear deflection was derived using energy equations, and is given below as Equation 4.3 (Boresi, et. al., 2003).

$$\Delta_V = \frac{4PL}{3AG} \tag{4.3}$$

where: P = load (lbs)
L = moment arm (in.)
A = cross-sectional area of bolt ($in.^2$)
G = shear modulus = $11x10^6$ psi for steel

Once the shear deflections were calculated and subtracted out, the remaining deflection values were taken to represent bending deflections (Δ_B). The loads recorded during testing were plotted against these bending deflections. In addition, a 5% offset line was generated for each sample according to the procedure described in section 2.4.5. One of the resulting plots containing a load-deflection curve and 5% offset line is shown below in Figure 4.34. This and all other data plots pertaining to the cantilever tests are also contained in Appendix C.

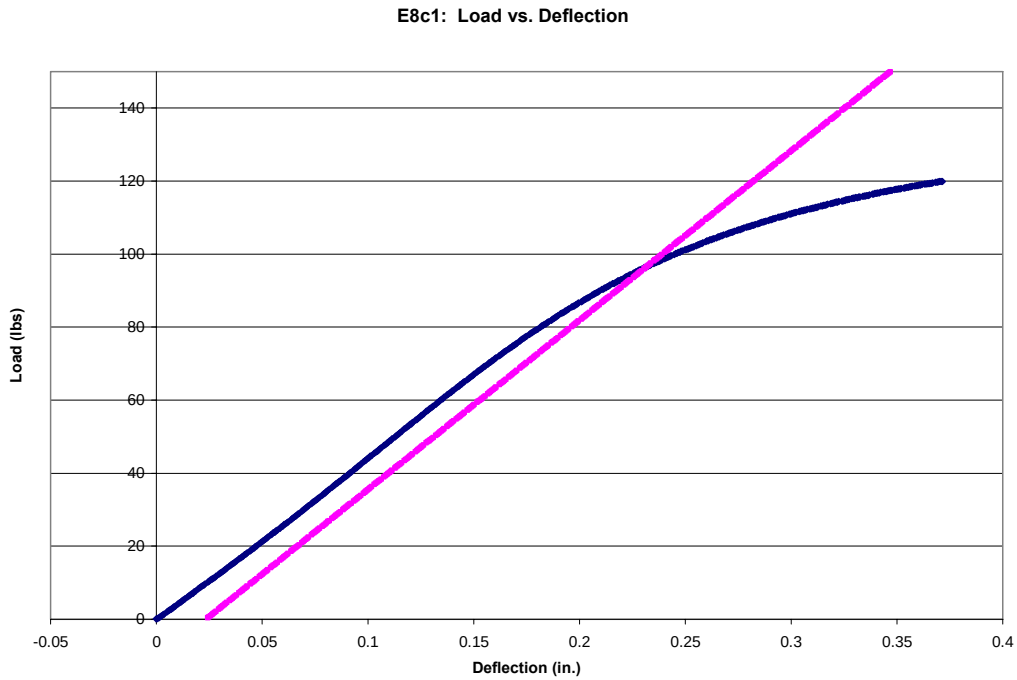

Figure 4.34: Example Load-Deflection Curve and 5% Offset Line, Cantilever Method

Finally, the bending yield strengths were calculated using the 5% offset yield loads, located at the intersections of the load-deflection curves and 5% offset lines (see Figure 4.34), and Equation 2.5 from section 2.4.6. The mean bending yield strengths for each of the nine sample sets are recorded below in Table 4.26. The 5% offset loads for each specimen are listed in Appendix C.

Table 4.26: Bending Yield Strengths (F_{yb}) for Cantilever Tests

Nominal Diameter (in.)	Length (in.)	Span (in.)	L/D	F_{yb} (psi)
3/8	4	2.00	5.33	59,400
	6	3.50	9.33	67,400
	8	5.00	13.33	56,200
1/2	4	2.00	4.00	91,100
	6	3.50	7.00	72,900
	8	5.00	10.00	55,800
3/4	4	1.25	1.67	91,100
	6	3.00	4.00	83,700
	8	4.00	5.33	55,200

As was the case for the 3-point tests, F_{yb} tended to decrease as L/D increased. The only deviation from this trend was likely due to a different bolt manufacturer for the 3/8"x6" specimens. Recall that the 3/8"x6" bolts featured manufacturer's stamps of "BL" while the 3/8"x4" and 3/8"x8" specimens featured manufacturer's stamps of "HKT." Further analyses of these results and their relationship to the results of the 3-point tests are included in section 4.4.5.

4.4.5 Comparison Between Bending Test Methods

Table 4.27 includes a comparison between the bending yield strengths measured using the 3-point method and those measured using the cantilever method.

Table 4.27: Comparison of F_{yb} from Both Bending Test Methods

Nominal Diameter (in.)	Length (in.)	3-point Fyb (psi)	Cantilever Fyb (psi)	% Difference
3/8	4	90,300	59,400	33.8
3/8	6	77,500	67,400	13.2
3/8	8	76,900	56,200	27.4
1/2	4	100,000	91,100	8.9
1/2	6	85,900	72,900	15.3
1/2	8	67,000	55,800	16.6
3/4	6	100,800	83,700	17.0
3/4	8	65,000	55,200	15.2

If both test methods provided accurate measurements of bending yield strength, then the data would be comparable. However, in all cases the 3-point test method resulted in higher values for F_{yb}, with the average difference between methods being 18.40%.

Various explanations for the lower cantilever values were considered. The first hypothesis held that the fixture used for the cantilever tests was slipping or rocking under load, resulting in excessive deflections. However, dial gauges placed to test this possibility reported negligible movement in the fixture. The second hypothesis held that

the lower yield strengths resulted from bolts slipping at the fixed end of the cantilever setup. It is difficult to tell whether or not this occurred. If it did, however, then the slipping was never great enough to be noticeable. A mark was placed on each bolt specimen prior to testing which designated the point at which the bolt was to align with the front of the fixed support. This mark never appeared to move relative to the face of the support. A third hypothesis suggested that the 5% offset method for determining yield load was responsible for magnifying the disparity between the test values. However, an analysis using the proportional limit (0.2% offset) for the yield load resulted in even greater differences for five of the eight data sets.

With each of these possibilities contributing minor influences at best, the differing yield strengths between test methods were likely related to the same factor or factors that led to decreasing yield strengths with increasing L/D ratios. The clear influence of the L/D ratio suggests that both test methods are tending to produce as much or more shear than bending in the cases of the shorter spans. Simply subtracting the shear deflections out of the displacement data is not enough to isolate the effects of bending. With shear exerting such a strong influence in both test methods, it is unlikely that either method can produce an accurate measure of the bending yield strength in the cases of small L/D ratios. On the other hand, the reoccurrence of F_{yb} values between 55,000 and 56,000 psi for some of the cantilever data sets with larger L/D ratios could indicate that the cantilever method is valid for long bolts with small diameters. However, it is difficult to determine whether these similarities are coincidental, and more testing is needed to provide a definitive conclusion.

Chapter 5: Conclusions

5.1 Summary

The primary objective of this project was to expand upon the research of Heine (2001), Anderson (2002), Billings (2004), and others concerning bolted timber connections under reverse-cyclic loading by addressing specific questions that remained following Billings' work. Despite intentions to the contrary, Billings was unable to consistently develop yield modes III and IV. Thus, she could not conclusively recommend a particular between-bolt spacing for connections subject to mode III and mode IV behavior. In response, the research presented in this document was aimed at developing and testing yield modes III and IV specifically. This objective was successfully realized with the help of preliminary yield limit calculations, complete with preliminary measurements of bolt bending yield strength (F_{yb}) and dowel bearing strength (F_e). With yield modes III and IV occurring regularly, optimization of the bolt spacing went forward. Optimization was based on the seven strength and serviceability parameters introduced by Billings. These included: maximum load, failure load, E.E.P. yield load, 5% offset load, elastic stiffness, E.E.P. energy, and ductility ratio.

A second question left over from Billings' work related to her use of a 7D-end distance for her 8D test specimens. Spatial constraints of the test apparatus prevented her from using an 8D end-distance to match her 8D between-bolt spacing, and she employed the 7D end-distance recommended by NDS (AF&PA, 2001) instead. This meant that the behavior of her 8D test specimens might have been controlled by the 7D end-distance rather than the 8D spacing between the bolts. In response, the research presented in this document employed a full 8D end-distance for all 8D specimens tested. This effort was enabled by the relatively small 3/8-in. (0.95 cm) diameter bolts used throughout. The use of these bolts resulted in a small between-bolt spacing and the spatial constraints encountered by Billings were thereby avoided.

In addition to addressing these questions, a second phase of this project was directed at the proper measurement of bending yield strength in bolts. Despite the direct influence

that this parameter has on the yield limit calculations, there was no reliable method for measuring it available to Billings and her predecessors. The 3-point, simple-span test procedure recommended by NDS was not applicable for short bolts with large diameters. Therefore, a cantilever test method was developed and used by Anderson and Billings. The second phase of this project involved extensive testing with both methods and a comparison between the data. In addition, specimens were tested in tension in hopes that a relationship between tensile yield strength and bending yield strength would emerge.

5.2 Conclusions

5.2.1 Connection Tests

Upon testing, the 8D spacing resulted in higher strength and comparable serviceability in the case of the mode III_s connections. However, a statistical analysis demonstrated that the differences in performance were not great enough to be statistically significant. In the case of the mode IV connections, the 8D spacing resulted in higher strength and superior serviceability. This time, however, the statistical analysis demonstrated that the higher mean values for maximum load, failure load, E.E.P. yield load, 5% offset load, and E.E.P. energy were statistically significant. In addition, both the mode III_s connections and the mode IV connections featured bolt behavior consistent with their predicted yield modes, meaning that the test results can be accurately applied in discussions of these yield cases. Thus, from the test data, it can be stated conclusively that an 8D bolt spacing results in better performance than a 7D spacing for connections subject to reverse-cyclic loading and mode IV yielding. It can also be stated that an 8D spacing tends to result in better performance for connections subject to reverse-cyclic loading and mode III_s yielding, though these results were not conclusive.

5.2.2 Bolt Tests

Both the tension and the bending tests proved inconclusive and call for further testing. The data generated by these tests should be viewed as supplemental to the search for a reliable test method rather than definitive proof in any particular direction.

The tension tests predictably resulted in failures located in the tapered or threaded regions of the bolts. This was the result of the small cross-sectional area of these regions relative to the bolt shafts, and it presented a challenge to measuring deformation with an extensometer. For effective readings, the span of the extensometer needs to include the location of failure, as this is where all critical yielding takes place (see Figure 4.32). This was not possible with failures occurring in and around the bolt threads. An accurate measure of the tensile yield strength would therefore require the relocation of the failure point to the bolt shafts. Suggested methods for this relocation are given in section 4.4.2 but were not tested during the course of this project.

The bending tests resulted in two consistent trends. Both the 3-point and cantilever specimens tended to exhibit decreasing bending yield strengths as the L/D ratios increased. In addition, the bending yield strengths of the 3-point specimens were significantly greater than their cantilever counterparts. Both of these trends contradicted the expectation of similar yield strengths across the board. The clear influence of the L/D ratio suggests that both test methods are tending to produce as much or more shear than bending in the cases of the shorter spans. With shear exerting such a strong influence in both test methods, it is unlikely that either method can produce an accurate measure of the bending yield strength in the cases of small L/D ratios. However, the reoccurrence of similar yield strengths for some of the cantilever data sets with larger L/D ratios could indicate that the cantilever method is valid for long bolts with small diameters. It is difficult to determine whether these similarities are coincidental, though, and more testing is needed to provide a definitive conclusion.

5.3 Limitations of the Research

There are various limitations to the research presented in this document. These limitations include:

CONNECTION TESTS

▪Only single-shear connections were tested
▪Only parallel-to-grain loading was tested
▪Only single rows of bolts were tested
▪Only rows consisting of five bolts were tested
▪Only spacings of 7D and 8D were tested
▪Only two species of timber were tested (Southern Yellow Pine, and Mixed Southern Pine)
▪Only specimens within a narrow range of moisture contents were tested
▪Only low-carbon steel bolts were tested (SAE J429 Grade 2, or ASTM A 307A)
▪Only 3/8-in. (0.95 cm) diameter bolts were tested
▪Only one load rate was used for monotonic testing [0.0714 in./min (1.81 mm/min)]
▪Only three specimens per data set were tested monotonically
▪Only ten specimens per data set were tested reverse-cyclically

BOLT TESTS

▪Only low-carbon steel bolts were tested (SAE J429 Grade 2, or ASTM A 307A)
▪Only three bolt diameters were tested [3/8-in. (0.95 cm), 1/2-in. (1.27 cm), and 3/4-in. (1.91 cm)]
▪Only three bolt lengths were tested [4-in. (10.16 cm), 6-in. (15.25 cm), and 8-in. (20.32 cm)]
▪Only one load rate was used [0.1 in./min (2.54 mm/min)]
▪Only ten specimens per data set were tested according to each method

5.4 Recommendations for Future Research

The successful development and testing of yield modes III and IV coupled with Billings' successes with mode II, means that the predominant yield modes have each been examined relative to reverse-cyclic loading. With Dolan and other researchers at Washington State University already testing multiple-row connections, the only potential directions remaining for connection testing derive from the list of limitations in section 5.3. For example, future research might be conducted using perpendicular-to-grain loading, or other species of wood, or double-shear connections, or connections with more than five bolts. In addition, spacings greater than 8D have not been tested yet. With the 8D spacing performing best in this project, it is not unreasonable to assume that a 9D spacing might also perform well. However, at some point the practicality of the bolt spacing must be considered, and spacings much greater than 8D would often be inapplicable due to other spatial constraints.

As for the bolt testing, more bending trials need to be performed on specimens with large L/D ratios. These data sets tended to exhibit the most consistent bending yield strengths during this project, and more testing might prove that the test methods, and especially the cantilever method, are indeed useful in these cases. Any future tension tests would first have to force the failures to occur in the bolt shafts, thereby avoiding the problems associated with measuring elongation. This relocation of the point of failure could be accomplished with the use of a threaded sleeve that covers the tapered and threaded portions of the bolt specimens. This concept is described in detail in section 4.4.2.

References

(1) American Forest and Paper Association (AF&PA). (2001) *National Design Specification for Wood Construction*. AF&PA, Washington, DC.

(2) Anderson, G.T. (2002) *Experimental Investigation of Group Action Factor for Wood Connections*. M.S. Thesis. Virginia Polytechnic Institute and State University. Blacksburg, VA, USA.

(3) Annual Book of ASTM Standards v01.08, (2003a) "Standard Test Methods for Determining the Mechanical Properties of Externally and Internally Threaded Fasteners, Washers, and Rivets." American Society of Testing and Materials Standard F 606-02. ASTM, Philadelphia, PA.

(4) Annual Book of ASTM Standards v01.08, (2003a) "Standard Test Method for Determining Bending Yield Moment of Nails." American Society of Testing and Materials Standard F 1575-01. ASTM, Philadelphia, PA.

(5) Annual Book of ASTM Standards v4.10, (2003b) "Standard Test Method for Mechanical Fasteners in Wood." American Society of Testing and Materials Standard F 1761-88(2000)e1. ASTM, Philadelphia, PA.

(6) Annual Book of ASTM Standards v4.10, (2003b) "Standard Test Method for Specific Gravity of Wood and Wood-Based Materials." American Society of Testing and Materials Standard D 2395-02. ASTM, Philadelphia, PA.

(7) Annual Book of ASTM Standards v4.10, (2003b) "Standard Test Method for Direct Moisture Content Measurement of Wood and Wood-Based Materials." American Society of Testing and Materials Standard D 4442-92(2003). ASTM, Philadelphia, PA.

(8) Annual Book of ASTM Standards v4.10, (2003b) "Standard Test Method for Evaluating Dowel-Bearing Strength for Wood and Wood-Based Products." American Society of Testing and Materials Standard D 5764-97a(2002). ASTM, Philadelphia, PA.

(9) ASTM. (1999) "Standard Test Method for Cyclic Properties of Connections Assembled with Mechanical Fasteners." American Society of Testing and Materials Standard E06.13. 7th Draft Standard. ASTM, Philadelphia, PA.

(10) Billings, M.A. (2004) *Optimization of Spacing Between Bolts in a Row in a Single-Shear Timber Connection Subjected to Monotonic and Reverse Cyclic Loading*. M.S. Thesis. Virginia Polytechnic Institute and State University. Blacksburg, VA, USA.

(11) Boresi, A.P. and Schmidt, R.J. (2003) Advanced Mechanics of Materials. Sixth Edition. John Wiley & Sons, Inc. Hoboken, NJ, USA.

(12) Chui, Y.H. and I. Smith. (1989) "Quantifying Damping in Structural Timber Components." *Proceedings, 2nd Pacific Timber Engineering Conference*, Auckland, New Zealand.

(13) Dodson, M. A. (2003) *The Effects of Row Spacing and Bolt Spacing in 6-Bolt and 4-Bolt Wood-to-Steel Connections*. M.S. Thesis. Washington State University. Pullman, WA, USA.

(14) Fastenal Company. (2000) "Fastenal Technical Reference Guide." http://www.fastenal.com/content/documents/FastenalTechnicalReferenceGuide.pdf Winona, MN, USA.

(15) Gutshall, S.T. (1994) *Monotonic and Cyclic Short-term Performance of Nailed and Bolted Timber Connections*. M.S. Thesis. Virginia Polytechnic Institute and State University. Blacksburg, VA, USA.

(16) Hamilton, Roger (NUCOR Fasteners). Telephone conversation. 8/5/2005.

(17) Heine, C.P. (2001) *Simulated Response of Degrading Hysteretic Joints with Slack Behavior*. Ph.D. Dissertation. Virginia Polytechnic Institute and State University. Blacksburg, VA, USA.

(18) Johansen, K.W. (1949) "Theory of Timber Connections." *International Association for Bridge and Structural Engineering*. 9:249-262.

(19) Jorissen, A. (1998) *Double Shear Timber Connections with Dowel Type Fasteners*. Ph.D. Thesis. Delft University Press. Delft, Holland.

(20) Krawinkler, H., Parisi, F., Ibara, L., Ayoub, A., Medina, R. (2000) *Development of a Testing Protocol for Woodframe Structures*. CUREE Publication No. W-02. Consortium of Universities for Research in Earthquake Engineering. Richmond, CA, USA.

(21) Lantos, G. (1969) "Load Distribution in a row of Fasteners Subjected to Lateral Load." Wood Science. Vol. 1(3): 129-136.

(22) McBain, N.S. and Uhlig, S. (1982) Choice of Technique in Bolt and Nut Manufacture. Scottish Academic Press. Edinburgh, Scotland.

(23) Murray, Dr. Thomas. Professor of Structural Engineering, Virginia Polytechnic Institute and State University. Electronic mail correspondence. August, 2005.

(24) Shackelford, James F. (2000) Materials Science for Engineers. Fifth Edition. Prentice Hall. Upper Saddle River, NJ, USA.

(25) Society of Automotive Engineers Standards. (1999) "Mechanical and Material Requirements for Externally Threaded Fasteners." Society of Automotive Engineers Standard J429. SAE, Warrendale, PA.

(26) Trayer, G.W. (1932) "The Bearing Strength of Wood Under Bolts." Technical Bulletin No. 332. USDA. Washington, D.C., USA.

(27) United States Department of Agriculture. (2002) Wood Handbook: Wood As an Engineering Material. Forest Products Laboratory. Madison, WI, USA.

(28) Wilkinson, T. (1980) "Assessment of Modification Factors for a Row of Bolts of Timber Connectors." USDA Forest Service Research Paper FPL 376. Forest Products Laboratory. Madison, WI, USA.

(29) Wilkinson, T. (1991) "Dowel Bearing Strength." Research Paper FPL-505. Madison, WI: US Department of Agriculture, Forest Service, Forest Products Laborory.

(30) Yeh, T.C., Hartz, B.H. and Brown, C.B. (1971) "Damping Sources in Wood Structures." *Journal of Sound and Vibration*. 19(4): 411-419.

(31) Young, J. F., Mindess, S., Gray R.J., Bentur, A. (1998) The Science and Technology of Civil Engineering Materials. Prentice Hall. Upper Saddle River, NJ, USA.